Development of a novel class of cyclic NGR peptides for targeted drug delivery

Andrea Angelo Pierluigi Tripodi

PhD thesis

Supervisor

Prof. Dr. Gábor Mező

Head of the Research Group of Peptide Chemistry

Doctoral School of Chemistry

Head of Doctoral School: Dr. Attila Császár

Doctoral Program:

Synthetic Chemistry, Materials Science and Biomolecular Chemistry

Director of the Program: **Prof. Dr. András Perczel**

Department of Organic Chemistry

MTA-ELTE Research Group of Peptide Chemistry

Eötvös Loránd University, Faculty of Science

Budapest, 2020

To whom has believed in me.

List of abbreviations

All applied three-letter and one-letter codes for α-amino acids are in agreement with the recommendations from the IUPAC-IUB Commission on Biochemical Nomenclature.

Aaa	amino acid
Ab	antibody
ADC	antibody-drug conjugate
AcOH	acetic acid
Aoa	aminooxyacetic acid
APN	Aminopeptidase N
>=Aoa	isopropylidene protected Aoa
Bn	benzyl
Boc	*tert*-butyloxycarbonyl
Boc-ON	2-(tert-butoxycarbonyloxyimino)-2-phenylacetonitrile
Boc_2O	di-*tert*-butyl dicarbonate (Boc-anhydride)
Bu	butyryl
Cbz	benzyloxycarbonyl

CD13	Aminopeptidase N
Cit	citruline
CLSM	confocal laser scanning microscopy
CPP	cell penetrating peptide
Dau	daunorubicin
DBU	1,8-diazabicyclo[5.4.0]undec-7-ene
DCC	*N,N'*-dicyclohexylcarbodiimide
DCM	dichloromethane
Dde	1-(4,4-dimethyl-2,6-dioxocyclohex-1-ylidene)ethyl
DDS	drug delivery system
DIAD	diisopropyl azodicarboxylate
DIC	*N,N'*-diisopropylcarbodiimide
DIPEA	*N,N*-diisopropylethylamine
DMEM	Dulbecco's Modified Eagle Medium
DMF	*N,N*-dimethylformamide
DMSO	dimethyl sulfoxide
DOTA	1,4,7,10-tetraazacyclododecane-1,4,7,10-tetraacetic acid

Dox	doxorubicin
DKP	diketopiperazine
EGF	epidermal growth factor
EDT	ethanedithiol
eq	equivalent
ESI	electrospray ionization
EtOAc	ethyl acetate
Et_2O	diethyl ether
EtOH	ethanol
FACS	fluorescence-activated cell sorting
FBS	fetal bovine serum
FDA	Food and Drug Administration
Fmoc	9-fluorenylmethoxycarbonyl
GnRH-III	gonadotropin-releasing hormone-III
HATU	1-[bis(dimethylamino)methylene]-1-*H*-1,2,3-triazolo[4,5-*b*]pyridinium3-oxid hexafluorophosphate
HCl	hydrochloric acid

HOAt	1-hydroxy-7-azabenzotriazole
HOBt	1-hydroxybenzotriazole hydrate
IC_{50}	half maximal inhibitory concentration
LC-MS	liquid chromatography-mass spectrometry
mAb	monoclonal antibody
MBHA	4-methylbenzhydrylamine (resin)
MeCN	acetonitrile
MeOH	methanol
MS	mass spectrometry
Mtr	4-methoxy-2,3,6-trimethyl benzene sulphonyl
Mtt	4-methyltrityl
MTX	methotrexate
$NaHCO_3$	sodium bicarbonate
Nle	norleucine
NGR	Asn-Gly-Arg
NMR	nuclear magnetic resonance
OAll	allyloxycarbonyl

OOI	National Institute of Oncology (Országos Onkológiai Intézet)
OtBu	*tert*-butyl ester
$Pd(PPh_3)_4$	palladium-tetrakis(triphenylphosphine)
PMe	Trimethylphosphine
PTX	paclitaxel
RP-HPLC	reversed-phase high-performance liquid chromatography
RMPI	Roswell Park Memorial Institute
RT	room temperature
R_t	retention time
sat.	saturated
SMDC	small molecule drug conjugate
SPPS	solid phase peptide synthesis
tBu	*tert*-butyl
TFA	trifluoroacetic acid
TMS	tetramethylsilane
TMSBr	bromotrimethylsilane
THF	tetrahydrofuran

Tic	1,2,3,4-tetrahydroisoquinoline-3-carboxylic acid
TIS	triisopropylsilane
Tris	tris-(hydroxymethyl)-aminomethane
Trt	triphenylmethyl/trityl
VEGF	vascular endothelial growth factor

Contents

Acknowledgment

On this day my special thank goes to all the people I met and supported me during this incredible and fascinating challenge, to all of them goes my gratitude for believing in me, even when I wanted to give up.

A big thank goes to my supervisor, Professor Dr. Gábor Mező for giving me the opportunity to start in his laboratory this wonderful experience, probably the most important of my life. I am very grateful for his guidance and continuous support, I will never forget his help from the beginning to the end of the PhD. He is a great supervisor and scientist. I feel privileged to have joined his team.

I am deeply grateful to my colleague and good friend Dr. Beáta Biri-Kovács for her extraordinary support and help during this past year of my PhD. Thanks a lot for the hard commitment you put in this project.

A special thank goes to Ivan, my colleague and great friend, he is so far the most gentle person I have been working with. Thank you for showing and teaching me the basics of biology and for being so patience in the laboratory when I was not sure what to do. I will never forget the days spent together at work and outside with you and Anna.

Sabine, what can I say? We started this adventure together and I am so glad I met you, thanks for being the best lab-mate I could ever ask for, thanks for the thousands of advices and long talks we had, I am honored I could share this adventure with you. Thank you for giving me the strength to carry on even when I thought this was not for me. You are a great friend and a great person. And as you always said we are the best team ever!

A special thank goes to Dr. József Tóvári for giving me the opportunity to work in his lab, a big thank goes to his coworkers who were involved in the in vivo evaluation for the PhD project.

A big thank goes to Dr. Szilvia Bősze for sharing part of the supplies and space in her laboratory, so that I could perform part of the biological experiments at ELTE.

Special thank goes to the team in Como headed by Professor Dr. Umberto Piarulli, thanks for the great environment at work and for the great welcome in the laboratory. A big thank here goes to Lizeth, Clemence and Sara who helped and supported me during the period spent in Italy.

Special thank to the group I have collaborated with at ITALFARMACO, in particular to Christian, Andrea, Barbara, Gianfranco, Ilaria, Mattia and Marilu', thank you for the great time spent together.

I am especially grateful to Dr. Gitta Schlosser for her support in mass spectrometry and for being always up to help me even when she was very busy. Special thanks to Arnold for his help as well.

Many thanks to Bálint Szeder and Professor László Buday who supported my project and analyzed the microscopy images.

I would like to thank all members of the European Training Network MAGICBULLET. In particularly I want to express my gratitude to Professor Dr. Norbert Sewald and Dr. Marcel Frese from the University of Bielefeld for the excellent organization of the network and the strong support within the four years.

Moreover, I would like to thank all the team members from ELTE, thank you very much to Kata, Lilla, Kriszti, and Klára for the great time spent together, I will never forget summer days in front of the HPLCs side by side (with no AC). Thank you for always helping each other as a good team.

Vorrei ringraziare dal profondo del mio cuore la mia famiglia, la mia vera forza in tutto questo, la fonte della mia energia e felicità. Grazie perché senza la vostra presenza, il vostro supporto non sarei mai stato in grado di affrontare queste difficili decisioni.

Infine, un sentito grazie ai miei genitori, non so da dove cominciare. Potrei iniziare ringraziandovi per avermi fatto nascere e per avermi amato e sostenuto ogni giorno, per avermi permesso di studiare, di scegliere la mia strada, di seguire le mie passioni, di vedere e conoscere il mondo. Resta il fatto che, pur essendo da oggi "dottore", l'insegnamento maggiore che ho ricevuto in vita mia me lo avete dato voi: amare, sempre. Siete la mia grande ricchezza. Questa laurea è anche vostra, che avete combattuto e stretto i denti al mio fianco, e che spero oggi possiate essere felici ed orgogliosi di me. Vi voglio bene.

Finally, I would like to express my appreciation to all institutions and organizations who provided the financial support for my PhD project and related research. This work was supported by the European Union's Horizon 2020 research and innovation program under the Marie Sklodowska-Curie Grant No 642004; and by the National Research, Development and Innovation Office under grant NKFIH K119552 and NVKP_16-1-2016-0036.

1. Introduction

1.1 Cancer today

Over the past years, almost 20 million new cases of cancer have been diagnosed around the globe, only in 2018 there were 9.6 million cancer-related deaths.[1–3] Cancer in fact is the second cause of death worldwide[4,5], the most fatal tumors for men are lung and prostate cancer, while for women are breast, colon and rectum cancer.[6] The figure below **(Figure 1)** shows the numbers in terms of incidence and mortality regarding some of the most aggressive cancer types.

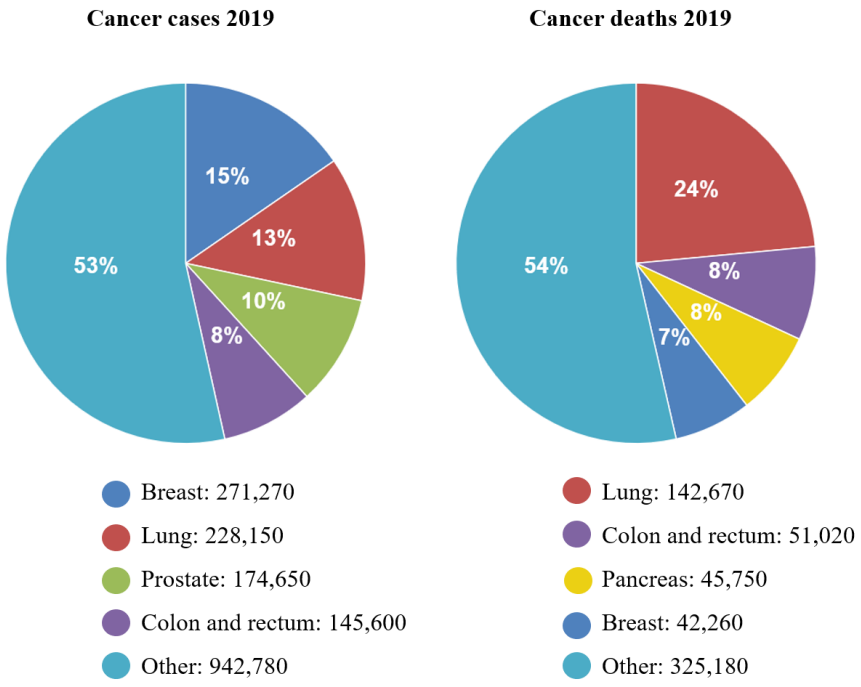

Figure 1: Major cancer types in 2019 (*seer.cancer.gov*).

Cancer is characterized by uncontrolled cell division and the ability of cells to invade other tissues leading to the formation of tumor mass, vascularization and metastasis.[7,8] Metastasis is the process of the spreading of cancer cells from the primary tumor to surrounding tissues and to distant organs.

Metastases are the main cause of cancer mortality[9–15] and studies confirm that they are responsible for about 90% of cancer deaths.[16] Metastasis includes a variety of serial and interconnected phases. In order to achieve the metastatic site, tumor cells have to detach from the primary tumor, intravasate into the circulatory and lymphatic systems, evade immune attack, extravasate at distant capillary beds, and invade into and proliferate in distant organs.[9,13,14,17,18] Those cells can create a microenvironment that facilitates angiogenesis and proliferation, resulting in the formation of malignant secondary tumors (**Figure 2**). Nowadays there is no therapeutic strategy that can efficiently fight metastasis. The most crucial difference is surgery, as widespread metastatic tumors are usually not surgically removed, beacause surgery is often limited to cases in which only a single metastatic lesion or a very small number of metastases are restricted to a specific area of the body or tissue.[16,19]

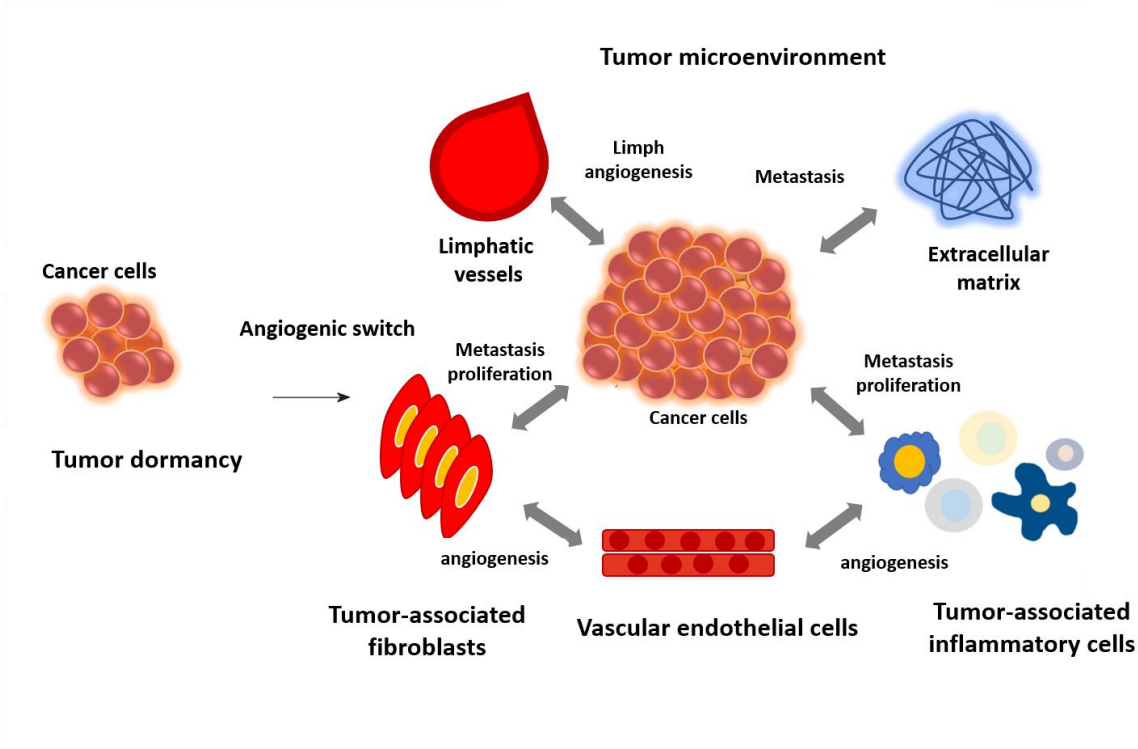

Figure 2: Tumor microenvironment, angiogenic switch and spreading. A change in the tumor microenvironment can facilitate metastasis and thereby allow cancer cells to exit from dormancy and interact with endothelial cells, tumor-associated fibroblasts and the extracellular matrix.[20]

The cause of cancer may be environmental agents, viral or genetic factors. We should keep in mind, that in most cancer cases we cannot point the disease to a single cause. Data taken from (*allaboutcancer.fi*)[21] shows that cancer risk factors can be divided into the following groups:

- biological or internal factors,
- environmental exposure, for instance to radon and UV irradiation,
- carcinogens such as many chemicals and radioactive materials,
- lifestyle-related factors.

Moreover, there are bacteria and viruses that may increase the risk of developing cancer as the below listed ones which are highly spread in the population around the globe:

- *Helicobacter pylori* (which causes gastritis),
- HBV, HCV (hepatitis viruses that cause hepatitis),
- HPV (human papilloma virus, papilloma virus, associated with cervical cancer),
- EBV (Epstein-Barr virus, the herpes virus that causes inflammation of the throat lymphoid).[21]

The main possible treatments of tumors are surgical resection[22], chemotherapy[23,24], radiation therapy[25,26], hormone therapies[27–29], but also targeted therapies[30–32], gene therapy and immunotherapy. The last one has become an important therapeutic alternative, and it is nowadays the first choice in many cases.[33,34] Nanotechnology has recently arrived on the scene offering alternative drug delivery systems, combining imaging and treatment and providing direct targeting among others.[35] The new approaches can be used in combination with other important components like peptides, monoclonal antibodies (mAb), folic acid[36], etc.

1.2 Traditional chemotherapy

Chemotherapy is one of the major approaches to treat cancer by delivering a cytotoxic agent to cancer cells.[37] The history of chemotherapy began in the early 20th century, but its use in treating cancer started in the 1930s.[24] The administration of anticancer drugs aims to induce apoptosis by interfering at various phases of the cell cycle. The main limitation of conventional chemotherapy is the inability to deliver the correct amount of drugs directly to cancer cells without affecting normal cells.[38,39] Drug resistance, biodistribution and drug clearance are also common issues to be taken in consideration during treatment of patients.[40] The unfavorable biodistribution combined with a mechanism of non-selective action can cause serious side effects and prevent the increment of doses of the active drug at therapeutic standards. Many healthy cells also have a rapid cell cycle, such as those in the gastrointestinal tract and hair follicles and thus, they are more susceptible to the effects of chemotherapy resulting in nausea and hair loss during treatment.[34] Main approaches have been studied to expand the therapeutic window: the combination of two or more cancer drugs with different mechanism of action and toxicity, and the introduction of highly potent drugs at very low dosage. Several strategies have been proposed which include alternative formulations, *e.g.* liposomes[41], resistance modulation, *e.g.* PSC833[42], antidotes/toxicity modifiers, *e.g.* ICRF-187[43] and gene therapy.

1.3 Targeted chemotherapy

Targeted therapy consists of delivering active compounds to specific genes or proteins that are unique to cancer cells or the tissue environment that promotes cancer growth.[44–48] One of the pioneer of this concept was Paul Ehrlich, a German scientist who had particular interest in alkylating agents and who came up with the term to describe the chemical treatment of disease. He coined for the first time the concept of MAGIC BULLET, as a drug which is selectively active on a particular pathogen

without harming normal cells. Firstly, he investigated this idea looking at infectious diseases and his first discovery (Salvarsan), provided the first effective treatment for syphilis before the advent of penicillin.[49–51] Overall, Ehrlich acknowledged that his idea of a 'magic bullet' could be optimized and further used in other classes of pathogens, and also for cancer. His findings enforced researchers to explore a new era with the development of new technologies in the field of targeted cancer therapy. Targeted active compounds specifically act on cell receptors which are overexpressed on the surface of cancer cells, improving the tolerability of the treatment, the compliance and quality of life of the individual. It is often used in conjunction with chemotherapy and other cancer treatments. Targeted therapy includes drugs that block cancer cell proliferation, promote cell cycle regulation or induce apoptosis and targeted delivery of toxic substances specific to cancer cells.[52] In the last decades, many new technologies in targeted therapy have been investigated and the obtained results are very encouraging. Many active agents have been used and these therapies including the application of proteins, monoclonal antibodies and peptides.[53,54]

Targeted therapies can actively influence different pathways:

- Release the toxic payload that act on cancer cells through different ways, *e.g.* inducing apoptosis, inhibiting their ability to proliferate and divide[34,48,35];
- Hinder angiogenesis which is the rate-limiting step in solid tumor growth[55], inhibit tumor-related kinases and other oncoproteins [53,54,56–59];
- Stimulate the immune system to identify and destroy cancer cells (immuno-oncology)[60,61];
- Influence the endocrine system through external administration of precise hormone or drugs that inhibit their production[62–65], *e.g.* anti-estrogens, aromatase inhibitors, GnRH agonists.

The first example, in particular, has been proposed as an alternative strategy to avoid the drawbacks of traditional therapies, allowing powerful cytotoxic payloads at their site of action by the help of ligands that are specific towards tumor associated targets.[66,67] The cytotoxic drug is covalently attached to the respective ligand using different linkers.[68–71] After binding to the membrane of the tumor cell, the complex is internalized, once inside, specific and non-specific enzymatic steps degrade the drug-conjugate allowing the release of the drug or its active metabolite.[67,72–74] The internalization of the active compound is not the principal requirement of its efficiency. Many conjugates can also work and be released efficiently at the tumor site, while drug release takes place outside the tumor cell and then it can enter through diffusion. Tumor microenvironment is a fundamental aspect to always consider when working with molecules such as peptides. Numerous conjugates have been discovered and some of them are already approved by Food Drug Administration (FDA) and waiting to be commercialized, some others are under clinical trial.

1.3.1 Antibody-drug conjugates (ADCs)

Biological compounds are widely used for the treatment of many diseases, nowadays they represent the most advanced therapies for the cure of some type of cancer. For example some of those are used in Crohn's [75–77], ulcerative colitis, rheumatoid arthritis, and other autoimmune diseases.[75,78,79] One of the most important biologics used are antibody-drug conjugates (ADCs) that are designed to afford therapeutic potency to the antibody and specificity to the anticancer agents, which can be targeted to the cancer cell and decrease the systemic drawbacks.[60] The main advantage of ADCs is their long half-life, activity upon binding to tumors and no systemic toxicity contributing to the maximum efficiency of administering the cytotoxic drug to the tumor cells.[80–83] However, monoclonal antibodies (mAbs) and large protein ligands have some major limitations compared to peptides:

expensive large-scale production[84], poor delivery to tumor due to their large size[85], and dose-limiting toxicity to the liver and bone marrow due to nonspecific uptake by endothelial cells.[47,86,87] It is important to mention some of the ADCs approved by the FDA: *e.g.* Adcetris® for the treatment of refractory Hodgkin's lymphoma and anaplastic large cell lymphoma, formed by the conjugation of chimeric mAb to monomethyl auristatin E (MMAE) across the protease cleavable Val-Cit linker, and Kadcyla® where the drug is attached by an uncleavable spacer, used for the treatment of HER2-positive metastatic breast cancer (**Figure 3**).[88] Despite the simple concept, various parameters must be considered when designing optimal ADCs, such as selection of the appropriate antigen target and conjugation method. Each component of the ADC (the antibody, linker and drug) must also be optimized to fully realize the goal of a targeted therapy with improved efficacy and tolerability. Advancements over the past several decades have led to a new generation of ADCs comprising non-immunogenic mAbs, linkers with balanced stability and highly potent cytotoxic agents. Although challenges remain, recent clinical success has generated intense interest in this therapeutic class. Mylotarg® is used for adult acute myeloid leukemia and Besponsa® (**Figure 3**) that got the approval in 2017 is used for the treatment of adult acute lymphoblastic leukemia.[64] Moreover, one of the most recent, Polivy®, the CD79b-directed ADC in combination with bendamustine plus Rituxan® (rituximab) is used for the treatment of adults with relapsed or refractory (R/R) diffuse large B-cell lymphoma (DLBCL).[89] Based on the success of such constructs, around seventy more ADCs are in different stages of clinical trial and development.[90]

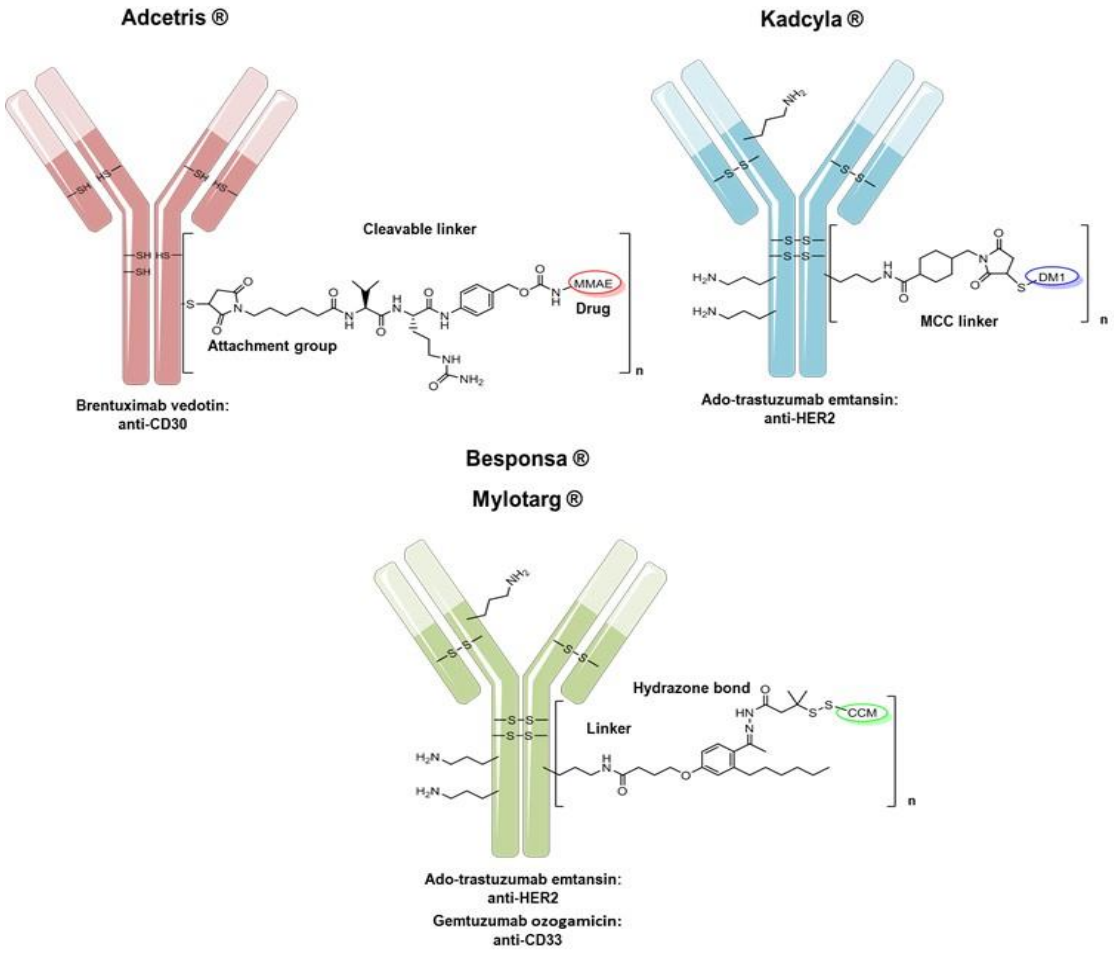

Figure 3: FDA approved ADCs. Drug-to-antibody ratio is different, depending from the conjugation strategy. n=4 (Adcetris), n=3.5 (Kadcyla), n=2.5 (Besponsa[91,92] and Mylotarg[93,94]).

A high drug-to-antibody ratio (DAR) is also affecting the propensity of the ADCs to aggregate, especially after being conjugated to very hydrophobic linker-drugs, so that the introduction of hydrophilic molecules could help to solve the major problem.[95] The optimal design to obtain homogeneous compounds with the same average and distribution of drug is the main feature to gain safe products, for this reason many efforts have been made in engineering the antibody sequence or by achieving site-selective conjugation strategies.

1.3.2 Small molecule drug-conjugates (SMDCs)

Considering the drawbacks of ADCs in terms of costs and pharmacokinetic profile which may eventually bring to a loss of antitumor activity, the development of small molecule drug-conjugates represent an important and effective alternative to mAbs for selectively targeting solid tumors.[96] In fact, small molecule-drug conjugates (SMDCs) have been thoroughly investigated as active anticancer agents[97]; however, while several SMDCs have been and are also currently evaluated in clinical trials, no SMDC has yet gained marketing approval. The most common targeting ligands are peptides[98], peptidomimetics and vitamins, those can be divided into two main categories, natural receptor ligands or synthetic derivatives. The general architecture of a SMDC consists of three building blocks: the tumor-homing peptide, the biodegradable connecting linker and the cytotoxic agent (**Figure 4**).

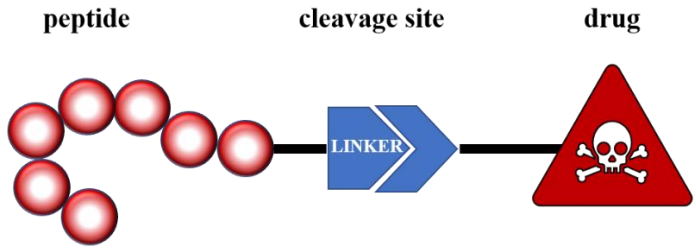

Figure 4: Schematic structure of a typical peptide drug-conjugate, containing the peptide sequence or ligand, the cleavage site also known as linker and the cytotoxic payload or drug.

The construct should be built in such way that the ligation with a cytotoxic agent is easily achievable. One of their main features is also their ability to resist to protease hydrolysis which increases their *in vivo* stability.[48,99–104] Conjugation typically takes place on lysine, cysteine and glutamic acid *via* orthogonal coupling or on the free *N*-terminus of the peptide during the synthetic route.[71,105] Moreover, important effort was made to increase their chemical and biological activity *in vivo* like cyclization, *N*-methylation and incorporation of D-amino acid.[66,106] However, the

conjugation site should be carefully selected, since variation induced in the peptide sequence and structure might reduce its binding activity to the targeted receptor.[71] Among the limited number of targets that have been addressed by SMDCs so far, the most prominent is the folate receptor. A vinblastine–folate conjugate (vintafolide) has been advanced to phase III clinical trials[107] but these trials have been terminated for confidential reasons. The group of Dario Neri at the ETH Zürich has recently described the SMDC AAZ-MMA that is derived from the known carbonic anhydrase IX (CAIX) inhibitor acetazolamide (AAZ) as the tumor-targeting moiety and incorporates the tubulin inhibitor monomethyl auristatin E (MMAE) as the cytotoxic payload.[108] Not only folate receptor but also prostate-specific membrane antigen, Aminopeptidase N (APN), integrins and hormone receptors like gonadotropin-release hormone and somatostatin receptors have been investigated as possible targets.

1.4 Solid phase peptide synthesis (SPPS)

In 1901 Emil Fisher discovered that amino acids can form peptide chains through condensation reactions.[109] The condensation reaction still leaves an amino and a carboxyl group at each end, which permits peptide elongation. In order to facilitate the condensation reaction, the carboxyl group should be activated while the amino group should be deprotonated, as an available lone pair can act as nucleophile. The demand of new peptides is still growing, and solution peptide synthesis becomes difficult for the synthesis of longer peptides. In fact, in this case, solubility and purification problems can occur, thus other strategies are required. In 1963 Merrifield described the synthesis of a tetrapeptide, carried out by adding one by one benzyloxycarbonyl (Cbz) protected amino acids to a peptide chain covalently bound to a polystyrene based resin. Once the peptide was synthesized, it was washed from the resin, purified and characterized. SPPS permits the ready removal of reagents, by-

products and impurities, without needing recrystallization steps. The use of the new method, in which the most significant change is the presence of a solid support, permits faster synthesis with high yields of pure peptide. However, the synthesis of bradykinin was the most relevant experiment performed by Merrifield on 1964, by changing the protecting groups to *t*-butyloxycarbonyl (Boc) derivatives, which are more acid labile. The loss of peptide from the resin was reduced using the new technique and the bradykinin possessed full biological activity.[110]

Merrifield's method is associated with many problems: premature cleavage of the protecting groups and the peptide due to harsh medium conditions, the difficulty to remove insoluble by-products and the solvation properties of the resin. The main cause of this was certainly the use of non-ideal protecting groups and resin linkers. In particular, the use of Boc group and benzyl derivatives (such as Z group) causes a non-selective cleavage, leading to impure final products, side reactions and lower yields.[111] Moreover, benzyl derivatives can be removed only using hydrogen fluoride which is highly toxic and can be used only with a special teflon apparatus. Finally, the strong acidic conditions can damage fragile peptides.[112] All these limitations led to a change in SPPS chemistry and moved towards the introduction of 9-fluorenylmethoxycarbonyl (Fmoc) strategy in SPPS.

1.4.1 Fmoc chemistry principles

The first example of Fmoc chemistry was reported by Carpino in 1970. In this case liquid ammonia was used for the deprotection step, but the reaction was unfavorable and not used by other scientists. Two years later, Carpino suggested the use of piperidine for the same purpose instead of ammonia. With this change, Fmoc chemistry started to be used more frequently. Later, in 1978, Atherton and

Sheppard reported a new combination of protecting groups and linkers which considerably improved Fmoc SPPS chemistry.[113]

This new technique differs from Merrifield's peptide synthesis because different types of protecting groups are used. Fmoc is a base labile α-amino protecting group, where the resin linker and side chain protecting groups are acid labile. This orthogonal chemistry is useful because temporary and permanent protecting groups are removed using completely different chemical reactions and under milder conditions.[111] The synthesis starts with the first Fmoc amino acid, covalently bound with the *C*-terminus *via* an acid labile linker to a solid support. The side chain of the Fmoc amino acid is protected by acid labile groups. Then the Fmoc group is removed by using a solution of 20% piperidine in DMF, in order to allow the addition of the second amino acid, which is added to the resin with activating agents dissolved in DMF. After deprotection, the resin is washed with DMF and methanol and the solution of the second Fmoc protected amino acid is added. The cycle needs to be repeated until the entire peptide chain is synthesized (**Figure 5**). Then the peptide is separated from the resin using trifluoroacetic acid (TFA) and it is ready to be purified.

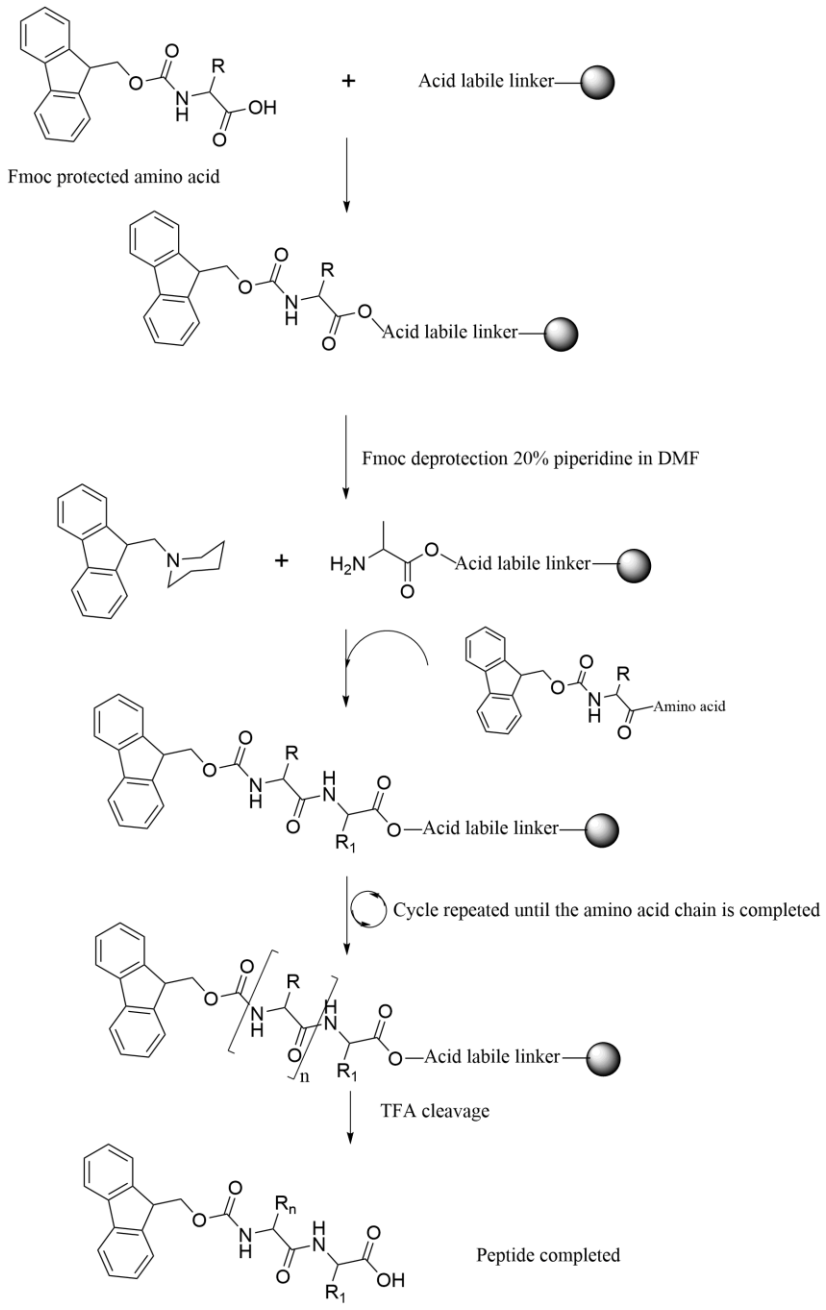

Figure 5: Generic scheme of the synthesis of a peptide using Fmoc strategy.

1.5 Receptor mediated uptake

Receptor-mediated uptake is an important process where specific ligands bind to receptor proteins of the cell membrane and can subsequently be internalized.[114] These receptors are overexpressed in

particular areas of the membrane called coated pits or migrate in these zones after binding to the molecule which has to be carried. The coated pits contain a layer of peripheral membrane proteins known as clathrins. Once the receptors are bound to specific molecules, the dimple folds back into the cell and forms a vesicle covered by the clathrin layer and containing the active molecule. Later on the vesicle loses the clathrin becoming an endosome, which then forms two vesicles: one containing the receptors and the other containing the ligand. The receptors are then recycled and returned to be available at the plasma membrane while the ligand-containing vesicle merges with the lysosome to form a secondary lysosome whose content, once digested, is released into the site of action in the cell (**Figure 6**). This process may be occur in many different ways *e.g.* caveolin-mediated process as well.

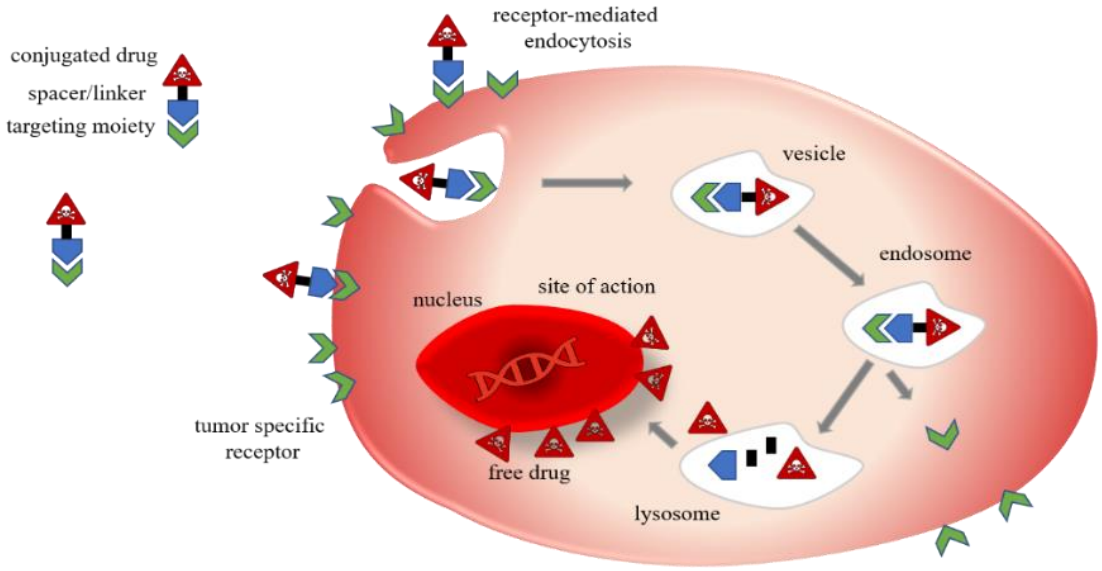

Figure 6: Simplified process of receptor-mediated uptake of drug conjugates: after internalization, the linker is cleaved in the lysosome, the free drug is released from the ligand and can express the activity on the particular target.

1.5.1 Integrins: structure and role in angiogenesis

Integrins are an important receptor family widely studied in active tumor targeting, they are heterodimeric transmembrane receptors that mostly mediate cell adhesion.[115–123] With their

extracellular head region, most integrins bind extracellular matrix (ECM) glycoproteins such as laminins and collagens in basement membranes or connective tissue components like fibronectin.[122] Others bind counterreceptors on neighboring cells, bacterial polysaccharides or viral coat proteins. Integrins (**Figure 7**) are formed through noncovalent association of two type I transmembrane glycoproteins, the α- and the β subunit.[124] The extracellular domains are approximately 700 amino acids for α- and 1000 amino acids for β subunits and form elongated stalks and a globular ligand-binding head region.[122,125] Those receptors are well known for their involvement in physiological mechanisms such as tissue growth and inflammation, considerable research has shown that they play crucial roles in diseases such as cancer, thrombosis and auto-immune diseases. The connection between ECM and cytoskeleton provided by integrins is highly dynamic and involves a bidirectional transfer of information.[126] For these reasons, the pharmacological targeting of these receptors has been the subject of numerous studies. Since cells that have undergone neoplastic transformation are less dependent on ECM adhesion for their survival and proliferation, it has been demonstrated that cancer cells enhance the expression of specific integrins that favor their proliferation and migration.[127] Among these, $\alpha_v\beta_3$ integrin has been widely investigated as receptor for tumor-targeting strategies, moreover, $\alpha_v\beta_1$, $\alpha_v\beta_5$, $\alpha_v\beta_6$, $\alpha_v\beta_8$, $\alpha_5\beta_1$, $\alpha_8\beta_1$ and $\alpha_{IIb}\beta_3$ integrins can also recognize the tripeptide RGD motif.[128] The importance of the RGD sequence was established in 1984 when Pierschbacher and Ruoslahti found that the ability of fibronectin to recognize its target receptors on cell membrane was achieved by this tripeptide sequence.[129] The presentation of the RGD motif in the binding site is important and it is a common feature for all the RGD proteins. Higher rigidity of the backbone and low flexibility of flanking residues, needed to properly fold the RGD sequence, were obtained in different ways; blocking the RGD sequence in a cyclic structure was the most used. Among the great variety of RGD peptidomimetic ligands found in literature, Cilengitide, discovered by Kessler *et al.*

in 1991, is surely the most famous.[130] Cilengitide has been the first integrin ligand to be tested for antagonistic behaviour in clinical trials; it failed phase III clinical trial for treatment of patients with glioblastoma[131] but it is currently undergoing phase II studies for the treatment of other tumors.[132–135]

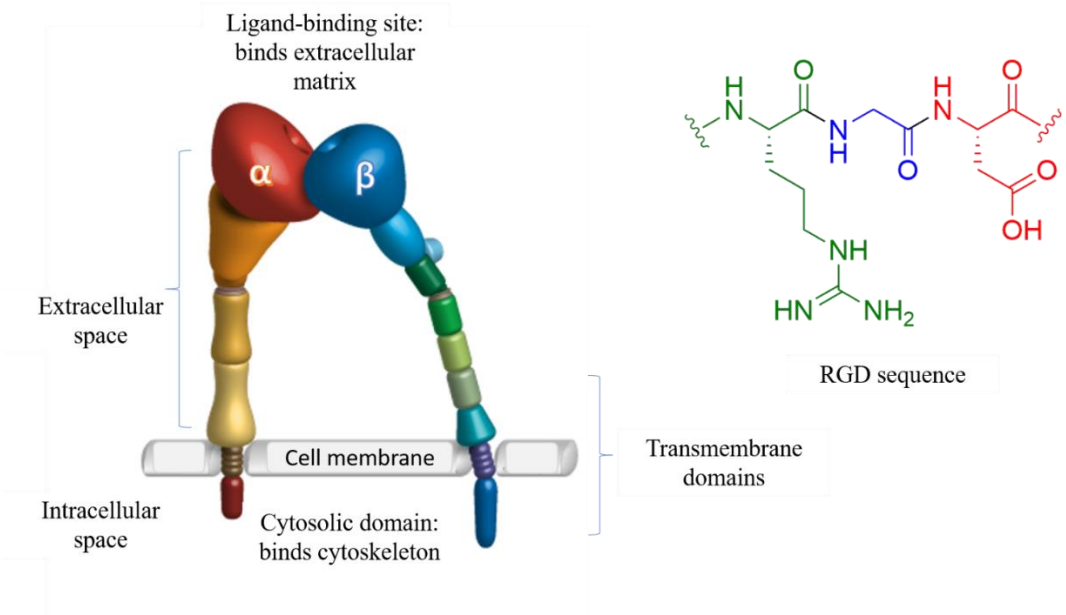

Figure 7: Schematic representation of the two integrin subunits and the RGD sequence.[136]

Moreover, it has been demonstrated that cyclic *iso*DGR and RGD peptides containing a 2,5 diketopiperazine (DKP) scaffold can more efficiently bind to integrin receptors, in fact, these ligands show a moderate affinity for $\alpha_v\beta_3$ integrin in competitive binding assays.[137] DKPs are heterocyclic scaffolds easily accessible form α-amino acids, these are the smallest cyclic peptides that provide an important class of biologically active compounds. This DKP scaffold provides increased affinity to the receptor, improved selectivity and chemical stability of the ligand.[138,139] The structural similarity of DKP to peptides opens a new way for medicinal chemistry in designing molecules with similar

characteristics. Reducing the susceptibility to metabolic amide bond cleavage and inducing conformational rigidity are the results of constraining the N-atom of amide bond into a DKP ring. Functional diversity and stereochemistry can be introduced at different positions. A DKP library was developed in the research group Prof. Dr. Piarulli at UNINS (Universita' Degli Studi Dell'Insubria, Italy) (**Figure 8**).[139–142] These DKPs differ for the stereochemistry at C3 and C6 and for the substitution on the endocyclic nitrogens.

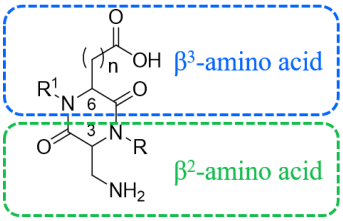

DKP1: (3*S*,6*S*), R = Ph, R^1 = H, n = 1
DKP2: (3*R*,6*S*), R = Ph, R^1= H, n = 1
DKP3: (3*S*,6*R*), R = Ph, R^1= H, n = 1
DKP4: (3*R*,6*S*), R = H, R^1= Ph, n = 1
DKP5: (3*R*,6*S*), R = R^1 = Ph, n = 1
DKP6: (3*S*,6*R*), R = H, R^1= Ph, n = 1
DKP7: (3*S*,6*R*), R = R^1 = Ph, n = 1
DKP8: (3*S*,6*R*), R = Ph, R^1= H, n = 2

Figure 8: DKP1-DKP8 scaffold library.[138,141]

1.5.2 Aminopeptidase N, APN (CD13): structure and role in angiogenesis

CD13 is a type II ectoenzyme of 150-240 kDa involved in the degradation of neutral or basic *N*-terminal residues of bioactive peptides.[143–148] This protein is a member of the M1 family of zinc metallopeptidases and consists of an enzymatic extracellular domain that has been implicated in signal transduction.[149–152] Originally APN was called aminopeptidase M referring to its location on the cell membrane, it was only demonstrated in 1989 that actually APN and CD13 were identical proteins.[153,154] The protein indeed is involved in many functions, including enzymatic regulation of peptides as well as tumor cell invasion, differentiation, proliferation and apoptosis, motility and angiogenesis.[143,145,155–161] This cascade is tipically activated by angiogenic signals as galectin-3 and

Ras, where Ras is crucial in signal transduction cascades.[162,163] Many studies demonstrate that APN is able to rescue angiogenesis.[164] Even if CD13 is not present on the surface of normal B and T lymphocytes and most lymphocytic tissues, it is now well known that the overexpression of CD13 is detected in acute myeloblastic leukaemia (AML) and also in acute lymphoblastic leukaemia (ALL).[165,166] It is also broadly expressed in the brush border of ephitelial cells from small intestine and renal proximal tubules, in bile duct canaliculi, in prostatic epithelial cells, mast cells and in some cases in fibroblasts and pericytes.[143,145,149,167,168] Taking in consideration the morphological aspect, a seven domain organization of CD13 has been identified. Three-dimensional models of human APN/CD13 (hCD13) and the crystal structure of APN from *E. coli* have been published.[169–172] The domain has a typical seahorse like shape, with four different regions that form dimers. The most important, zinc-dependent catalytic region contains a wide opening that can better interact with the peptide substrates, so being potentially exposed to proteins.[173]

1.6 NGR peptides for tumor targeting

A growing body of evidence suggests that CD13 plays an important role in NGR-peptide homing to the tumor vasculature.[67,155,174,175] The NGR sequence (**Figure 9**) was first discovered by injecting phage peptide libraries into nude mice bearing human breast carcinoma xenografts.[58,176] A huge variety of different compounds have been coupled to NGR peptides by different investigators, with good results.

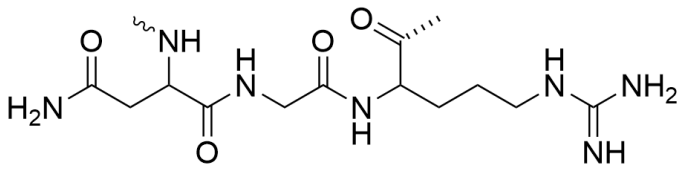

Figure 9: Structure of linear Asn-Gly-Arg

Since the cyclic scaffold is more stable and has higher stability, those studies are mostly focused on the cyclic versions. [153,175] It is important to mention that these molecules rely on the use of different peptide sequences having the NGR (Asn-Gly-Arg) inserted into different scaffolds, such as disulfide-bridged CNGRC (**Figure 10**), acetylated-CNGRC, linear GGCNGRC, CVLNGRMEC, CNGRCGK, and the head-to-side chain cyclized cKNGRE (**Figure 10**) and many others.[177] Constructs are generally chemically ligated and attached to proteins or in some cases even incorporated in the protein itself. Linear NGR has shown successful accumulation in APN-positive lung carcinoma tumors, indicating that despite their lower stability the sequence can be effective in certain cases.[178] Cyclic CNGRC and linear GNGRG motifs have been applied successfully for targeting tumor necrosis factor alpha (TNF-α) and interferon gamma.[176,179–181] This fusion protein (TNF-α-NGR) is currently being evaluated in phase III trials for the treatment of pleural mesothelioma[182], advanced solid tumors and metastatic colon cancer.[183]

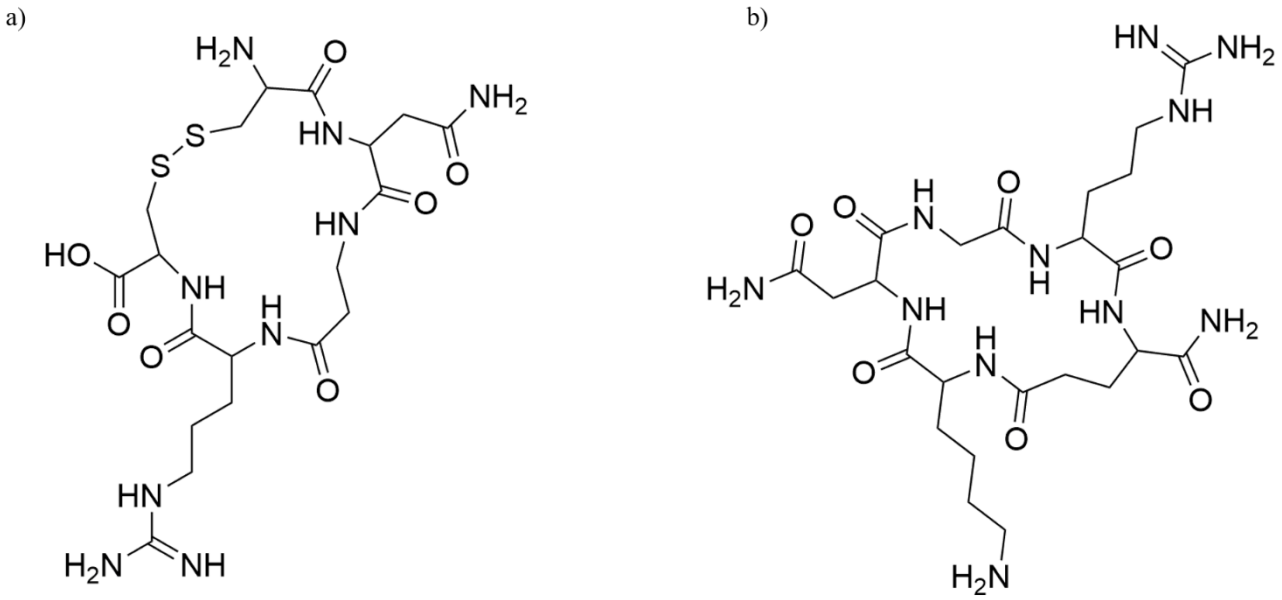

Figure 10: Nonreactive peptide-based APN-targeting agents: (a) cCNGRC; (b) cKNGRE.

It is important to highlight that different molecular scaffolds of NGR might lead to the generation of CD13 ligands with different biochemical, biological and toxicological properties, suggesting that different flanking residues can affect NGR affinity and selectivity for CD13.[184] In fact it has been demonstrated that the affinity of CNGRCG peptide for CD13-positive endothelial cells is higher than that of linear GNGRGG.[177] Cyclic CNGRC is susceptible to biodegradation due to the disulfide bond, for this reason a new targeting unit was developed that lacked the disulfide bridges. According to literature data, one of the most stable and tumor-selective cyclic NGR-peptides is cKNGRE in which the α-amino group of the *N*-terminal Lys is coupled to the γ-carboxyl group of the glutamic acid residue. *In vitro* fluorescence microscopy studies of an Oregon Green (OG) labeled cKNGRE, where OG is attached to the side chain of lysine revealed selective binding to CD13-receptor positive HT1080 human fibrosarcoma cells and minimal to receptor negative MCF-7 human breast adenocarcinoma cells.[185] Moreover, a ^{68}Ga-radiotracer labeled derivative of the cyclic KNGRE and

cyclic CNGRC has been successfully used for tumor diagnostic studies by positron emission tomography (PET), indicating its specific binding to CD13 receptor expressing tumor tissue.[174,186] Cytotoxic drugs have been successfully ligated to NGR peptides, for instance, a conjugate made of doxorubicin and the cyclic CNGRC peptide was less toxic and more effective against human cancer xenografts in nude mice than free doxorubicin.[187] Other payloads have been coupled to NGR like platinum[188], carboplatin[189], 5-fluorouracil prodrug[190] and most importantly daunorubicin *via* oxime linkage used in this study.[66,67,72,175] A chemotherapeutic drug chlorambucil (CLB), was ligated to a cyclic CNGRC and conjugated to a chelator for radiolabeling with ^{99m}Tc. The targeted probe shows an inhibition of cancer cell proliferation, and its high hydrophilicity could lead to a rapid clearance from the body[191], by the addition of this probe to a PEG2 linker no change was shown.[192] These results indicate that it is possible to improve the therapeutic index of several cytotoxic drugs following the NGR-targeting approach. It is well known that the NGR sequence, has a strong propensity to undergo deamidation of Asn side chain.[193–196] This process can activate important pharmacological and toxicological repercussions as Asn can easily form (*iso*Asp or *iso*D) derivative. The process of deamidation occurs by nucleophilic attack of the back bone NH (Gly) center at the carbonyl group of Asn side chain, which brings the formation of a five ring member succinimide.[197,198] The same step is then followed by fast hydrolysis that can occur at both carbonyl groups of the cyclic imide leading to the formation of *iso*Asp and Asp residues (**Figure 11**), this happens usually with a ratio of 1:3 (DGR:*iso*DGR).[193–196] It is very important to say that the speed of this process can be addressed to many reasons, but the main one is the presence of a glycine residue that follows asparagine, this sequence can often accelerate this reaction[199–201], otherwise the process itself is much slower.

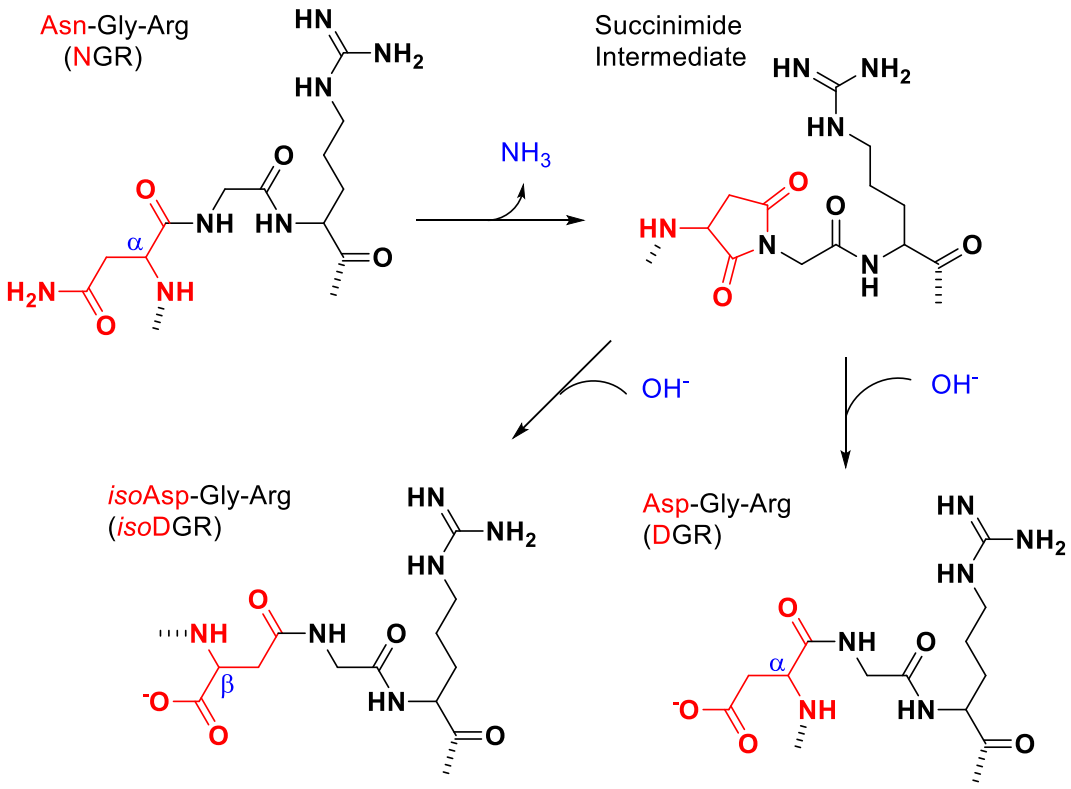

Figure 11: Schematic representation of the intramolecular deamidation process at neutral pH, the peptide bond nitrogen of the N +1 amino acid attacks the carbonyl carbon of the asparagine side chain forming a five-membered ring structure referred to as a succinimide or cyclic imide. The succinimide is then rapidly hydrolyzed at either the alpha or beta carbonyl group to yield *iso*-aspartate and aspartate.

At acidic pH (<2), direct hydrolysis of the side chain can occur with the generation of aspartate as the only product, on the other hand the exposure to alkaline pH results in an increased rate of deamidation due to greater deprotonation of the peptide bond nitrogen that increases its nucleophility resulting in easy succinimide formation. Solvent properties also can partially influence the deamidation process.[202,203] Thus, different asparagines in a protein may show high variability in their deamidation kinetics. Moreover, temperature-induced loss of function in proteins could be influenced by the amount of deamidation in that specific peptide/protein. Even if the process of deamidation tipically causes a loss of function, it is fundamental to say that in the case of NGR, the formation of the *iso*DGR derivative is highly important. This derivative in fact can mimic RGD, an integrin

recognition motif, and recognize the RGD-binding site of integrins, such as $\alpha_v\beta_3$, $\alpha_v\beta_5$, $\alpha_v\beta_6$, $\alpha_v\beta_8$ and $\alpha_5\beta_1$.[192,194,195] *Iso*DGR is a natural ligand for the RGD-binding pocket especially for $\alpha_v\beta_3$ integrin.[137,204–206] Notably, those receptors (also known as the vitronectin receptor) appear to be the most important among all integrins regarding cell proliferation, invasion and angiogenesis.[207] This integrin is overexpressed on activated endothelial cells, new-born vessels and other tumor cells, making it a suitable target for anti-angiogenic therapy.[136,157] It is very important to stress the concept that $\alpha_v\beta_3$ and CD13 are tumor biomarkers and thus, the combination of *iso*DGR derivative (derived from Asn deamidation) and NGR can simultaneously bind to the target tissue, which for obvious reason would enhance the incorporation of the cytotoxic agent, obtaining the so called dual-targeting effect. Lately, an amide bond containing cyclic NGR peptide (Dau=Aoa-GFLGK(c[KNGRE]-GG)-NH_2) with higher resistance against succinimide formation has been described, in which cargos such as fluorescent labels or chelated ^{68}Ga for PET were attached to lysine side chain. In the Research Group of Peptide Chemistry (RGPC), several cyclic NGR peptides with thioether linkage were developed. Compared to the amide bond or the disulfide bridge, the enzyme stability of the thioether linkage is significantly higher and it can be formed more easily. Additionally, it was suggested that the conjugates with thioether linkage have a lower chemostability to deamidation compared to the previously mentioned disulfide and amide bond containing versions. However, the deamidation process is highly altered by the structure of the cyclic peptides.[175,208]

1.7 Linker strategies

One of the most important and crucial aspect to be considered in case of an ADC or SMDC is the design of a linker which is the connection between the cytotoxic payload as an active drug/prodrug and the ligand scaffold. The linker has to be carefully chosen to avoid any drawbacks in binding affinity to the target receptors. Using the wrong linker may obstruct the release of the drug inside the cell, and by doing so decrease the therapeutic potency. The design of a linker is not an easy task, it is always fundamental to keep in mind important aspects like stability, length, functional groups, and hydrophobicity/hydrophilicity.[71] Acid-labile linkers for example could be hydrolyzed in the slightly acidic environment and allow the drug to be released inside the tumor cell (in particular imine, oxyme under pH 2, and hydrazone which are stable in blood circulation). Another important class is the stimuli-responsive linkers which are cleaved when there is a specific signal (like ultrasound, temperature), and the exposure to radiation can also trigger the same effect leading to drug release in the tumor tissue.[209,210] The third important class of linkers are the enzymatically cleavable linkers that rely on the drug activation realized by different enzymes overexpressed on cancer cells (*i.e.*, proteases or glycosidases), especially those influenced by proteases that have been studied intensively and the most representative members are the MMP-2/9 (matrix metalloproteinases) and the cathepsin B peptide substrates. MMPs and cathepsin B are important proteolytic enzymes, they are predominantly expressed in cancer cells, and they are well known to take part in human tumor invasion and metastasis. Cathepsin B is able to specifically recognize peptide sequences like Val-Ala (valine-alanine), Val-Cit (valine-citrulline)[211] and GFLG (glycyl-penylalanyl-leucyl-glycine) tetrapeptide sequence[212–214]; this last one has been widely used as a linker in the development of peptide-drug conjugates (**Figure 12**).

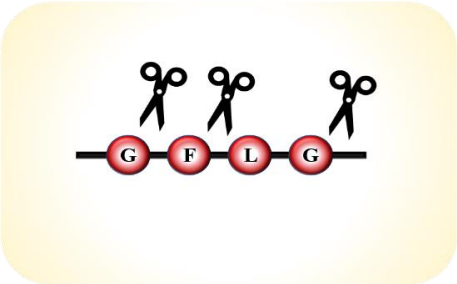

Figure 12: Tetrapeptide spacer GFLG containing the enzymatically cleavable portions essential for the drug release.

The cleavage sites of the GFLG linker were reported to be the amide bond between F, L, and also G and F, and the amide bond after the *C*-terminal G.[67,175]

1.8 Cytotoxic payloads

According to the National Cancer Institute (*cancer.gov*), there are more than 250 FDA-approved anticancer drugs utilized to treat malignancies at the moment. Among this large pool of cytotoxic drugs, an array of them has been utilized as toxic vehicles for SMDCs and ADCs and some of the most important representatives are doxorubicin, daunorubicin, camptothecin and gemcitabine (**Figure 13**). The main feature, side effect of these drugs is their high toxicity effects which result in a very narrow therapeutic window and consequently in very low compliance for treated patients. The addition of the targeting moiety is crucial, as without it, the used drug does not distinguish between cancer cells and normal healthy cells. Furthermore, the linkage of a peptide as a ligand can ameliorate the pharmacokinetic properties and widen the therapeutic window of the drug itself. Every drug has a specific mechanism of action and a way to be conjugated, they must contain specific functional groups for conjugation with the peptide, usually an enzymatically cleavable linker. It is fundamental in fact that the conjugation site chosen does not alter the biological activity, neither the release of the active drug or active metabolite. The selected payload needs to be potentially active at low-nanomolar IC_{50} values on

cancer cells. The most common problem is the low potency of the drug, this may occur when the drug is released not in its free form, this important issue can be solved by the loading of several drug molecules of the same carrier compound, however, this is a challenging step and not always feasible due to poor physicochemical characteristic of the constructs.

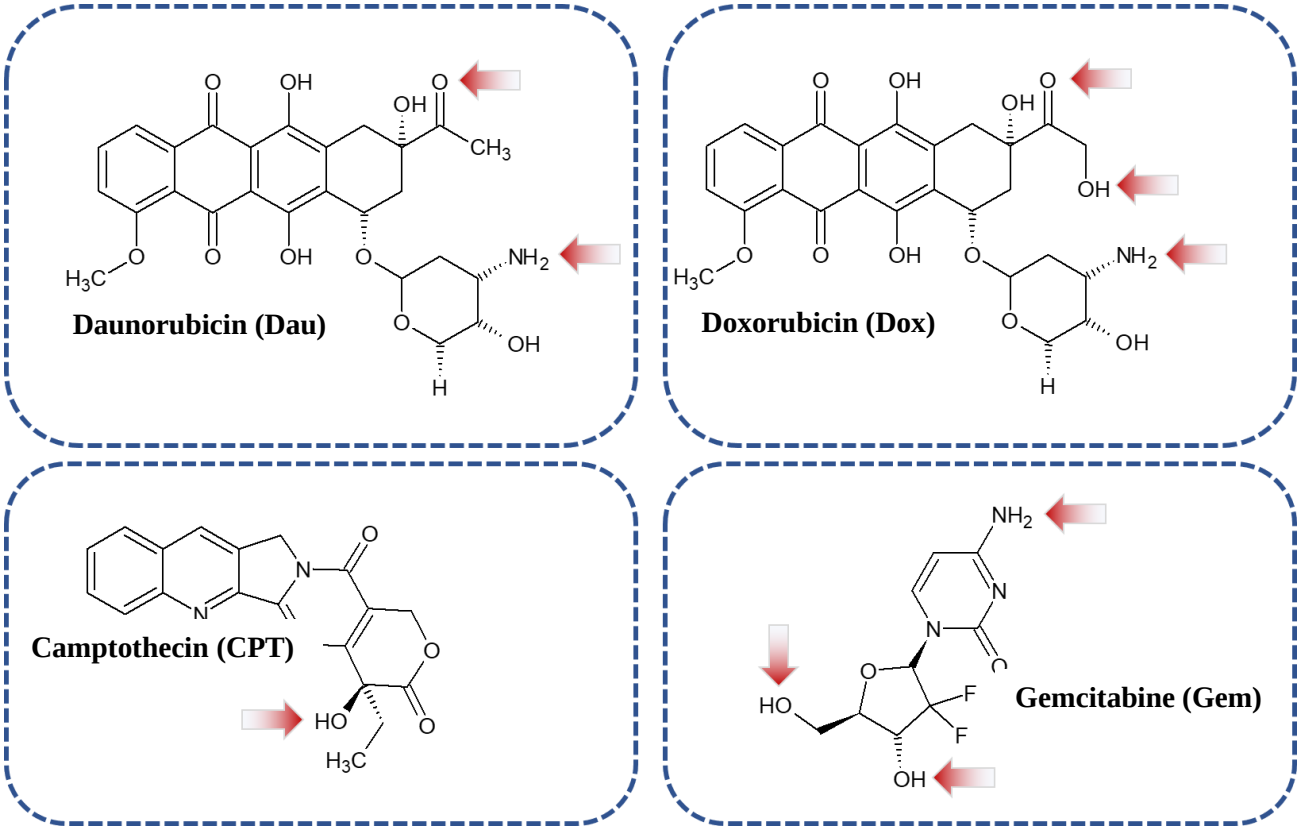

Figure 13: Anticancer drugs used for the synthesis of SMDCs. The most common functional groups used for the conjugation reaction are marked with arrows.

Gemcitabine is used for the treatment of various cancers including breast, ovarian and pancreatic cancer, its main disadvantages are high systemic toxicity and hydrophobicity, multidrug resistance (MDR).[215] It enters cells through nucleoside transporters and after internalization is phosphorylated by kinases.[216,217] Those phosphorylated forms can actively intercalate into the DNA during polymerization and stop cell proliferation.[218] The other drug often used in SMDCs is camptothecin (CPT), first

discovered by Wall *et al*. 1966.[219] Camptothecin forms a stable ternary complex, preventing normal DNA re-ligation, and causes the complex to collide with the replication fork, leading to a DNA double-strand break and cytotoxicity.[219–221] CPT can be conjugated to targeting elements to enhance its efficacy *via* its primary alcohol marked in (**Figure 13**). Considering its low water solubility, new analogs have been proposed with same mechanism of action, topotecan and irinotecan are both approved by FDA for the treatment of different types of tumors. CPT works as an anticancer drug in combination with targeting peptides like somatostatin derivative and c(RGDyK).[222,223] Daunorubicin (Dau) and doxorubicin (Dox) are the parent compounds of anthracycline antibiotics. Anthracyclines are among the main anticancer drugs that are applied in combination with other chemotherapeutic agents. Mostly isolated from natural sources (*Streptomyces peucetius*)[224], they are extensively used for the treatment of cancer and are widely investigated as cytotoxic agents conjugated to tumor homing peptides.[67,71,175]

Anthracyclines consist of a tetracyclin aglycon part and a daunosamine sugar moiety. They are very effective but also very toxic, leading to cardiotoxicity.[225,226] The main difference between Dau and Dox is a hydroxy group substituted at the C-14 carbon atom on Dox providing an extra conjugation site for ester linkage. Despite this small structural difference, their activity spectrum is not the same. Dox has significant applications on solid tumors[117–119] while the main indication for Dau is acute leukemia.[227] The mechanism of action of anthracyclines is based on their DNA intercalation ability inhibiting the macromolecular biosynthesis.[228] Numerous results have indicated topoisomerase II as its main target. This nuclear enzyme relaxes DNA by forming a phosphodiester bond between the OH group of its active-site tyrosyl residue and the phosphoric group of DNA, allowing the free end of nucleic acid to rotate. Hydroxy groups can now restore the continuity of the helix by attacking the activated phosphate.[118] By intercalating the DNA, they stabilize topoisomerase II preventing transcription.

2. Aims and objectives

Therapeutic peptides are a promising and powerful approach to treat many diseases including cancer. Usually cyclic peptides show better biological activity compared to their linear counterparts due to their conformational rigidity. They have several advantages over proteins or antibodies as they are easy to synthesize, have a high target specificity, selectivity and low toxicity. Among various homing devices, peptides containing the NGR (L-asparaginyl-glycyl-L-arginine) tripeptide sequence represent a promising approach to selectively recognize the Aminopeptidase N (CD13) receptor isoforms overexpressed in tumor neovasculature. There are several examples in both linear and cyclic NGR peptides, but as a general rule, small cyclic NGR peptides are superior in terms of selectivity than their linear forms. The project is based on the observation that the expression of CD13 is up-regulated in endothelial cells within mouse and human tumors especially on neovasculature to which NGR peptides can bind efficiently. One of the most stable and tumor selective cyclic NGR-peptide is c[KNGRE]-NH_2, in which the α-amino group of the *N*-terminal Lys is coupled to the γ-carboxyl group of the glutamic acid residue (head-to-side chain cycle).[175] Due to this fact, the central goal of the present work was the development and evaluation of efficient NGR-based drug delivery systems for targeted tumor therapy. Additionally, certain key aims have been defined:

Improvement of the antitumor activity of oxime bond-linked NGR-Dau conjugates:

- synthesis and characterization of oxime bond-linked NGR-Dau conjugates with various amino acids in the sequence, using solid phase peptide synthesis (SPPS) and ligation of Dau in solution;

- evaluation of the cytostatic effect of the compounds on CD13 and integrin expressed on human Kaposi's sarcoma, fibrosarcoma and colon cancer cells in comparison to cyclic KNGRE peptide Dau conjugate by cell viability assays;
- additional analyses of (best) candidates to analyze the cellular uptake (by flow cytometry) and localization (by confocal laser scanning microscopy (CLSM)), stability in plasma and in presence of lysosomal enzymes (by LC-MS assay);
- establishment of a suitable tumor model and evaluation of the activity, selectivity and toxicity on animals. Additionally, considering the great importance of those bioconjugates in angiogenesis, the proliferation and vascularization index was planned to be evaluated *ex vivo* on all the tumor samples.
- development of new cyclic NGR peptides using 2,5-diketopiperazine (DKP) scaffold, and the study of their stability against deamidation.

3. Results and discussion

3.1 NGR as targeting moiety and daunorubicin as cytotoxic payload

In this work, the NGR derivatives were concepted in the RGPC laboratory by developing a unique synthetic route for these conjugates targeting mainly the CD13 receptor, those conjugates were ligated with daunorubicin as cytotoxic payload. A new library of cyclic bioconjugates have been synthesized and characterized by using the Dau=Aoa-GFLGK(c[KNGRE]-GG)-NH_2 peptide drug-conjugate as a reference which shows the best resilience against deamidation.[67,175] The main goal of this work was to replace lysine present inside the cyclic moiety with a variety of amino acids with diverse characteristics: alanine, leucine, norleucine, proline and serine were chosen to form five novel different peptide drug-conjugates with different propensity in terms of stability and biological activity. Those amino acids were chosen considering their different nature in terms of hydrophilicity/hydrophobicity and flexibility. The main advantage in replacing the lysine in the cyclic scaffold is the avoidance of the removal of the protecting group from the ε-amino group of lysine, usually an Fmoc group, which brought to a longer synthetic route with decreased yield. Considering the fact that the attachment of the drug at the sugar moiety causes a drastical decrease in the activity, it could be concluded that daunorubicin has an important part in the interaction with DNA[229,230]; hence, to ligate the toxic drug to the peptide, the amide bond formation with the amino group of the sugar was not feasible without the contemporary drastic loss of activity. Considering its structure, daunorubicin cannot be attached to the targeting moiety by ester bond like doxorubicin but the carbonyl group allows the formation of oxime bonds originating conjugates with high stability under physiological conditions. For the preparation of the bioconjugates an enzymatically cleavable linker, the tetrapeptide Gly-Phe-Leu-Gly (GFLG), well known for its high stability in plasma, was added to

allow the release of the drug after cleavage by enzymes (*e.g.* Cathepsin B) overexpressed in tumor cells.[231,232] It has been shown that the release of the free drug is not essential for the antitumor activity of the conjugates since the smallest releasing Dau=Aoa-Aaa-OH metabolite can also bind to the DNA with satisfactory efficiency.[233] By using this strategy, it was possible to obtain fair selectivity with a small loss in activity compared to the free highly toxic drug.

3.1.1 Synthesis of cyclic NGR-Dau conjugates

All derivatives, linear precursors were synthesized by SPPS on a Rink-Amide MBHA Resin, using Fmoc/tBu strategy. In all conjugates the enzyme labile spacer GFLG with isopropylidene protected aminooxyacetyl moiety was built up using a Fmoc-Lys(Mtt)-OH, as the *C*-terminal amino acid derivative attached to the resin. The isopropylidene protected aminooxyacetyl moiety is stable under the conditions of synthesis and removal from the solid support. The following step was the deprotection of the Mtt as lysine side chain protecting group. After removal of the Mtt two glycines were attached that are essential to increase the flexibility of the construct by giving some distance between the tetrapeptide cleavable spacer and the cyclic ligand. The anticancer drug daunorubicin was conjugated to the Aoa-GFLGK spacer *via* oxime linkage.[175] The GFLG spacer is degraded by lysosomal enzymes ensuring the release of the Dau=Aoa-Gly-OH as the smallest bioactive metabolite in lysosomes.[233] It is well known from our previous findings that not only the free Dau but also Dau containing metabolites like Dau=Aoa-Gly-OH bind to DNA efficiently resulting in antitumor activity. The substitution of the Lys in the cycle simplified the cyclization step and due to the avoidance of the Fmoc cleavage in solution (**Figure 14**) the compounds could be obtained with an easier synthetic route in higher yields compared to the control (**1**). Isopropylidene protected aminooxyacetyl moiety was used to avoid unwanted reactions with aldehydes or ketones. This protecting group was removed

with 1 M methoxylamine in 0.2 M NH_4OAc buffer solution (pH 5.0) prior to the Dau conjugation. The final cyclic NGR peptide ─ Dau conjugates were characterized by analytical HPLC and mass spectrometry, whereby the purity was over 95% in all cases. In comparison with the control conjugate (**1**) significantly higher overall yield was observed in the case of conjugates **2**, **3**, **4**, **5** and **6** (**Table 1**). The improvement was observed especially in the cyclization step that might be explained by the absence of bulky protecting group on amino acids used instead of lysine. ESI-MS spectra are shown on **Figure 29-33** in Appendix.

Table 1: List of the synthesized peptide drug-conjugates

Code	Compounds	Yield[a] (%)	RP HPLC R_t (min)[b]	ESI-MS[c] M(*calc*)/M(*exp*)
1	Dau=Aoa-GFLGK(c[KNGRE]-GG)-NH_2	2.0	23.0	1783.6/1783.0
2	Dau=Aoa-GFLGK(c[NleNGRE]-GG)-NH_2	10.6	22.6	1767.8/1767.2
3	Dau=Aoa-GFLGK(c[ANGRE]-GG)-NH_2	2.2	22.2	1725.8/1725.8
4	Dau=Aoa-GFLGK(c[LNGRE]-GG)-NH_2	7.0	22.4	1767.8/1767.4
5	Dau=Aoa-GFLGK(c[PNGRE]-GG)-NH_2	6.2	17.3	1751.1/1751.4
6	Dau=Aoa-GFLGK(c[SNGRE]-GG)-NH_2	1.8	20.1	1741.9/1741.7

[a]The overall yield was calculated for the starting amount and capacity of the resin. [b]HPLC: KNAUER 2501; column: Phenomenex Luna C18 (250 mm x 4.6 mm, 5 µm silica, 100 Å pore size; gradient: 0 min 0% B; 5 min 0% B; 50 min 90% B; eluents: A) 0.1% TFA/water, B) 0.1% TFA/MeCN-H_2O (80:20, v/v); flow rate: 1 mL/min; detection: λ=220 nm. [c]ESI-MS: Bruker Daltonics Esquire 3000+ ion trap mass spectrometer; spectra were acquired in the 50-2500 *m/z* range.

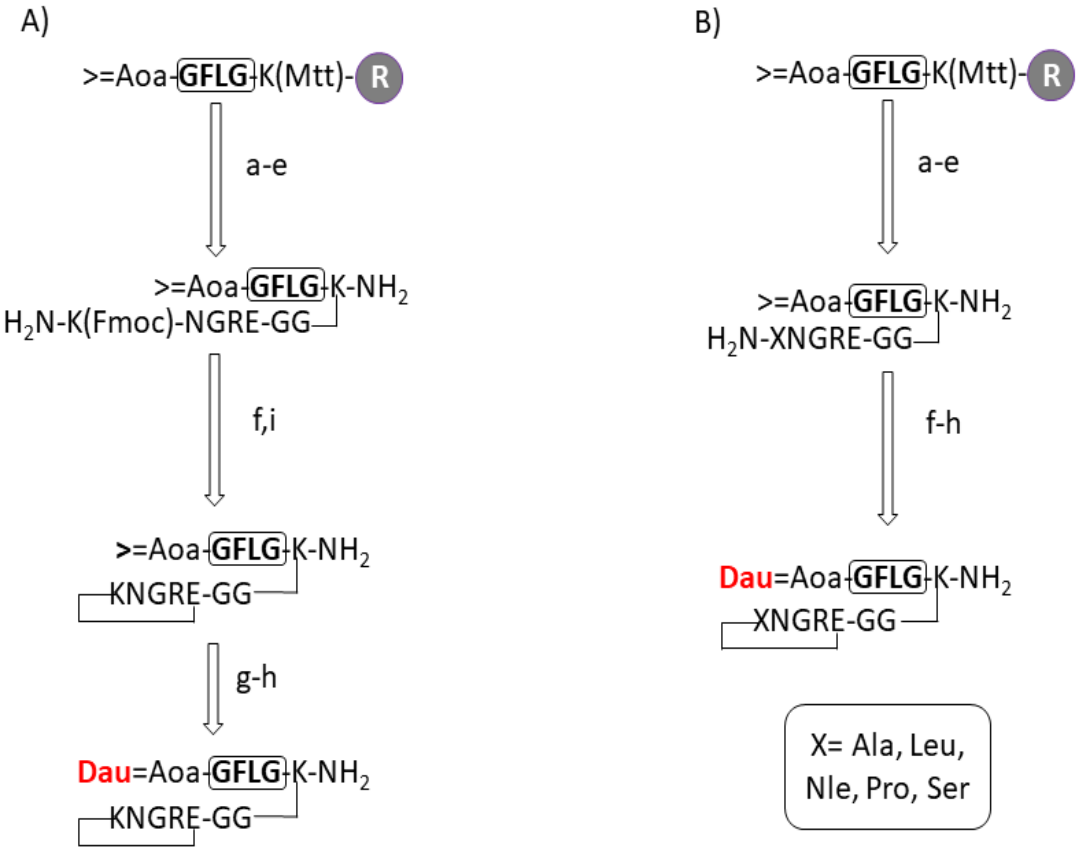

Figure 14: Schematic representation of the synthesis of cyclic KNGRE (A) and XNGRE (B) drug-conjugates. a) Mtt-cleavage: 2% TFA/DCM; b) Fmoc-Aaa(X)-OH coupling; c) Fmoc-cleavage 2% piperidine/2% DBU/DMF, 0.1 M HOBt; d) cleavage from resin 2.5% TIS/ 2.5% H_2O/ 95% TFA (RT, 3 h); e) salt exchange Pyr.HCl 10 eq/MeOH (1h); f) cyclization: BOP 3 eq/HOBt 3 eq/DIPEA 6 eq/DMF (c=0.5 mg/mL, RT, 24 h); g) deprotection of aminooxyacetic acid 0.2 M NH_4OAc solution (pH 5.0)/1 M methoxylamine (RT, 1 h); h) daunorubicin conjugation (RT, 24 h) in 0.2 M NH_4OAc solution (pH 5.0); i) Fmoc-cleavage 4% hydrazine/DMF (RT, 2 h).

3.2 Stability of cyclic NGR peptide-daunorubicin conjugates in cell culture medium

Chemical stability of cyclic NGR bioconjugates was investigated under the treatment conditions used for the *in vitro* cytotoxicity experiments. Samples were analyzed at 0 min, 6 h and 72 h. Deamidation rate was evaluated by HPLC-MS. In contrast to the (lysine containing) control conjugate that showed high stability in our previous study, the novel conjugates rearranged in time. The results presented similar *iso*Asp/Asp (~3:1) rates after deamidation of conjugates **2**, **3**, **4**, **5** and **6** calculated from the area under the curve (AUC) see Appendix (**Figures 34-38**). After 6 h, reasonable rearrangement was observed which increases over time. Nevertheless, 54-58% of the parent cyclic NGR conjugates was still intact after 72 h (**Table 2**). Decreased stability was detected in the case of the Pro-containing conjugate (**5**) with faster deamidation and higher ratio of DGR. Except deamidation no other decomposition could be observed during the entire execution of the study.

Table 2: Stability of cyclic NGR peptide-Daunorubicin conjugates

Ratio of Asn-/Asp-/*iso*Asp-derivatives (DMEM CM, 37 °C)							
Code	**Aaa in position X of the conjugates**	**6 h**			**72 h**		
		NGR	**DGR**	***iso*DGR**	**NGR**	**DGR**	***iso*DGR**
1	Lys	100	0	0	100	0	0
2	Nle	93	1	6	58	9	33
3	Ala	96	0	4	58	11	31
4	Leu	93	0	7	54	11	35
5	Pro	73	14	13	19	46	35
6	Ser	93	0	7	56	12	31

3.2.1 Degradation of NGR peptide-daunorubicin conjugates in lysosomal homogenate

For medical compounds it is extremely important to understand and study the metabolic processes that lead to the degradation and elimination of the active substance from the body. The drug-containing peptide-conjugate may release the free drug in the living organism, but upon degradation other drug-containing metabolites may also be formed producing a different biological effect from the effect of the parent drug. An important aspect is, therefore, the detailed knowledge of the enzyme-induced release of the active species. In the assay that was carried out during the study, the degradation of the conjugates was investigated with lysosomal enzymes. Naturally, bioconjugates need to be processed in the cells, particularly in lysosomes, in order to release the free drug or to generate drug-containing metabolites displaying antitumor activity. The stability and degradation processes of the peptide conjugates were investigated in the presence of a rat liver lysosomal homogenate incubated at 37 °C. The main disadvantage of this process was the inability to exactly determine the proteolytic activity of the homogenate, so the protein content of the lysosomal homogenate was used as reference: the weight ratio of conjugate and lysosomal proteins was 1:1 in the reaction mixture. Due to the enzyme activity, it was possible to see the action of the enzymes even after 5 minutes. The original conjugates were still present in the reaction mixture, but their degradation started in a short time. Metabolites were detectable in the chromatogram, which were identified based on their molecular weight. During the measurements, it was found that the glycine-lysine bond is cleaved first in the tested compounds forming the drug-containing metabolite Dau=Aoa-GFLG-OH (this is the same for all five conjugates). In addition, the respective cyclopeptide-containing moieties could be also detected. (**Table 3**).

Table 3: List of metabolites detected during the experiment after 5 minutes incubation and their analytical characterization.

Metabolite	Conjugate	M_{calc} **([M+H]$^+$)**	M_{meas} **([M+H]$^+$)**	t_r / min
H-K([NleNGRE]cyclicGG)NH_2	**2**	810.5	810.6	7.5
H-K([ANGRE]cyclicGG)-NH_2	**3**	768.8	768.6	2.1
H-K[(LNGRE)cyclicGG]-NH_2	**4**	810.5	810.6	7.6
H-K([PNGRE]cyclicGG)-NH_2	**5**	794.4	794.6	6.2
H-K([SNGRE]cyclicGG)-NH_2	**6**	784.6	784.4	1.9
Dau=Aoa-GFLG-OH	**All**	974.4	974.4	20.7
Dau=Aoa-GFL-OH	**All**	917.4	917.5	21.3
Dau=Aoa-GF-OH	**All**	804.3	804.3	20.1
Dau=Aoa-G-OH	**All**	657.2	657.3	18.0

The results exhibited that all bioconjugates fragmented within the time range used for the experiment with a maximum of 72 h (end of the study) see in the Appendix (**Figures 39-48**). No free daunorubicin was detected by LC-MS, indicating substantial chemical and enzymatic stability of the oxime bond, some sugar (daunosamine) loss of Dau was detected due to the experimental MS conditions. The smallest drug containing metabolite generated in case of all bioconjugates in the presence of lysosomal enzymes and identified by ESI-MS was Dau=Aoa-Gly-OH (*m/z*: 657.2). The core cleavage site of the conjugates could be detected between Gly-Phe within the enzyme labile spacer. No substantial alteration in degradation speed of the conjugates was observed. Therefore, we concluded that the replacement of lysine has no influence on the biological activity through the lysosomal degradation.

3.2.2 Stability of NGR peptide-daunorubicin conjugates in sodium acetate solution

In addition to *in vitro* degradation assays, it is important to investigate the stability of the tested compounds under the experimental conditions. To verify this, control samples were prepared without the presence of the lysosomal enzymes, only the bioconjugate and sodium acetate solution. The mixture was then allowed to incubate and samples were periodically measured using HPLC-MS. The findings from the study confirm that the bioconjugates were stable under the experimental conditions that were used (37 °C, pH 4.8 sodium acetate solution) and did not degrade. Chromatograms of the conjugates are shown in the Appendix (**Figure 49**), (leucine containing) by HPLC-MS measurements are shown in (**Figure 15**) below.

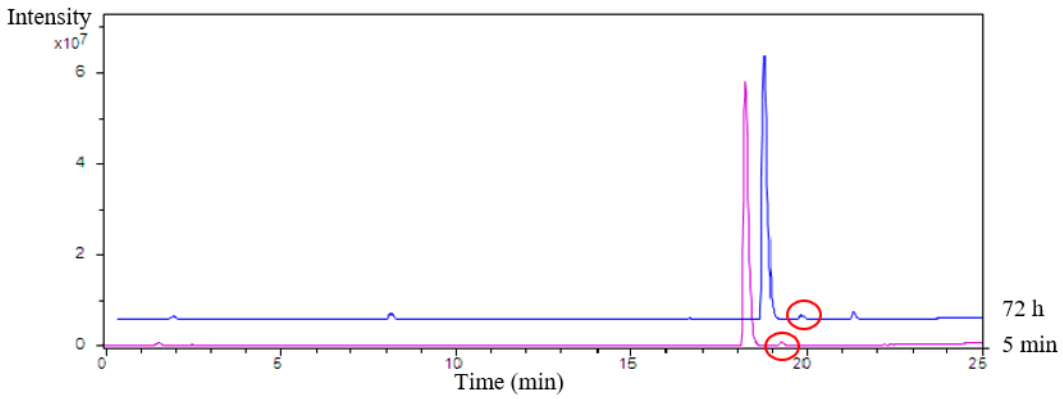

Figure 15: Control samples of conjugate **4**: The LC-MS base peak after 5 min and after 72 h incubation (37 °C, pH=4.8, 0.2 M sodium acetate solution).

The chromatograms show that no new components appeared in the sample injected between 5 minutes and 72 hours of the experiment, and the amount of conjugate did not decrease. Although contaminants could be detected with low intensity, it is important to mention that those impurities were also present in the original sample. Thus, those findings prove that the all compounds are stable under the experimental conditions.

3.3 In vitro studies of NGR peptide-daunorubicin conjugates

The antitumor effects of bioconjugates were examined *in vitro* on CD13(+) HT-1080 human fibrosarcoma and on CD13(−) HT-29 human colon adenocarcinoma cells. Both cell types are integrin receptor positive.[234,235] The effect of the new drug-conjugates was associated with the toxicity of free payload and our lead compound Dau=Aoa-GFLGK(c[KNGRE]-GG)-NH_2 (**1**). The bioconjugates enter cancer cells most likely by receptor-mediated endocytosis (at least at lower micromolar concentration) followed by the release of the active metabolite Dau=Aoa-Gly-OH by lysosomal degradation. In contrast, free Dau enters the cells in an unspecific manner which might explain the lower antitumor effect of conjugates in comparison with the free drug. In this experiment we evaluated the cytostatic effect (6 h treatment and further 66 h incubation after washing out of the compounds) and the cytotoxic effect (72 h treatment). The results are shown in **Table 4**. In contrast to compound **1** that is taken up by HT-1080 cells slightly more efficiently than by HT-29 and therefore shows higher antitumor effect against CD13(+) cells, the novel bioconjugates showed higher cytostatic/cytotoxic effects on the CD13(−) HT-29 colon cancer cells. It seems that the replacement of Lys by the hydrophilic amino acid Ser is not favored. However, the incorporation of hydrophobic amino acids was well accepted. The conjugate with bulky side chain in this position (Leu) had higher IC_{50} values that might be explained by steric hindrance. The bioconjugates with Ala or Nle showed the best antitumor activity on both cell lines. The Nle containing compound showed similar activity on HT-1080 and higher activity on HT-29 cells compared to the control conjugate **1**. It is important to mention that Nle has linear hydrocarbon side chain with the same length as Lys, but the amino functional group is not present on the side chain. To further characterize the biological activity of the conjugates, their lysosomal degradation and cellular uptake were also investigated.

Table 4: *In vitro* cytostatic/cytotoxic effects of compounds on HT-29 and HT-1080 cells

Compounds	HT-1080 (6 h) IC_{50} (μM)	HT-29 (6 h) IC_{50} (μM)	HT-1080 (72 h) IC_{50} (μM)	HT-29 (72 h) IC_{50} (μM)
Daunorubicin	1.4 ± 0.6	0.3 ± 0.2	0.5 ± 0.2	0.1 ± 0.1
Dau=Aoa-GFLGK(c[KNGRE]-GG)-NH_2 (1)	5.7 ± 0.5	8.7 ± 1.2	1.4 ± 0.7	3.0 ± 0.6
Dau=Aoa-GFLGK(c[NleNGRE]-GG)-NH_2 (2)	5.5 ± 0.3	2.2 ± 0.2	2.3 ± 0.6	1.3 ± 0.2
Dau=Aoa-GFLGK(c[ANGRE]-GG)-NH_2 (3)	8.9 ± 0.8	4.3 ± 0.5	3.6 ± 0.7	3.2 ± 0.8
Dau=Aoa-GFLGK(c[LNGRE]-GG)-NH_2 (4)	57.5 ± 6.3	47.0 ± 5.4	20.6 ± 0.4	14.1 ± 0.7
Dau=Aoa-GFLGK(c[PNGRE]-GG)-NH_2 (5)	9.4 ± 4.0	14.6 ± 4.7	3.5 ±1.0	3.7 ± 0.8
Dau=Aoa-GFLGK(c[SNGRE]-GG)-NH_2 (6)	>100	64.7 ± 4.9	63.7 ± 9.5	39.4 ±2.9

In this study our goal was to compare the *in vitro* antitumor activity of the conjugates. We believe that the measurement of binding affinity on isolated receptors, that was not task of this experiment, could not have properly explained the efficiency and selectivity. The receptor profile of both cell types is very complex. HT-1080 cells express different integrins (RGD, collagen, etc) next to CD13 receptor[236], HT-29 cells express all the known β_1 RGD dependent receptors furthermore $\alpha_v\beta_3$, $\alpha_v\beta_5$, $\alpha_v\beta_6$, $\alpha_v\beta_8$.[237] Most of the mentioned integrins bind *iso*DGR peptides with different affinity from nM up to μM concentration that depends on the structure of the peptide.[204] Furthermore, there is only a few binding affinity study for CD13 suggesting several hundred nM IC_{50} values for NGR peptide derivatives.[238] The biological activity of NGR and *iso*DGR peptides might be influenced also by the amount of the different receptors on the tumor cells, which is not easy to detect in case of such complex receptor profile. Therefore, *iso*DGR derivatives might provide similar activity both on CD13(+) and CD13(−) cells.

3.3.1 Cellular uptake studies

Daunorubicin is used for the tratment of different types of cancer including lymphoma, bladder, stomach, breast, prostate and several others.[239] This compound contains a tetrahydroxy-anthraquinone, a six-member daunosamine sugar with a hanging glycosyl moiety, essentially representing the structure of anthracycline antibiotics.[240–242] Daunorubicin has intrinsic fluorescence which can be used as a valuable tool in cancer imaging and research.[243,244] The cellular uptake of Dau containing conjugates can be followed by flow cytometry (**Figure 16**). The accumulation of conjugates **2**, **4** and **5** increased significantly higher in HT-29 cells than HT-1080 in comparison with the other conjugates. The low cytostatic/cytotoxic effects of conjugate **6** can be deducted by the results of cellular uptake study. The Ser-containing conjugate did not enter HT-1080 cells, while a slightly higher cellular uptake was detected in HT-29 cells, although the uptake for this conjugate was still much lower than in the case of the other tested bioconjugates.

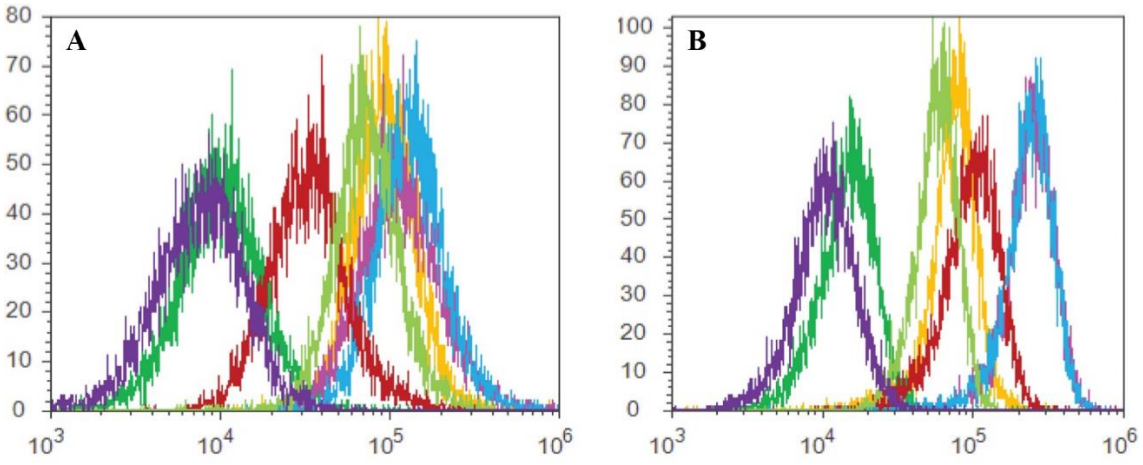

Figure 16: Direct uptake of Dau of conjugate **1** (yellow); **2** (light blue) **3** (light green); **4** (red); **5** (pink); **6** (green) by (A) HT1080 and (B) HT-29 cells, using 10 µM conjugate for each sample. Untreated control is marked with purple detecting the autofluorescence of the cells.

From these findings we could conclude that replacement of Lys in the Dau=Aoa-GFLGK(c[KNGRE]-GG)-NH_2 conjugate by different amino acids provides a more convenient and cost-effective synthetic route. By doing so the resulting conjugates could be obtained in a higher yield, which might be relevant for larger scale synthesis needed for further investigations. We have shown that the modifications reduce the chemical stability of the cyclic NGR moiety, boosting the affinity to integrin receptors as compared to the CD13 receptor. Among the new cyclic NGR peptide – daunorubicin conjugates the most effective compound was Dau=Aoa-GFLGK(c[NleNGRE]-GG)-NH_2, which showed similar activity on HT-1080 CD13(+) cells to Dau=Aoa-GFLGK(c[KNGRE]-GG)-NH_2, and a significantly higher antitumor effect on HT-29 CD13(−) but integrin receptor positive cells. To summarize the results of this first part of the project, the synthetic and biological data collected suggest that compound **2**, norleucine containing cyclic NGR peptide is more suitable for drug targeting with dual acting propensity than our control lead lysine containing conjugate which was obtained from a longer and more difficult synthetic route.

3.4 Further investigations: in vitro, in vivo and ex vivo studies

Considering the relevance of the *in vitro* antitumor effect, the second part of the current work involved the investigation of the *in vivo* biological activity of the best peptide-drug conjugates synthesized. For this reason great effort was given on scaling-up the synthesis of the two chosen bio-conjugates (**1**) and (**2**). Our main goal was to better understand how these highly similar bioconjugates can impact the *in vivo* antitumor effect, taking into count the dual-targeting strategy especially in the case of Nle containing peptide conjugate which shows higher versatility in the previously reported data.[67] We investigated the *in vivo* antitumor activity of the best peptide-drug conjugates (**Figure 17**) and their ability to suppress the tumor growth and the development of new blood vessels in cancer

bearing mice. Moreover, we performed *in vitro* and *in vivo* experiments on CD13 (+) Kaposi's sarcoma (KS) cell line[245–247], human colon adenocarcinoma, CD13 (-) but integrin positive HT-29 cells to compare the targeting effect of conjugates, finally MRC-5 fibroblasts were used as negative control. To better clarify their action on the treated animals, proliferation index and *ex vivo* blood vessel formation was evaluated on every tumor model.

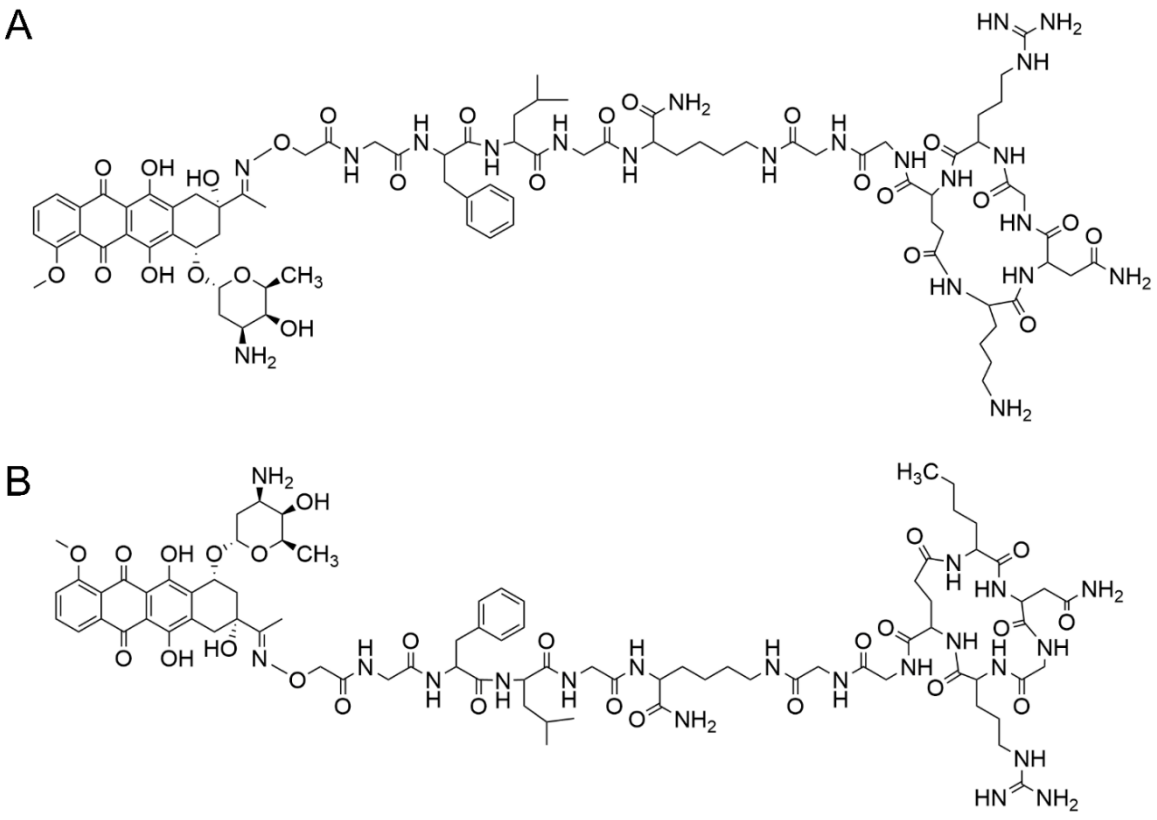

Figure 17: Structures of peptide-drug conjugates, Lys containing compound **1** (A) and Nle containing compound **2** (B).

The large scale synthesized Dau NGR conjugate (Nle containing) was analyzed by ESI-MS and analytical RP-HPLC. ESI-MS spectrum shows one single signal with an *m/z* ratio of 884.63 (**Figure 18A**), belonging to the $[M+2H]^{2+}$ ionized compound. This leads to an experimental molecular mass of 1767.25 g/mol. Therefore, the experimental molecular mass is in accordance with the

calculated molecular mass (1767.92 g/mol). Additionally, also the analytical RP-HPLC, besides the injection peaks at 3.5 min, revealed only one peak at 34.2 min, with an absorbance of 1.09 (**Figure 18B**). This peak belongs to the eluted conjugate **2** compound and demonstrates high compound purity.

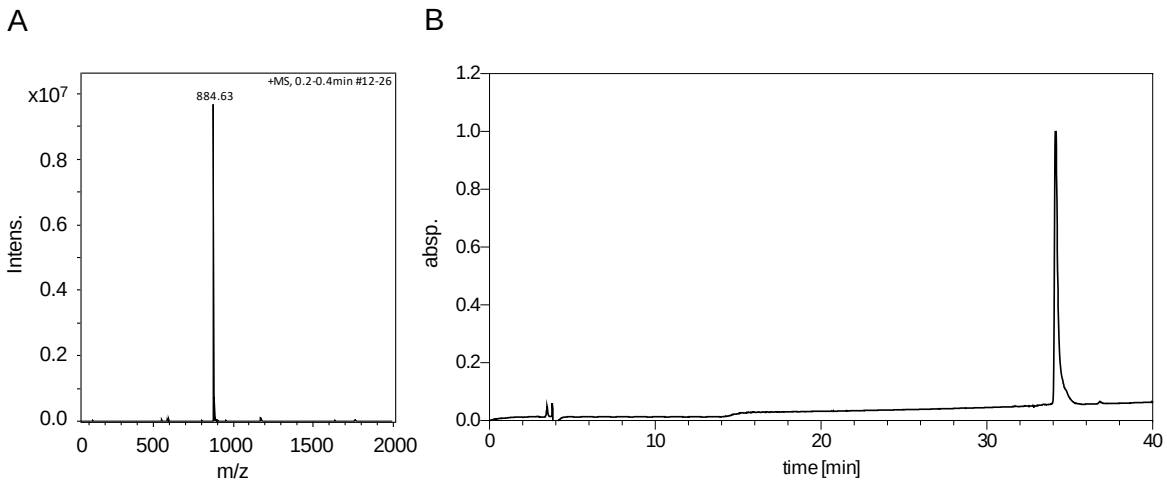

Figure 18: Purity control of Nle containing conjugate **2** *via* ESI-MS and analytical RP-HPLC. (A) ESI-MS revealed a pure signal of the $[M+2H]^{2+}$ ionized compound with an *m/z* ratio of 884.63, leading to a calculated experimental molecular weight of 1767.25 g/mol. The expected molecular weight is 1767.92 g/mol. (B) Analytical RP-HPLC shows one peak at 34.2 min.

Thus, the synthesis of the conjugate **2** was successful, 222.0 mg pure compound could be obtained. The final Dau coupled NGR conjugate **1** was analyzed *via* ESI-MS and analytical RP-HPLC. ESI-MS spectrum shows two signals with *m/z* ratios of 595.13 ($[M+3H]^{3+}$), and 892.04 ($[M+2H]^{2+}$) (**Figure 19A**), leading to an experimental molecular mass of 1782.24 g/mol. Therefore, the experimental molecular mass is in accordance with the calculated molecular mass (1782.93 g/mol). Additionally, the analytical RP-HPLC, besides the injection peaks at 3.5 min, revealed only one peak at 32.4 min, with an absorbance of 0.61 (**Figure 19B**). This peak belongs to the eluted conjugate **1** and demonstrates high compound purity.

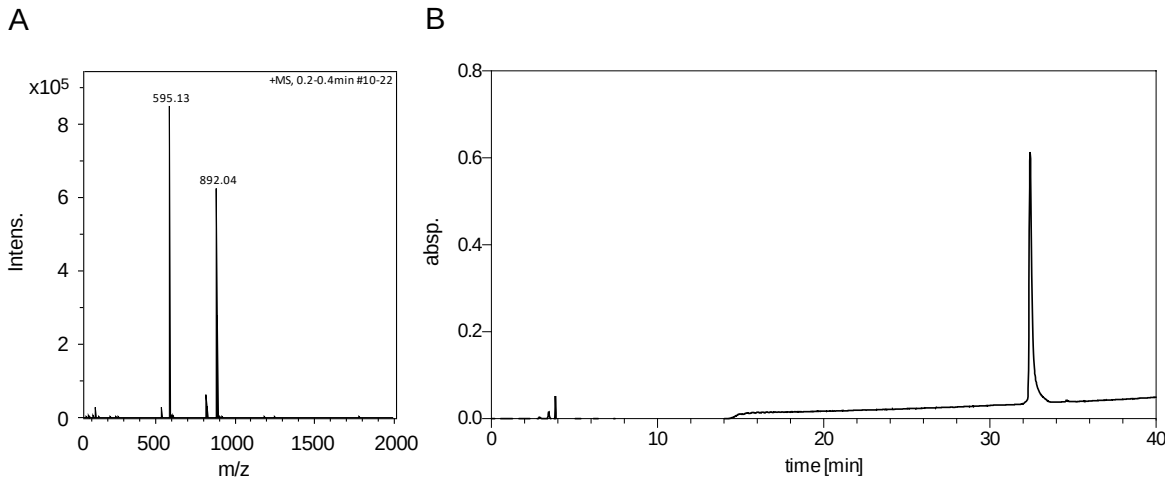

Figure 19: Purity control of conjugate **1** (Lys containing) via ESI-MS and analytical RP-HPLC. (A) ESI-MS revealed two signals of the $[M+3H]^{3+}$ and $[M+2H]^{2+}$ ionized compound with *m/z* ratios of 595.13 and 892.04, respectively, leading to a calculated experimental molecular weight of 1782.24 g/mol. The expected molecular weight is 1782.93 g/mol. (B) Analytical RP-HPLC shows one peak at 32.4 min.

3.4.1 In vitro antiproliferative activity of NGR-Dau conjugates and free Dau

The antiproliferative effect of the NGR-Dau conjugates **1** and **2** and free Dau was investigated *in vitro* on CD13(+) Kaposi's sarcoma cells (KS) and on CD13(-), but integrin positive[248] HT-29 human colorectal adenocarcinoma cells, as well as on MRC-5 (human fibroblast) as non-cancerous control cell line. Prior to the antiproliferative activity studies, cell surface CD13 expression of KS and HT-29 cells was detected by immunocytochemistry and visualized by confocal microscopy (**Figure 20**). As stated in the literature, KS cells express a higher level of CD13 receptors at their cell membrane compared to HT-29 cells.[164,249]

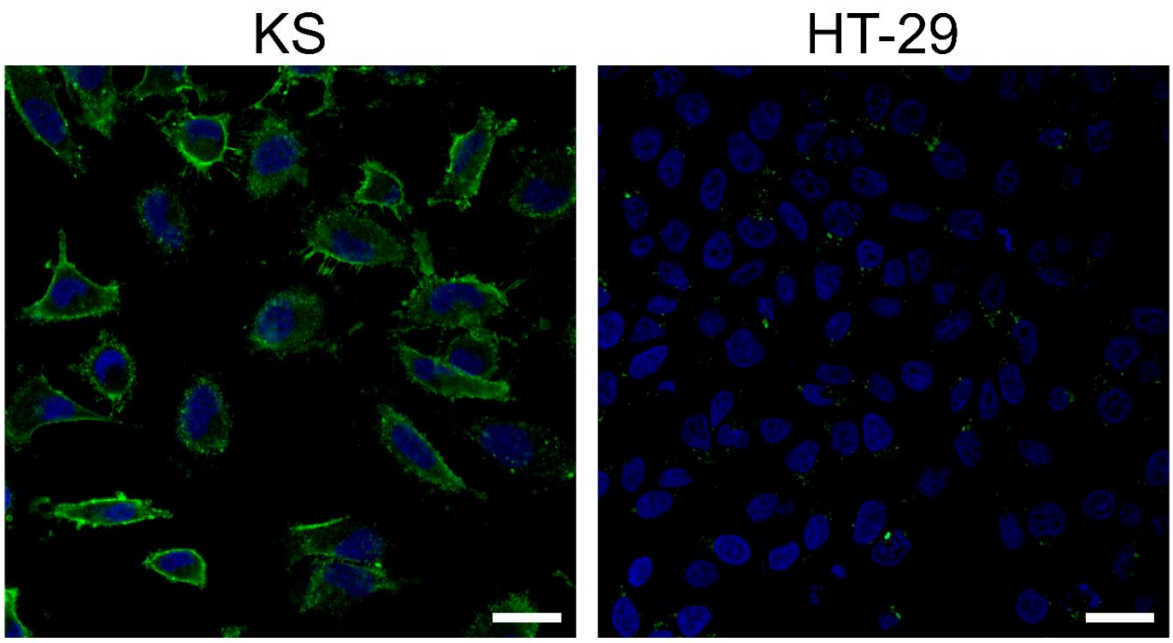

Figure 20: Determination of cell surface CD13 expression on KS (left) and HT-29 cells (right) by immunocytochemistry. CD13 was detected by anti-CD13-FITC antibody (green). The nuclei were stained with Hoechst 33342 (blue). The scale bars represent 20 µm. [a]

The results of the MTT assay showed that both bioconjugates have antiproliferative effect on cancer cells (**Table 5**). Conjugate **2** (Nle) displayed higher antiproliferative activity than conjugate **1** (Lys). The selected conjugates showed higher antiproliferative activity on CD13(+) KS cells, then on CD13 (-) HT-29 cells. The IC_{50} values of both conjugates are lower after longer time of exposure, particularly for conjugate **2**. High IC_{50} values of conjugates were obtained on MRC-5 cells, showing selectivity of conjugates for cancer cell lines, especially in case of conjugate **1**.

[a] All CLSM samples were prepared with the help of Beáta Biri-Kovács and images were processed by Bálint Szeder

Table 5: *In vitro* antiproliferative activity of NGR-Dau conjugates and Dau on KS, HT-29 and MRC-5 cells

	KS (24 h) IC_{50} (µM)	KS (72 h) IC_{50} (µM)	HT-29 (24 h) IC_{50} (µM)	HT-29 (72 h) IC_{50} (µM)	MRC-5 (72 h) IC_{50} (µM)
Dau	0.1 ± 0.01	0.07 ± 0,01	0.09 ± 0.01	0.1 ± 0.01	0.25 ± 0.06
1	22.7 ± 2.3	15.2 ± 0.3	32.4 ± 1.4	29.3 ± 1.0	> 100
2	8.0 ± 0.8	4.3 ± 0.1	13.9 ± 1.6	7.2 ± 0.2	25.4 ± 3.5

All IC_{50} values represent average ± SD.

3.4.2 Cellular uptake of NGR-Dau conjugates

The cellular uptake of the NGR-Dau conjugates by KS and HT-29 cells was measured by flow cytometry. The results that were obtained displayed that the uptake on both cell lines was concentration dependent, but the new conjugate **2** (Nle) entered the cells more efficiently than **1** (Lys containing), especially at lower concentrations (**Figure 21**). At 50 µM concentration, conjugate **2** showed almost 100% uptake, whereas conjugate **1** was lower (~20%). At 100 µM concentration, conjugate **1** was already taken up by around 50% of cells. Moreover, at 50 µM and 100 µM concentrations, the uptaken level of conjugate **2** by CD13(+) KS cells was similar to those in HT-29 cells, while for conjugate **1** higher values were measured in case of HT-29 cells.

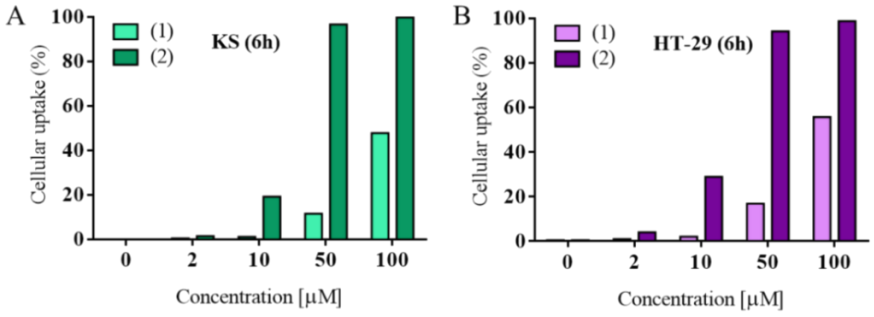

Figure 21: Cellular uptake of NGR-Dau conjugates **1** (Lys containing) and **2** (Nle containing) at concentrations 2, 10, 50 and 100 µM, after 6 h treatment by KS cells (A) and HT-29 cells (B).

3.4.3 Stability of NGR peptide-daunorubicin conjugates in mouse plasma

NGR peptides might have several benefits in targeted tumor therapy. However, the easy deamidation of NGR peptides, resulting in both *iso*Asp and Asp derivatives, indicates the difficulties in their biological evaluation and synthetic route. Therefore, known that preclinical studies of anticancer drug conjugates are mostly performed using xenograft mouse models, stability of the two bioconjugates was determined in murine plasma, using HPLC-MS. Both conjugates were stable at experiment conditions for at least 8 h at 37 °C (**Figure 22**). This indicates that both compounds possess a high stability towards plasma-specific enzymes providing a reliable durability during circulation. Those results are promising if we consider their importance for *in vivo* applications.

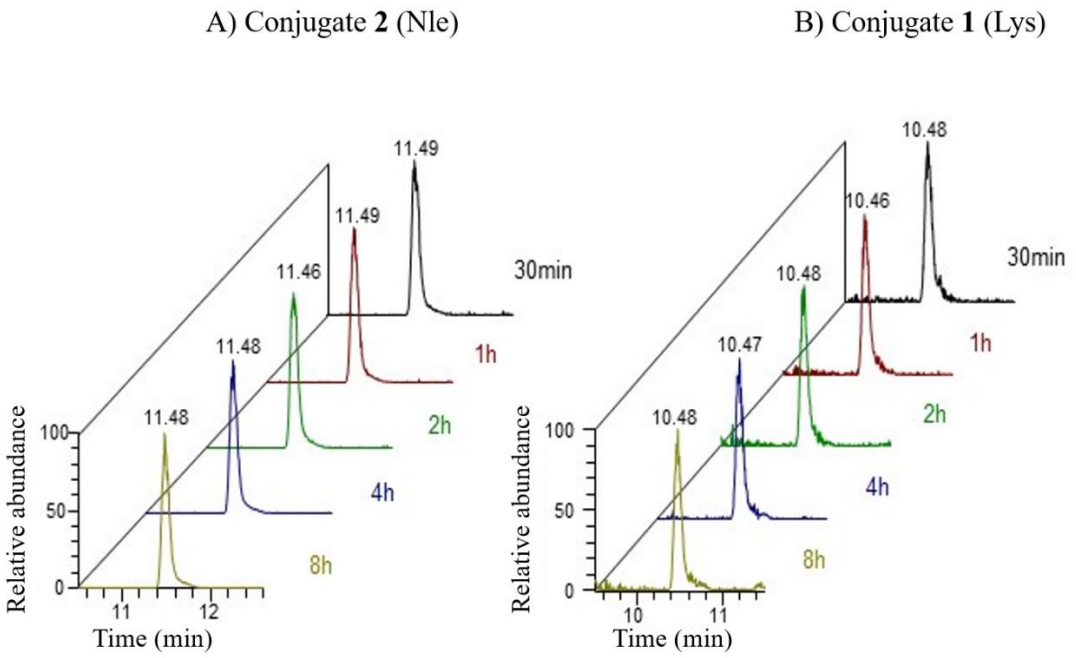

Figure 22: Stability of the bioconjugates in murine plasma 90%, 10µM peptide concentration. A) Nle containg conjugate, B) Lys containing conjugate: LC-MS chromatograms in murine plasma of the conjugates after 30 min, 1, 2, 4, 8 h incubation at 37 °C.

3.4.4 Acute and chronic toxicity studies of NGR-Dau conjugates

Acute toxicity experiment was completed for 14 days in adult male BALB/c mice. No significant change in body weight could be observed (**Figure 23 A,B**), also the general looking and behavior of experimental animals were adequate, even when 25 mg/kg Dau content of both NGR-Dau conjugates was used. Chronic toxicity studies were also performed for 14 days, and animals were treated with both conjugates 5 times at a dose of 10 mg/kg Dau content. Similar to the acute toxicity experiment, we could not observe a significant change in body weight (**Figure 23 C**), general looking and behavior of the mice.

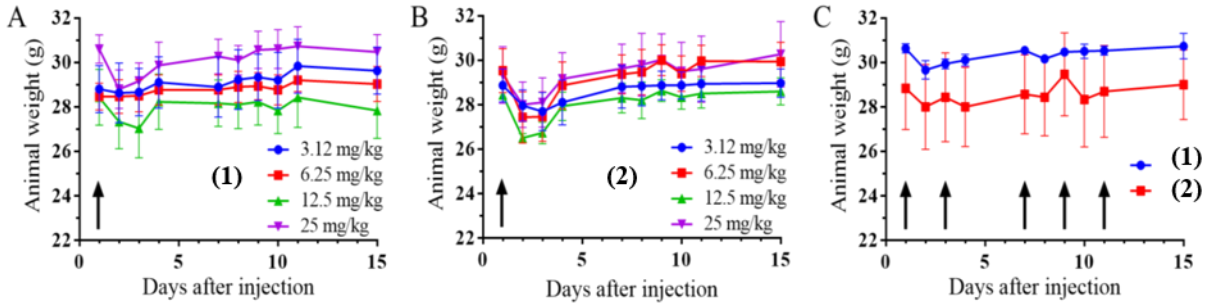

Figure 23: Animal body weight (average ± SEM). A) Acute toxicity study of conjugate **1** with doses of 3.125, 6.25, 12.5 and 25 mg/kg Dau content. B) Acute toxicity study of conjugate **2** with doses of 3.125, 6.25, 12.5 and 25 mg/kg Dau content. C) Chronic toxicity study of NGR-Dau conjugates **1** and **2** with dose of 10 mg/kg Dau content, 5 treatments: marked by black arrows, 3 mice per group. [a]

[a] Toxicity, *in vivo* and *ex vivo* studies were performed in collaboration with Ivan Ranđelović.

3.5 Effect of NGR-Dau conjugates and free drug in Kaposi's sarcoma subcutaneous model in vivo

Subcutaneous Kaposi's sarcoma bearing SCID mice were treated with NGR-Dau conjugates **1** and **2** at dose of 10 mg/kg Dau content 3 times during the first week and two times per week during the next 4 weeks, as well as with free Dau at a dose of 1 mg/kg (maximum tolerated dose) once per week, and their effect on the animal body weight was evaluated (**Figure 24 A**). The animal body weight was decreased non-significantly in the control and conjugate **2** treated groups (2.5% and 4.6%, respectively), while non-significant increase was obtained in conjugate **1** treated group (3%). In comparison, administration of free Dau from day 63 after cell inoculation resulted in a significant decrease of mice body weight which was at the end of experiment reduced by 16.7%. Considering that some animals of the control group and all animals in the free Dau treated group were in bad condition, the experiment was terminated on day 70 after cell inoculation. The antitumor effect of NGR-Dau conjugates **1** and **2** and free Dau was evaluated by measuring the tumor volume in each group. All treated groups showed decreased tumor volume in comparison to control group at the end of the experiment (**Figure 24 B**). Treatment with conjugate **1** was the most effective, whereby the tumor volume was inhibited by 37.7% compared to the non-treated control. Conjugate **2** inhibited tumor growth by 24.8%, while the group treated with free Dau showed the lowest inhibition of tumor volume, only 18.6% compared to control. The effect of NGR-Dau conjugates and free Dau on liver toxicity was evaluated by measuring the liver weight at completed experiment (**Figure 24 C**). The average liver weight from mice in the group treated with free Dau decreased significantly by 21.8% in comparison to control group. The decrease was also significant compared to both groups treated with conjugates. The groups treated with conjugates **1** and **2** showed no significant changes in liver weight in comparison to the control.

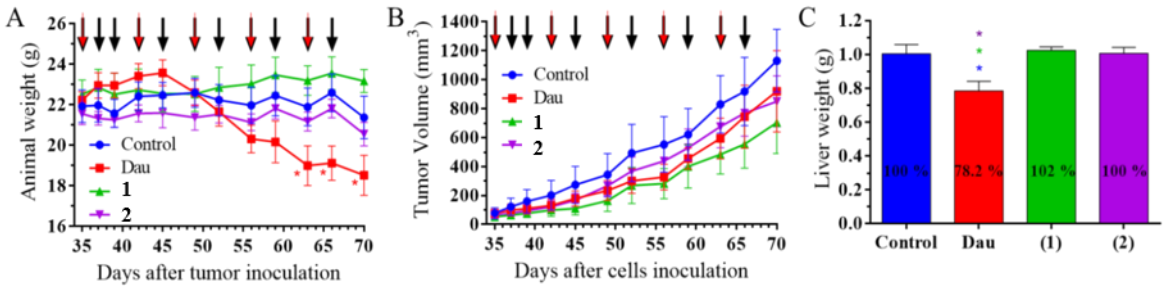

Figure 24: Effect of NGR-Dau conjugates **1** and **2** (10 mg/kg Dau content, 11 treatments, black arrows) and free Dau (1 mg/kg, 5 treatments, red arrows) on subcutaneous Kaposi's sarcoma bearing mice. A) Animal body weight (g, average ± SEM). B) Tumor volume (mm^3, average ± SEM). C) Liver weight (g, average ± SEM) after termination of experiment, 70 days after cell inoculation, 5 animals per group. Statistical analysis was performed by Mann-Whitney test. * means significantly different at $p<0.05$.

3.6 Effect of NGR-Dau conjugates and free drug in orthotopic HT-29 human colon tumor model in vivo

Orthotopic HT-29 human colon carcinoma bearing SCID mice were treated according to the same doses and schedule as subcutaneous Kaposi's sarcoma bearing mice. The animal body weight decreased in all groups at the end of the experiment compared to the start (**Figure 25 A**). The mice treated with free Dau showed a significant reduction in body weight from day 17 after tumor transplantation, whereby the experiment was terminated on day 24 (day 19 of treatment). Conjugate **1** caused significant decrease in body weight from day 22, while the body weight of the control group significantly decreased on the last day of the experiment and due to this the experiment was terminated on day 27 after tumor transplantation. No significant change in the body weight was obtained during the treatment period with conjugate **2**. The antitumor effect of the NGR-Dau conjugates and free drug was assessed by measuring the tumor weight in each group after termination (**Figure 25 B**). The obtained results reveal that the free Dau inhibited the tumor growth significantly, whereby the tumor weight was reduced by 67.7% compared to the control group. Conjugate **1** inhibited tumor growth by

16.9%, while inhibition by conjugate **2** was 45.7% in comparison to the control group. The toxicity of the free drug was detected in this experiment as well. The average weight of livers from the mice treated with free Dau was significantly decreased by 28.9% in comparison to the control group (Figure 24 C). In contrast, there was no significant change in liver weight in the groups treated with the conjugates (92.4% and 110% of the control, respectively). The antimetastatic effect of NGR-Dau conjugates was evaluated by counting and measuring the weight of metastases near the primary tumor in each group at the end of the experiment (**Figure 25 D**). Lower number of metastases was observed near the primary tumor in the treated groups compared with the untreated control group. While in control group metastases were found in 7 out of 8 animals, in treated groups using Dau, conjugates **1** and **2**, metastases were found in 1, 5 and 4 out of eight animals, respectively. Free Dau inhibited the weight of metastases by 78.3%. Conjugate **1** did not show significant inhibition (4.9%), while conjugate **2** inhibited metastases by 22.2% in comparison to control group.

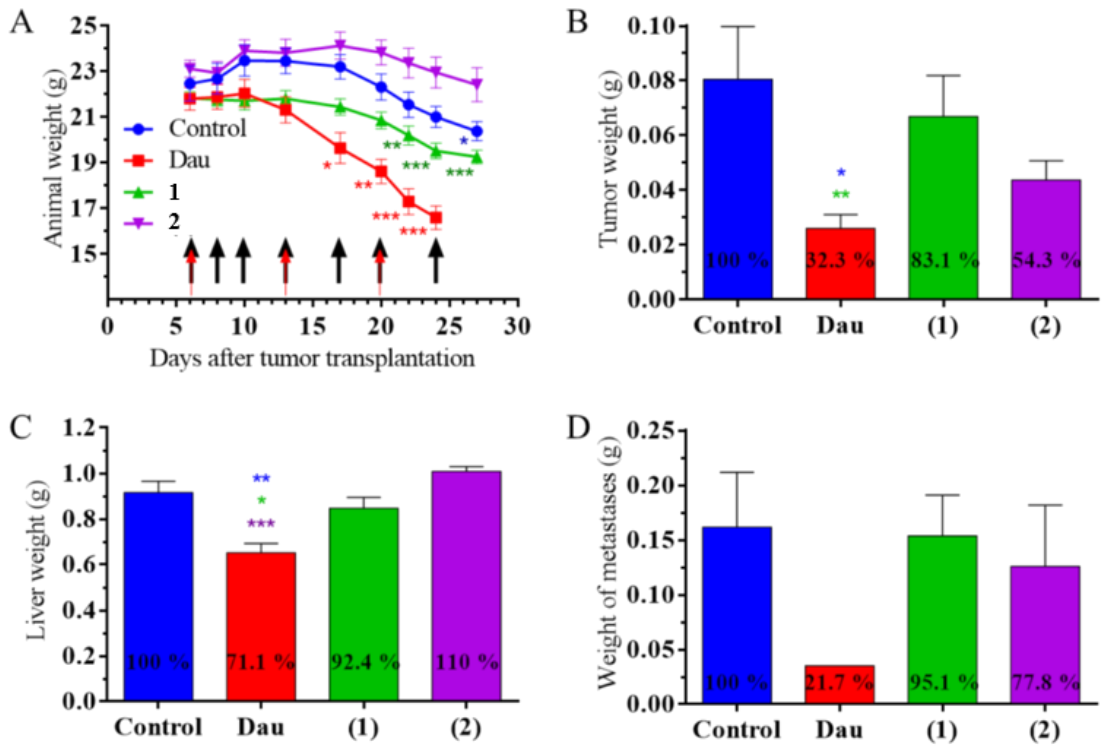

Figure 25: Effect of NGR-Dau conjugates **1** and **2** (10 mg/kg Dau content, 7 treatments, black arrows) and free Dau (1 mg/kg, 3 treatments, red arrows) on orthotopic HT-29 human colon carcinoma bearing mice. A) Animal body weight (average ± SEM). B) Tumor weight (average ± SEM). C) Liver weight (average ± SEM). D) Weight of metastases near the primary tumor (average ± SEM). Control and groups 1 and 2 were measured after the termination of the experiment (on day 27 after transplantation), while Dau group was measured on day 24 subsequent to transplantation. 8 animals were used per group. Statistical analysis was performed by Mann-Whitney test. *, ** and *** mean significantly different at $p<0.05$, $p<0.01$, and $p<0.001$, respectively.

3.7 Effect of NGR-Dau conjugates and free daunorubicin on proliferation and vascularization in primary tumor

The effect of NGR-Dau conjugates and free Dau on proliferation was evaluated in the primary tumor by proliferation index, presented by the percentage of proliferation marker (KI-67) positive cells out of all cells per field of view in subcutaneous Kaposi's sarcoma and orthotopic HT-29 human colon primary tumors (**Figure 26 A, B**). In KS primary tumor, all treated groups showed decreased proliferation, but only the group treated with conjugate **1** displayed significant inhibition of proliferation by 17.4% compared to the control. However, in HT-29 primary tumor, all treated groups showed significant inhibition of proliferation by 11.2, 12.9 and 15.1% for Dau, and conjugates **1** and **2**, respectively. The effect of NGR-Dau conjugates and free Dau on vascularization in the primary tumor was evaluated counting CD31 (endothelial marker) stained blood vessels per field of view in subcutaneous Kaposi's sarcoma and orthotopic HT-29 human colon primary tumors (**Figure 26 C, D**). In KS primary tumor, all treated groups showed lower blood vessel formation, but we could detect significant inhibition only in groups treated with conjugates: 31.0% (**1**) and 38.8% (**2**) compared to the control. In HT-29 primary tumor, all treated groups showed inhibition of vascularization which was significant only when treated with conjugates **1** and **2** by 41.5% and 36.1%, respectively.

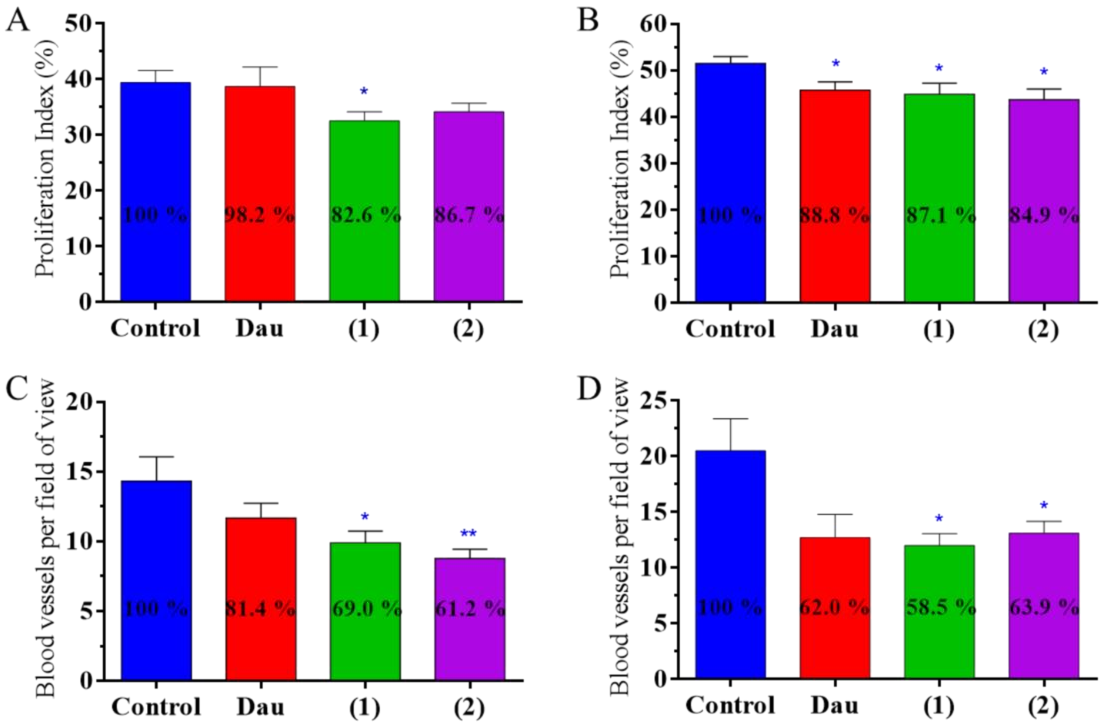

Figure 26: Effect of NGR-Dau conjugates **1** and **2** and free Dau on proliferation in primary tumor in Kaposi's sarcoma (A) and HT-29 human colon carcinoma (B) bearing mice. Effect of NGR-Dau conjugates **1** and **2** and free Dau on vascularization in primary tumor in Kaposi's sarcoma (C) and HT-29 human colon carcinoma (D) bearing mice. Statistical analysis was performed by Mann-Whitney test. * and ** mean significant at $p<0.05$ and $p<0.01$, respectively.

3.8 Highlights and outcomes of the project

Kaposi sarcoma was described for the first time by the Hungarian dermatologist Móritz Kaposi in 1872 is a tumor of vascular origin developing in many different clinical-epidemiological forms with several lesions of the skin.[246,250,251] This type of angio-proliferative disease represents today one of the most deadly and aggressive type of tumors in HIV-1-infected people.[252] It has been confirmed that primary lesions of KS express a high level of CD13/APN and this is a key factor for the contribution of increased vascularization of the tumor.[253,254] The main focus of the present study is also attentive on a colon carcinoma tumor model which is one of the most lethal types of tumor in developed countries. Colon carcinoma cells can express a variety of integrins and often a lower level of CD13.[255,256] Targeted tumor therapy is a promising approach to decrease all the drawbacks of

chemotherapeutic drugs.[257] In the present project, cyclic NGR-Dau bioconjugates were used as targeting vehicles due to their affinity to the aminopeptidase N CD13 and a variety of integrins, in particular the ones closely related to angiogenesis (RGD integrins). The recognition of integrins by NGR peptides is rather based on the rearrangement of NGR to *iso*DGR peptides established by succinimide formation followed by fast hydrolysis. *Iso*DGR peptides similarly to RGD ones can efficiently be recognized by different integrins like $\alpha_v\beta_3$, $\alpha_v\beta_6$, etc.[258–260] The important value of these homing devices counts on the fact that they possess their own *in vitro* antiproliferative effect. Our recently published findings show that the bioconjugates with daunorubicin connected *via* chemo selective ligation (oxime bond formation) can have noteworthy antitumor action *in vitro.* after the characterization and screening of the bioconjugates the second part of the project involved the investigation of the antitumor activity of our two best conjugates in comparison with the free highly cytotoxic drug, that was evaluated *in vitro* on CD13(+) KS and CD13(-) HT-29 cells, while MRC-5 normal fibroblasts were used as negative control. While the free drug is internalized through cells *via* diffusion, the conjugates are ideally internalized through receptor-mediated endocytosis leading to the release of the active metabolites in lysosomes. Our studies were mainly focusing on the formation of a small metabolite Dau=Aoa-Gly-OH which can bind to the DNA causing cell death.[261] The results of the MTT assay *in vitro* indicated that both bioconjugates have stronger antitumor effect on KS (CD13+) than HT-29 (CD13-) cells. Moreover, we need to highlight that conjugate **2** with Nle instead of conjugate **1** (Lys in the cycle) provided drastically higher efficiency on both cell lines, which is also confirmed by cellular uptake studies where conjugate **2** entered the cells more efficiently than **1**, even at lower concentrations. The higher antitumor activity might be caused by the faster rearrangement from NGR to *iso*DGR in case of conjugate **2** in comparison with conjugate **1** resulting in dual acting tendency of the conjugate.[262] Moreover, key role in this study to better understand the

selectivity of the conjugates was the experiment made on MRC-5 cells, in this case the antiproliferative effect of the bioconjugates was lower compared to the tumor cells. The selectivity towards cancer cells was especially high in case of conjugate **1** that it has higher stability against the deamidation process. Considering the obtained outcomes, it could be proposed that the biological activity of the NGR-Dau conjugates depends strongly on the expression of CD13 receptor which ensures the selectivity of the conjugates and their cellular uptake capacity. Due to the promising *in vitro* results with conjugates **1** and **2**, we decided to analyze their *in vivo* antitumor activity on tumor-bearing mice. Initially, we determined the stability of the compounds in mice plasma detecting that both conjugates were stable for at least 8 hours.[262,263] For the drug development process, the studies of the toxicity effect of new compounds on healthy mice is essential. Thus, acute toxicity study was performed, showing that neither the body weights of mice, nor the general looking and behavior of experimental animals were significantly different, even at a dose of 25 mg/kg Dau content of both conjugates. Moreover, to evaluate the effect of the compounds on healthy mice, chronic toxicity was investigated where animals were treated with both conjugates 5 times with a dose of 10 mg/kg in terms of drug content. After 14 days, we could not observe any substantial differences in the body weights, general looking and behavior of the treated mice. Based on these results, it could be concluded that both drug-conjugates were suitable for treatment of tumor bearing mice at this concentration. First, the *in vivo* antitumor activity of NGR-Dau conjugates and free Dau was determined on a subcutaneous KS model. The animal body weight of mice indicated significant decrease for the Dau group, while in control and in conjugates treated groups, no significant change in animal body weight could be observed indicating that the conjugates did not cause toxic side effects to the animals during the treatment in comparison with the free payload. The antitumor effect of the NGR-Dau conjugates **1** and **2**, as well as the free Dau was evaluated by measuring the tumor volume

in each group during the experiment. We obtained tumor growth inhibition of KS tumor in all treated groups compared to the control group. Interestingly, in contrast to the *in vitro* experiments, the inhibition effect of conjugate **1** was higher in comparison with Dau and conjugate **2**. Data showed antitumor effect of the conjugates against KS tumor, especially in case of conjugate **1** which inhibited tumor volume by 37.7% compared to control. The number of dividing cells in tumor tissues, as well as the formation of blood vessels are strictly associated with cell proliferation and tumor progression. Therefore, the proliferation index of KI-67 positive cells and blood vessel density by CD31 marker in the primary tumor were determined.[264,265] Both the cell proliferation index and blood vessel formation were lower in case of mice treated with conjugates in comparison with the Dau-treated and control group. The differences were higher in case of conjugate **1** than in case of **2**. The data obtained can explain the higher tumor growth inhibition of conjugate **1**. We can also conclude that for the treatment of a highly CD13 positive tumor type, a stable NGR peptide derived conjugate might be a better choice. Moreover, not only the elicited antitumor activity is of high relevance for the success of an anticancer drug, but also the targeting action to cancerous cells and reduction of side effects, thus, liver toxicity was determined. Since the liver is the vital organ in drug metabolism, this analysis provides a better understanding of drug toxicity.[266] Free Dau caused a significant decrease of liver weight in comparison to control and conjugates treated groups, revealing that treatment with Dau resulted in toxic side effect in treated mice. In contrast, non-significant liver weight changes could be detected in NGR-Dau conjugates treated groups proving evidences for their selectivity and non-toxicity to healthy tissue. Next to the *in vivo* studies on KS bearing mice, we were interested in analyzing the anticancer activity of the two NGR-Dau conjugates and free Dau on a tumor that has a lower expression of CD13 receptors but expresses integrin receptors.

Regarding our evaluation of CD13 receptor expression and based on studies that pointed out that HT-29 cell line shows increased integrin receptor expression level, this human colon adenocarcinoma might represent an adequate model for this experiment.[235] Although orthotopic colon cancer xenograft models are technically challenging and labor-intensive, orthotopic transplants can mimic human tumors more accurately. This approach simulates the natural microenvironment for tumor development better, providing an effective approach to better understand tumor pathophysiology and to develop therapeutic strategies which consent a better prediction of a patient's response to chemotherapy in comparison with heterotopic transplants.[267] A variable number of therapeutics have been used which target receptors, and hence revealed a significant tumor growth inhibition *in vitro* and *in vivo*. Thus, HT-29 human colon tumors were implanted to the intestine of immunodeficient SCID mice.[250]

We observed that the free drug produced a significant reduction in mice body weights which compelled us to terminate the experiment for this group on day 24 after tumor transplantation. For similar reasons, conjugate **1** treated group was also terminated on day 27. Significant changes of animal weight were not observed in case of mice treated with conjugate **2** (terminated also on day 27). This indicates that both drug-conjugates induce less damaging side effects than the free daunorubicin, especially conjugate **2** with no significant effect. Additionally, it might be possible that the decrease in body weight was caused by a higher susceptibility of the immunodeficient animals after surgery procedures which was required to establish the orthotopic colon cancer model.[269] The antitumor effect of the conjugates and free Dau was evaluated after isolation of the tumors at the end of the experiment.[270] We found a significant inhibition of the tumor weight only in Dau treated group compared to the control, which showed significant inhibition compared to conjugate **1** also. High

inhibition of tumor weight (45.7%) was obtained in the treatment with conjugate **2**, though the decrease was not significant. The better efficacy of conjugate **2** on orthotopically developed CD13(-) HT-29 colon cancer might be explained by the faster rearrangement of conjugate **2** to *iso*DGR derivative that identifies integrins in comparison with conjugate **1**. By studying the proliferation index in primary tumors, we could perceive that both conjugates and free Dau as well reduce the proliferation rate supporting their significant inhibitory activity in primary tumors. This can also be reinforced by the significant inhibition of new blood vessel formation by both NGR-Dau conjugates revealing their suppressing effect on angiogenesis in HT-29 primary tumor. It has been reported that in SCID mice, the remaining innate immune cells reduce the metastasis formation in distal organs. Consequently, the antimetastatic effect of the conjugates and free drug was evaluated based on the number of animals containing metastases close to the primary tumor and also on the total weight of metastases. The obtained results showed that the antimetastatic effect of Dau was the highest with only 1 animal with metastases close to the primary tumor, while conjugate **2** showed better antimetastatic effect than conjugate **1** (4 and 5 animals with metastases close to the primary tumor, respectively) which reduced total metastasis weight by 22% compared to control where 7 out of 8 animals were with metastases suggesting that these two conjugates has potential antimetastatic therapeutic effect for colon cancer. In addition, we did not detect significant changes in the liver weights of the groups treated with the conjugates, while a significant decrease was observed for the group which was treated with the free drug. This indicates that the conjugates did not cause toxicity in mice, unlike free Dau. The combination of the NGR sequence with the cathepsin B cleavable linker proved to be a very promising strategy that is worth to be further investigated in the future also with other constructs. Anyhow, there is still a long way to go and a lot of room for improvement. From the results obtained in the project we can conclude that both NGR-Dau conjugates, as well as free Dau

inhibited tumor growth and metastasis development. Since the construct showed remarkable toxicity only at the highest tested concentration after 72 h, it could be demonstrated that the compound could be safely used as drug delivery system *in vivo*. The chemical stability in cell culture medium and the lysosomal degradation were also crucial experiments that allowed us to confirm our findings. The designed synthetic strategy worked well, and after optimization and scale up, the bioconjugates could be obtained in high yields. Conjugate **2** showed higher antitumor and antimetastatic effect against colon cancer compared to conjugate **1**, while its effect on the animal body weight and liver weight was the lowest. Both bioconjugates demonstrate significant effect on inhibition of proliferation in the primary tumor and inhibition of blood vessel formation making them promising candidates for targeting angiogenesis processes in tumor tissues.

3.9 Development, synthesis and characterization of diketopiperazine (DKP) scaffold for CD13 ligand

Considering the great potential of DKP-RGD library as targeting integrin ligand, we decided to use it and develop for the first time a novel class of NGR cyclic peptides with the insertion of the DKP scaffold to improve the affinity to CD13. The new DKP-NGR Dau cyclic peptides shall be synthesized and their biological activity investigated *in vitro* on different tumor cell lines. Moreover, further studies shall be performed to analyze the impact of the scaffold on the stability of the NGR peptide. Before that, the synthesis and characterization of the cyclo[DKP-3-NGR] non-functionalized and functionalized cyclo[DKP-f3-NGR] have been evaluated (**Figure 27**). The latter one and most important can be used for drug conjugation.

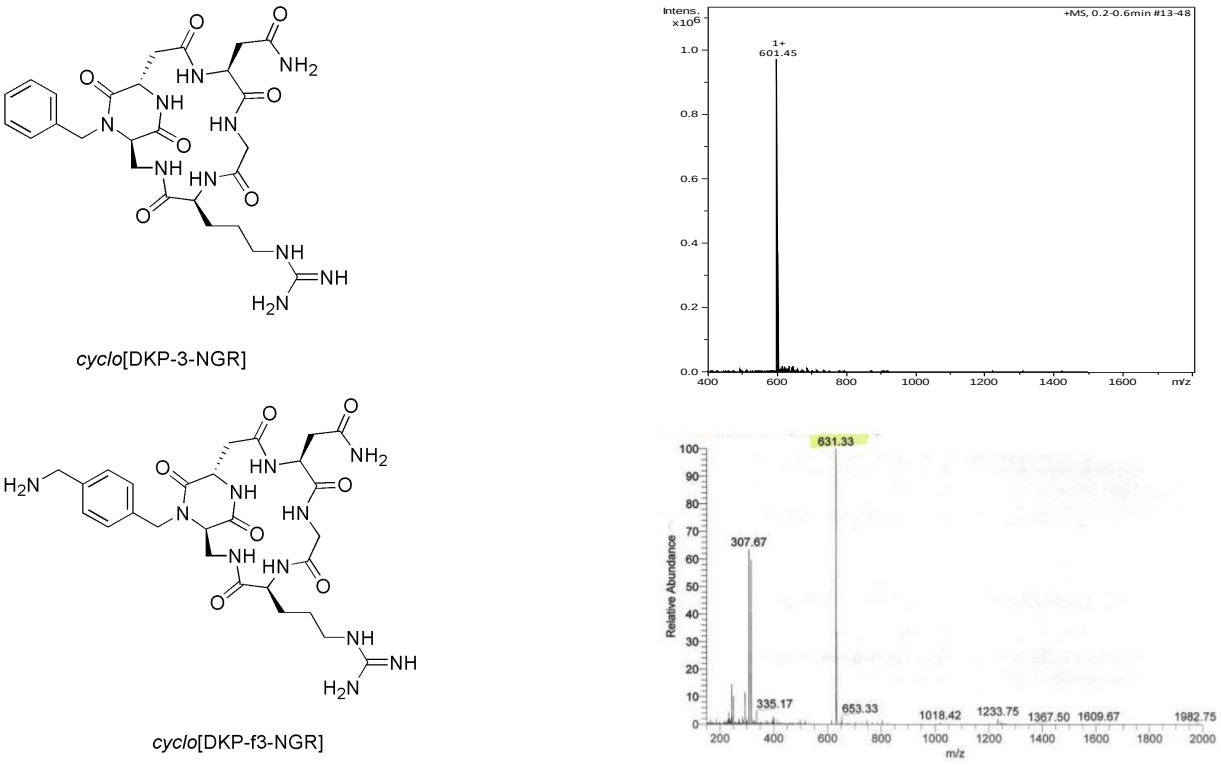

Figure 27: Cyclo[DKP-3-NGR] and Cyclo[DKP-3-f3-NGR] scaffold for CD13 ligand and ESI-MS spectra.

3.9.1 Summary of the synthetic route to obtain the cyclic[DKP3-f3-NGR] scaffold

The synthesis of the functionalized DKP-f3 scaffold was achieved as presented in (**Figure 28A**), starting from commercially available D-aspartic acid and L-serine methyl ester.

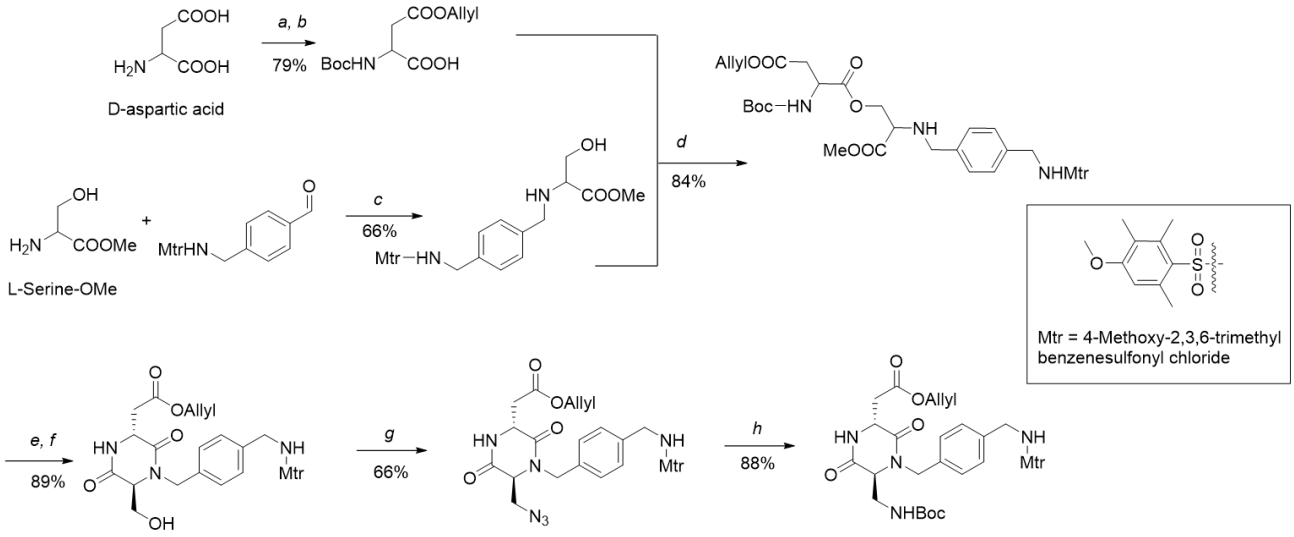

Figure 28A: Synthesis of DKP3-f3 scaffold: (a) Allyl alcohol, acetyl chloride; (b) Boc_2O, TEA, dioxane, water, 79% over two steps; (c) $NaBH(OAc)_3$, THF, 3 h, rt.; (d) HATU, HOAT, DIPEA, DMF, 3 h, 0 °C to rt.; (e) TFA/DCM 1:2, 3 h, 0 °C to rt.; (f) DIPEA, iPrOH, overnight, rt., 89% over two steps; (g) HN_3·toluene, DIAD, Ph_3P, DCM/toluene 1:2, 4 h, −20 °C; (h) Me_3P, BOC-ON, THF, 3 h, −20 °C to rt.

Once the intermediate was obtained in gram scale, the synthesis of *cyclo*[DKP3-f3-NGR]-CH_2-NH_2 continued as indicated in (**Figure 28B**). This strategy was entirely performed in solution allowing to synthesize the NGR, CD13 ligand.

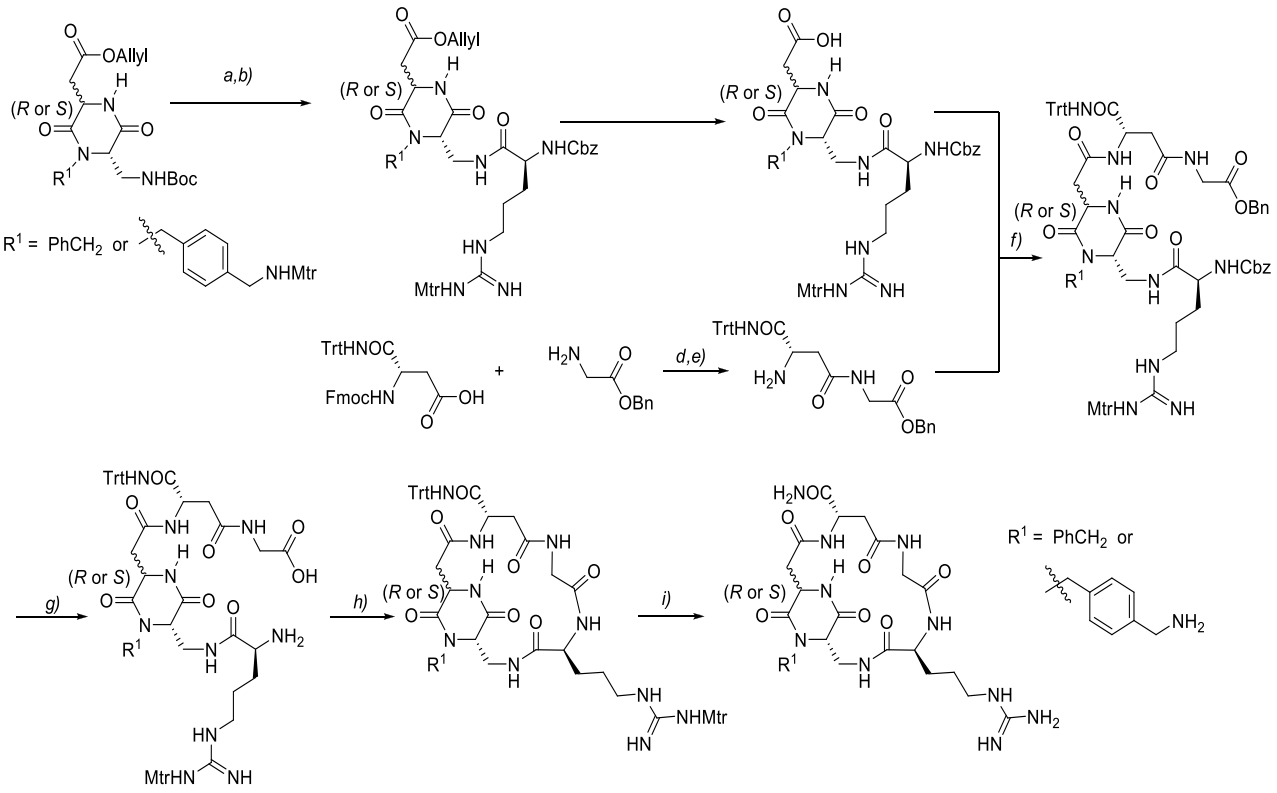

Figure 28B: a) PMe_3 in toluene, Boc-ON, THF, -20 °C, rt 5 h; a) TFA, DCM, rt 2 h; b) Cbz-Arg(Mtr)-OH; HATU, HOAt, DIPEA, DMF, 0 °C, rt, overnight; c) [$Pd(PPh_3)_4$], *N*-methylalanine, DCM, 0 °C, 1 h; d) HATU, HOAt, DIPEA, DMF, 0 °C, rt overnight; e) piperidine, DMF, 3 h, rt; f) HATU, HOAt, DIPEA, DMF, 0 °C, rt, overnight; g) H_2, 10% Pd/C, THF/water 1:1, 1 h 0°C, then rt overnight; h) HATU, HOAt, DIPEA, DMF (1.4 mM), 0 °C 1 h, then rt, overnight; i) TFA/TMSBr/thioanisole/EDT/phenol 70:14:10:5:1(v/v/v/v/m) 3 h, 0°C.

The DKP3-f3-NHBoc was Boc-deprotected and reacted with Cbz-Arg(Mtr)-OH under coupling conditions (HATU, HOAt, DIPEA), then the allyl protecting group was cleaved in presence of N-methylaniline and [$Pd(PPh_3)_4$] to obtain the Arg-DKP fragment. The dipeptide, Asn-Gly, was achieved by regular coupling of Fmoc-Asn(Trt)-OH with glycine benzyl ester, followed by cleavage of Fmoc group. Intermediates were attached under coupling conditions (HATU, HOAt and DIPEA) to give the linear protected compound. Afterwards, the benzyl and Cbz protecting groups were removed by palladium catalyzed hydrogenation in water/THF 1:1. The linear peptidomimetic was then treated with coupling agents (HATU, HOAt, DIPEA) under high dilution conditions (1.4 mM in

1:1 DCM/DMF) to promote an intramolecular cyclization, giving the cyclic intermediate. Finally, the 4-methoxy-2,3,6-trimethylbenzenesulphonyl (Mtr) and tert-butyl protecting groups were removed by using TFA in presence of scavengers thioanisol, phenol, EDT and trimethylsilyl bromide to afford cyclo[DKP-3-f3-NGR]-CH_2-NH_2 as a TFA salt after purification by reversed-phase HPLC and freeze-drying from water. NMR spectra of intermediates can be found in the Appendix (**Figure 50-55**). Preliminary studies of binding affinity and stability to deamidation are in progress, but due to a very low amount of scaffold synthesized, the compound will need to be synthesized again on a higher scale.

4. Materials and methods

4.1 Reagents for solid phase peptide synthesis (SPPS)

All amino acid derivatives, K-Oxyma Pure®, Rink-Amide MBHA were obtained from Iris Biotech GmBH (Marktredwitz, Germany), Novabiochem®/Merck-Millipore (Darmstadt, Germany) and Bachem (Bubendorf, Switzerland). Aminooxyacetic acid, coupling agents (1-hydroxybenzotriazole hydrate (HOBt), *N,N'*-diisopropylcarbodiimide (DIC)), and cleavage reagents (triisopropylsilane (TIS), thioanisole, 1,2-ethanedithiol (EDT), phenol, piperidine, 1,8-diazabicyclo[5.4.0]undec-7-ene (DBU), trifluoroacetic acid (TFA)), diisopropylethylamine (DIPEA), methanol (MeOH), *tert*-butanol, hydrochloric acid (HCl) and acetonitrile (MeCN) for RP-HPLC were purchased from Sigma-Aldrich Kft. (Budapest, Hungary). Daunorubicin hydrochloride was provided from IVAX (Budapest, Hungary). *N*,*N*-dimethylformamide (DMF), dichloromethane (DCM) and diethyl ether (Et_2O) were purchased from Molar Chemicals Kft. (Budapest, Hungary).

4.2 Solid phase peptide synthesis for linear NGR peptides

The protocol of the SPPS was as follows: (i) swelling of the resin in DCM (2 x 5 min) followed by DMF washing (4 x 0.5 min), (ii) Fmoc removal with 2% DBU, 2% piperidine, 0.1 M HOBt in DMF (4 times; 2+2+5+10 min), (iii) DMF washing (10 x 0.5 min), (iv) coupling of Fmoc-protected amino acid derivative : DIC : HOBt (4 eq each) in DMF (1 x 60 min), (v) DMF washing (3 x 0.5 min), (vi) DCM washing (2 x 0.5 min), (vii) ninhydrin test. Rink-Amide MBHA resin as solid support and standard Fmoc protected amino acids were used for the synthesis except Fmoc-Lys(Mtt)-OH that was applied for the development of branching in the peptide. The Mtt group was removed by using 2% TFA in DCM (8 x 5 min). The peptidyl resin was neutralized with 10% DIPEA in DCM (4 x 5 min),

afterwards. Coupling of isopropylidene protected aminooxyacetic acid (>=Aoa-OH) was carried out with K-Oxyma Pure® and DIC (5 eq each) in DMF for 2 hours. The cleavage from the solid support was performed at RT in a solution of 95% TFA, 2.5% TIS, 2.5% water for 3 h. The resin was then filtered, and the crude product was precipitated with cold diethyl ether and centrifugated for 5 min at 4000 rpm to allow the removal of the cleavage agents. After washing (3 times with ether) the remaining pellet was dissolved in water or in 10% acetic acid and lyophilized for 24 hours (overnight?). The lyophilized compound was then purified by RP-HPLC prior to the cyclization.

4.3 Cyclization of NGR conjugates

Before the head-to-side chain cyclization, a salt exchange was performed using 10 eq of pyridinium hydrochloride in 5 mL MeOH. After 20 min, volatiles were removed under reduced pressure, the remaining oily compound was dissolved in dry DMF at a concentration of 0.5 mg/mL. The pH of the mixture was adjusted to pH 8.0 with DIPEA, then BOP and HOBt (3 eq each to the peptide) were added to the stirring reaction mixture. The termination of the reaction was followed by analytical HPLC till the total conversion. At the end the solvent volatiles were removed, and the remaining oily compound was dissolved in acetonitrile-water and purified by RP-HPLC, the collected fractions were lyophilized.

4.4 Removal of isopropylidene group

To remove the isopropylidene protecting group of the >=Aoa-moiety, the compound was dissolved in 0.2 M NH_4OAc buffer solution (pH 5), containing 1 M of methoxylamine hydrochloride at a peptide concentration of 5 mg/mL. The reaction was stirred at RT for one to two hours. Reaction process was controlled by analytical RP-HPLC till complete conversion. When the reaction was

completed, the reaction mixture was directly purified by RP-HPLC. Product-containing fractions were evaporated and used for chemo-selective ligation of daunorubicin.

4.5 Coupling of daunorubicin

To avoid undesired side reactions with carbonyl groups (acetone or formaldehyde), the concentrated compound was dissolved at once in 0.2 M NH_4OAc solution (pH 5), and daunorubicin was added in 20% molar excess and the reaction was stirred overnight at RT. In order to remove unreacted Dau, the reaction mixture was directly injected into the HPLC on a semipreparative RP-HPLC column. MeCN/H_2O with 0.1% TFA were used as eluents. The collected fractions were evaporated to remove volatiles and lyophilized to obtain the purified peptides with >95% purity.

4.6 Kaiser test

With the Kaiser test, any primary amine can be detected through a colorimetric reaction with ninhydrin, thus the completion of a coupling or deprotection reaction can be proved. Some dry resin beads were transferred in a closable 1.5 mL tube and three drops of each of the following solutions were added:

- solution A: 1 g of ninhydrin in 20 mL of ethanol (absolute);

- solution B: 80 g of phenol in 20 mL of ethanol (absolute);

- solution C: 0.4 mL of 1 mM aqueous KCN solution in 20 mL of pyridine.

The reaction mixture was inserted for 2 min at 100 °C in a dry block A blue color of the solution or the resin beads suggested the presence of free amines, indicating the unfinished coupling reaction

(positive test). In contrast, a yellow color implied the absence of free amino groups (negative test). The duration of the test may vary depending on the protecting groups attached to the sequence.

4.7 Analytical RP-HPLC

Purity of the different peptides was confirmed by using analytical column Phenomenex Luna C18 (250 mm x 4.6 mm), 5 µm silica as stationary phase, 100Å. Linear gradient elution (0 min 0% B; 5 min 0% B; 50 min 90% B). Peaks were detected at λ = 220 nm. Flow rate 1 mL/min.

4.8 Preparative RP-HPLC, purification of the crude peptides

The crude products and the conjugates were purified on a KNAUER 2501 HPLC system (KNAUER, Bad Homburg, Germany) using a preparative Phenomenex Luna C18 column (250 mm x 21.2 mm) with 10 µm silica (100 Å pore size) (Torrance, CA). Linear gradient elution (0 min 15% B; 5 min 15% B; 55 min 70% B) with eluent A (0.1% TFA in water) and eluent B (0.1% TFA in MeCN-H_2O (80:20, v/v)) was used at a flow rate of 12 mL/min. Peaks were detected at 220 nm.

4.9 Mass spectrometry

Electrospray (ESI) mass spectrometric analyses were carried out on an Esquire 3000+ ion trap mass spectrometer (Bruker Daltonics, Bremen, Germany). Spectra were acquired in the 50-2500 *m/z* range. Samples were dissolved in a mixture of 20% MeCN and 80% water.

4.10 Cell culturing

KS (Kaposi's sarcoma) cells derived from human Kaposi sarcoma and HT-29 (human colorectal adenocarcinoma) cell line obtained from ATCC were cultured in RPMI 1640 medium with glutamine (Roswell Park Memorial Institute Medium, Lonza, Basel, Switzerland), and MRC-5 (normal

fibroblast) cells were cultured in DMEM (Dulbecco's Modified Eagle's Medium, Lonza). All media were supplemented with 10% heat-inactivated FBS (Fetal Bovine Serum, Euroclone, Milan, Italy), and with 1% penicillin/streptomycin (Sigma-Aldrich). All the cell culture experiments were carried out under a laminar flow hood in sterile conditions. The culturing of cells was carried out at 5% CO_2 at 37 °C.

4.11 Cell viability assay for NGR peptides-drug conjugates

For evaluation of *in vitro* antiproliferative activity of NGR-Dau conjugates and free Dau, cell viability was determined by MTT assay (3-(4,5-dimethylthiazol-2-yl)-2,5-diphenyl-tetrazolium bromide (Sigma Aldrich)). After standard harvesting of the cells by trypsin-EDTA (Lonza), 5×10^3 till 10×10^3 cells per well depending on cell line, were seeded in serum containing growth medium to 96-well plates and incubated. After 24 hours, cells were treated with various concentrations of conjugates (32 nM-100 μM) or free Dau (0.1-10 μM), dissolved in serum free medium, and incubated under standard conditions. Control wells were treated with serum containing medium. Two treatment regimens were used. According to the first type, after 24 hours of treatment, cells were washed with serum free medium, and then cultured in serum containing medium for an additional 48 hours. In case of the second type, cells were treated for 72 hours continuously. Afterward, MTT assay was performed in order to determine cell viability, by adding 20 μL of MTT solution (5 mg/mL in PBS) to each well and after 2 hours of incubation at 37 °C, the supernatant was removed. The formazan crystals were dissolved in 100 μL of a 1:1 solution of DMSO (Sigma-Aldrich):EtOH (Molar Chemicals) and the absorbance was measured after 15 min at λ = 570 nm by using a microplate reader (Bio-Rad, model 550, Hercules, CA, USA). The IC_{50} values of the conjugates and free drug were calculated using

GraphPad Prism 6 (GraphPad Software, San Diego, CA, USA). The experiments were done in triplicate, and each experiment was repeated twice.

4.12 Flow cytometry studies

The cellular uptake of the bioconjugates was studied on KS and HT-29 cells. Cells were seeded (1.5×10^5 cells/well) to 24-well plates (Sarstedt, Nümbrecht Germany), incubated 24 h at 37 °C, and treated with conjugates at concentrations of 2, 10, 50 and 100 µM for 6 h. After harvesting, cells were washed with PBS. Fluorescence intensity was detected using the PE-A channel of Attune NxT Flow Cytometer (Thermo Fisher Scientific, USA). Number and proportion of the cells with intracellular fluorescence were evaluated and calculated using Attune NxT 2.6. software (Thermo Fisher Scientific).

4.13 CD13 cell surface expression level detection with immunocytochemistry

CD13 expression was detected by confocal microscopy. KS and HT-29 cells were seeded (10^5 cells/well) to coverslip-containing (Assistant, Karl Hecht GmbH&Co KG, Sondheim/Rhön Germany) 24-well plates (Sarstedt) one day before immunostaining. Nuclei were stained with Hoechst 33342 solution (0.2 µg/mL, Thermo Fisher Scientific, diluted in serum-free medium) for 10 min at 37 °C. After washing, cells were fixed with 4% paraformaldehyde (Sigma-Aldrich) for 20 min at 37 °C followed by blocking with 3% Bovine Serum Albumine (BSA, Sigma-Aldrich, dissolved in PBS) for 1 h at room temperature. Anti-CD13 antibody (clone: WM-15, FITC-conjugated, eBioscience, 1:100, diluted in 1% BSA containing PBS) was added to the wells overnight at 4 °C. After washing three times with PBS, coverslips were mounted to cover glasses using Mowiol 4-88 (Sigma-Aldrich). Imaging was carried out using a ZEISS LSM-710 system (Carl Zeiss microscopy GmbH, Jena,

Germany with a 40x/1.4 Plan-Apochromat oil immersion objective. Images were processed with ZEN (Carl Zeiss microscopy GmbH).

4.14 Stability studies

4.14.1 Stability in cell culture medium

To measure the stability, each of the conjugates were dissolved in DMSO (2% of the final volume), following the addition of 10% FBS containing complete cell culture medium (DMEM CM) up to the 1 mg/mL final peptide concentration. Every conjugate was incubated at 37 °C. Samples were taken at experiment time of 0 h, 6 h and 72 h, respectively, and components were purified with Amicon Ultra Centrifugal Filters (cut off 10K, Merck Millipore). The membranes were washed with eluent A (used for HPLC) to a final volume of 0.5mL, and centrifugated at 13000 rpm for three times, this for each sample. Considering the adsorption characteristic of Dau only the small molecules of the medium eluted in this step. The final stage was the washing step with eluent B (used for HPLC) 1 x 15 min centrifugation at 13000 rpm, followed by lyophilization to concentrate and analyze the samples.

4.14.2 Stability in murine plasma

The conjugates were dissolved in water and diluted with plasma (90%) to a final peptide concentration of 10 µM. The mixture was incubated at 37 °C and aliquots were taken after 0.5, 1, 2, 4, and 8 h. To quench the reaction, 10 µL of acetic acid was added. Large human plasma proteins were excluded using ultra centrifugal filters with a cut-off of 10 kDa. The lower molecular weight fractions were analyzed by LC-MS. As controls, 90% plasma plus 10% water and 10 µM of bioconjugate in 100% water were incubated and analyzed in the same manner. The rat liver lysosomal homogenate was set as previously described.[261] Murine plasma was collected, isolated and provided

from the research group of Dr. József Tóvári at the National Institute of Oncology in Budapest (OOI). Water for chromatography (LC-MS Grade) LiChrosolv®, MeCN hypergrade for LC-MS LiChrosolv®, formic and acetic acid 98% - 100% for LC-MS LiChropur®, NH_4OAc and NaOAc were provided by Merck Millipore.

4.14.3 Degradation in rat liver homogenate

For this experiment rat liver lysosomal homogenate was prepared. Protein concentration was detected with bicinchoninic acid (Pierce BCA protein assay) following the manufacturer's protocol (Thermo Fischer Scientific), and it was 17.4 μg/μL. Bioconjugates were dissolved in double destilled water till 4 μg/μL of concentration. The components were further diluted to a concentration of 0.2 μg/μL using 0.2 M of NH_4OAc (pH 5.0). The homogenate was then suspended with 0.2 M NH_4OAc (pH 5.0) to a concentration of 3.48 μg/μL. The homogenate was then added to the conjugates in a ratio of 1:1 w/w. All the degradation mixtures were incubated at 37 °C, samples of 13 μL were collected at experimental time of 0 h, 6 h and 72 h. Reaction mixtures were quenched by the addition of 2 μL of formic acid. LC-MS analysis was performed at the end.

4.15 In vivo antitumor activity studies

4.15.1 Experimental animals

Adult inbred BALB/c mice from a specified pathogen free (SPF) breeding of the National Institute of Oncology (Budapest, Hungary) were used in acute and chronic toxicity studies. Mice were kept in a sterile environment in Makrolon® cages at 22-24 °C (40-50% humidity), with a lighting regulation of 12/12 hours light/dark. The animals had free access to fresh water and were fed with a sterilized standard diet (VRF1, autoclavable, Akronom Kft., Budapest, Hungary) *ad libitum*. The

immunodeficient SCID mice on a C.B.-17 background were bred in specific opportunistic and pathogen free isolator breeding rooms. The breeding isolator was supplied with corn-cob bedding and standard VRF1 rodent chow and with acidified (pH 3) sterilized distilled water. The mice from the breeding rooms were used for the subcutaneous model of KS and orthotopic model of human colon cancer. They were held in filter-top boxes in the experimental barrier rooms, and every box-opening was performed under a Class 100 laminar flow hood. The animal housing density was in accordance with the international recommendations. The cage components, corn-cob bedding and food (VRF1 from Special Diet Services) were steam-sterilized in an autoclave (121 °C, 20 min). The animals used in these studies were cared for according to the "Guiding Principles for the Care and Use of Animals" based upon the Helsinki declaration, and they were approved by the local ethical committee. Permission license for breeding and performing experiments with laboratory animals: PEI/001/1738-3/2015 and PEI/001/2574–6/2015.

4.15.2 Acute and chronic toxicity studies on in vivo model

In order to determine toxicity of conjugates on healthy animals *in vivo*, acute and chronic toxicity studies were performed. In acute toxicity study, adult BALB/c male mice (26-32 g) were treated by a single intraperitoneal (*i.p.*) injection of both conjugates at the start of the experiment, administrating 4 different doses: 25, 12.5, 6.25 and 3.125 mg/kg Dau content (3 mice per group). In chronic toxicity studies, adult male BALB/c mice (25-31g) were treated with both conjugates at dose of 10 mg/kg Dau content on day 1, 3, 7, 9 and 11 (5 treatments, 3 mice per group). The toxicity was evaluated on the basis of life span, behavior and appearance of the mice, as well as body weight. Parameters were followed for 14 days.

4.15.3 Kaposi's sarcoma tumor model

Kaposi's sarcoma (KS) cells were injected into SCID female mice (19-24 g) (*s.c.*), 3 x 10^6 cells per animal in volume of 200 µL M199 medium per animal. Treatment started 35 days after cell inoculation when average tumor volume was 66 mm^3, by *i.p.* administration. Four groups by 5 animals were established and treated with the following doses and schedule: control group was treated with solvent; free Dau group was treated with a dose of 1 mg/kg on days 35, 42, 49, 56 and 63 after cell inoculation, while the groups treated with conjugates **1** and **2** were administered with a dose of 10 mg/kg Dau content, that are 33.8 and 33.5 mg/kg of each conjugate respectively, on days 35, 37, 39, 42, 45, 49, 52, 56, 59, 63 and 66 after cell inoculation. Animal weight and tumor volumes were measured initially when the treatment started and at periodic intervals according to the treatment schedule. A digital caliper was used to measure the longest (a) and the shortest diameter (b) of a given tumor. The tumor volume was calculated using the formula $V = ab^2 \times \pi/6$, whereby a and b represent the measured parameters (length and width). The experiment was terminated on day 70 after tumor transplantation (day 36 of treatment). The mice from all groups were sacrificed by cervical dislocation. Their primary tumors and livers were harvested and weighed.

4.15.4 Human colorectal adenocarcinoma tumor model

HT-29 human colon cancer cells were injected into SCID female mice subcutaneously (*s.c.*), 3 x 10^6 cells per animal in volume of 200 µL M199 medium per animal, in order to establish tumor for transplantation. After 2 weeks, the mice with palpable tumors were sacrificed by cervical dislocation, and the subcutaneous tumor was dissected out aseptically. Tumor pieces of 2 mm^3 were transplanted orthotopically, under aseptic conditions into anesthetized (narcotic mixture: tiletamine, zolazepam, xylazine, butorphanol) SCID female mice (19-25 g). A small midline incision (0.5 cm) was made and

the colorectal part of the intestine was exteriorized. Serosa of the site where the tumor pieces were to be implanted were removed. Tumor tissue fragments of HT-29 human colon tumor were implanted on the top of the animal intestine; an 8/0 surgical (polypropylene) suture was used to suture it on the wall of the intestine. The intestine was returned to the abdominal cavity, and the abdominal wall was closed with 4/0 surgical (polyglycolic acid) sutures. The wound was sterilized, and the animals were kept in a sterile environment. On the next day, no sign of pain and/or stress of the mice was observed. The treatments started 6 days after tumor transplantation by *i.p.* administration of the compounds dissolved in distilled water for injection. 8 mice per group were used. One group of mice were treated with free Dau (1 mg/kg body weight) on days 6, 13 and 20 after tumor transplantation. Animal groups treated with compounds **1** and **2** were administered with a dose of 10 mg/kg Dau content (33.8 and 33.5 mg/kg of each conjugate, respectively) on days 6, 8, 10, 13, 17, 20 and 24 after tumor transplantation. Control group was treated with sterile water (Pharmamagist Kft., Budapest, Hungary) as solvent. The experiment was terminated on day 27 after tumor transplantation (day 22 of treatment). Daunorubicin treated group was terminated on day 24 after tumor transplantation (day 19 of treatment) due to significant weight loss of the animals. The mice from all groups were sacrificed by cervical dislocation. Their primary tumors and livers were harvested and weighed, while metastases were counted in other organs.

4.15.5 Ex vivo studies: proliferative index and vascularization in tumor tissues

The routinely formalin-fixed tumors were dehydrated in a graded series of ethanol, infiltrated with xylene and embedded into paraffin at a temperature not exceeding 60 °C. Two microns thick sections were mounted on Superfrost slides (Thermo Shandon, Runcorn, UK) and manually deparaffinized. To block endogenous peroxidase activity, slides were treated for 20 min at RT with 3% H_2O_2 in

methanol. Slides were immersed in 6% citrate buffer (pH=6) and exposed to 98 °C water bath for 40 min. Afterwards, slides were primarily treated with antibody against human KI-67 (DAKO, Glostrup, Denmark, 1:40) and endothelial marker CD31 (Dianova, Hamburg, Germany, 1:20) incubated for 1 hour at RT. After washing, Biotinylated Link (Dako) secondary antibody was applied for KI-67 samples for 10 min at RT, while rabbit anti-rat IgG (Novus Biologicals, Centennial, CO, USA) was applied for CD31 samples for 1 h at RT. For visualization of KI-67 samples, supersensitive one step polymer HRP (Biogenex, Fremont, CA, USA) was used with 3-amino-9-ethylcarbazole (AEC) as chromogen, while for visualization of CD31 samples match 2 rabbit-HRP polymer (Biocare Medical, Concord, CA, USA) with AEC (Vectorlabs, Burlingame, CA, USA) were used. Staining without the primary antibody served as negative control. The KI-67-positive tumor cells were counted manually per fields of vision under light microscope (400-fold magnification), and 3 fields of view per tumor were evaluated. Proliferation index was calculated as percentage of KI-67 positive cells from all cells in the field of view. The CD31-positive blood vessels were counted manually using light microscope (200-fold magnification), and 3 fields of view per tumor were evaluated.

4.15.6 Statistical analysis

The statistical analyses were performed by GraphPad Prism 6 (GraphPad Software) using the non-parametric Mann-Whitney (independent samples) test. The experimental data were filtered by Gaussian statistics where P-values lower than 0.05 were considered statistically significant.

4.16 General methods to prepare DKP3-f3 scaffold

All manipulations requiring anhydrous conditions were carried out in flame-dried glassware, with magnetic stirring and under a nitrogen atmosphere. All commercially available reagents were used as

received. Anhydrous solvents were purchased from commercial sources and withdrawn from the container by syringe, under a slight positive pressure of nitrogen. Reactions were monitored by analytical thin layer chromatography using 0.25 mm pre-coated silica gel glass plates (DURASIL-25 UV254) and compounds visualized using UV fluorescence, a ceric ammonium molibdate solution (Pancaldi's reagent) and ninhydrine. Flash column chromatography was performed according to the method of Still and co-workers103 using Chromagel 60 ACC (40-63 μm) silica gel.

4.16.1 Nuclear magnetic resonance (NMR)

Proton NMR spectra were recorded on a spectrometer operating at 400.16 MHz or with a spectrometer operating at 500.13 MHz. Proton chemical shifts are reported in ppm (δ) with residual solvent referenced relative to tetramethylsilane (TMS) as the internal standard.

4.16.2 Mass spectrometry studies of DKP-peptides

ESI-MS spectra were recorded on the ion trap mass spectrometer Finnigan LCQ Advantage analysing a solution H_2O/MeCN 1:1(v/v) + 0,1% TFA.

4.17 Conversion of N-Boc-protected Aaa

To a solution of the *N*-Boc-protected compound in DCM (0.13 M) was added half volume of TFA and the reaction was stirred for 2 h at room temperature. The solvent was evaporated, toluene (2×) was added followed by evaporation, and then Et_2O was added and evaporated to afford the corresponding TFA salt.

4.18 Synthesis and preparation of hydrazoic acid

In a three-necked flask, NaN_3 (3 g) was dissolved in H_2O (3 mL). Once completely dissolved, toluene (20 mL) was added and the reaction mixture was cooled to 0 °C under vigorous stirring. Concentrated H_2SO_4 (1.2 mL) was added extremely slowly, so that the solution temperature did not exceed 10 °C. The reaction was stirred for one hour at 0 °C and then filtered on cotton wool. The residue was washed twice with toluene. 1 mL of HN_3 solution in toluene was diluted in distilled water (50 mL) and titrated by adding NaOH (0.1 M), using phenolphthalein as indicator.

4.19 Synthesis of N3-DKP3-f3-OAll

To a solution of DKP3-f3-OH (500mg, 1 eq) in DCM/toluene (20 mL, 4:6), under nitrogen atmosphere and at -15 °C, PPh_3 (1.1 g, 1.2 eq) was added and the mixture was stirred. After complete dissolution, hydrazoic acid (0.75 M in toluene, 5 mL, 2 eq) was added followed by dropwise addition of Diisipropyl azodicarboxylate DIAD (200 µL, 1.2 eq): the reaction was stirred at -15 °C for 4 h. The reaction mixture was loaded on silica gel without previous evaporation and purified by flash chromatography (EtOAc/hexane from 1:1 (v/v) to EtOAc 100%) affording the desired product as a white foam.

4.19.1 Synthesis of Boc-DKP3-f3-OAll

To a solution of azide (100 mg, 1 eq) in THF (4 mL), at -20 °C and under nitrogen atmosphere, Me_3P (1.2 mL of 1 M solution in THF, 2.5 eq) and 2-(*t*-butoxycarbonyloxyimino)-2-phenylacetonitrile (Boc-ON, 300 mg, 2.5 eq) were added: the reaction was stirred at room temperature for 5 h. The mixture was diluted with DCM (100 mL) and washed with H_2O (4×100 mL) and brine (1×100 mL). The organic phase was dried over Na_2SO_4 and volatiles were removed under reduced

pressure. The residue was purified by flash chromatography on silica gel (DCM/MeOH from 100% DCM to 9:1) affording the desired product as a white foam.

4.19.2 Synthesis of Cbz-Arg(Mtr)-DKP3-f3-OAll

Cbz-Arg-(Mtr)-OH (112 mg, 1.2 eq) was dissolved in DMF (3 mL) under nitrogen atmosphere. HATU (70 mg, 1.2 eq), HOAt (25 mg, 1.2 eq) and DIPEA (30 μL, 3 eq) were added at 0 °C: the mixture was stirred at 0 °C for 30 minutes. Boc-(3S,6R)-DKP-f3-OAll was deprotected according to (conversion of *N*-Boc Aaa). The corresponding trifluoroacetate salt (65 mg, 1 eq) was dissolved in DMF (2 mL) and DIPEA (80 μL, 1 eq) was added: the reaction mixture was stirred at 0 °C for 1 h, then at room temperature overnight. The mixture was diluted with EtOAc (150 mL) and washed with $KHSO_4$ 1 M (3×90 mL), saturated aqueous $NaHCO_3$ (3×90 mL) and brine (1×100 mL). The organic phase was dried over Na_2SO_4 and the volatiles were removed under reduced pressure.

4.19.3 Synthesis of the dipeptide Fmoc-Asn(Trt)-Gly-OBn

To a solution of Fmoc-Asn(Trt)-OH (1.15 g, 1.2 eq) in DMF (28 mL), at 0 °C and under nitrogen atmosphere, HATU (735 mg, 1.2 eq), HOAt (270 mg, 1.2 eq) and DIPEA (950 μL, 2.0 eq) were added: the reaction was stirred at 0 °C for 30 min. A solution of H_2N-Gly-OBn·TFA (300 mg, 1 eq) in DMF (30 mL) and DIPEA (3 eq) was added dropwise to the previous solution: the reaction mixture was stirred at 0 °C for 1 h and at room temperature overnight. The mixture was diluted with EtOAc (300 mL) and washed with $KHSO_4$ 1 M (3×100 mL), saturated aqueous $NaHCO_3$ (3×100 mL) and brine (1×100 mL). The organic phase was dried over Na_2SO_4 and volatiles were removed under reduced pressure. The residue was purified by flash chromatography on silica gel (DCM/MeOH from DCM 100% to DCM/MeOH 9:1 (v/v), solid load) affording the desired product as a white foam.

4.19.4 Fmoc cleavage from dipeptide

To a solution of Fmoc-Asn(Trt)-Gly-OBn (680 mg, 1 eq) in DMF (30 mL), at 0 °C under nitrogen atmosphere, piperidine (500 µL, 5 eq) was added and the reaction mixture was stirred at 0 °C for 10 min and at room temperature for 3 h. The mixture was diluted with EtOAc (300 mL) and washed with H_2O (4×100 mL). The organic phase was dried over Na_2SO_4 and volatiles were removed under reduced pressure. The residue was purified by a Grace Reveleris system (column: Reveleris Silica 40 g; liquid load; flow rate: 33 mL/min; gradient: from DCM/MeOH 98/2 (v/v) to 8/2 (v/v) in 35 min) affording the desired product as a white foam.

4.19.5 Allyl cleavage and synthesis of Cbz-Arg(Mtr)-DKP3-f3-OH

To a solution of Cbz-Arg(Mtr)-DKP3-f3-OAll (50 mg, 1 eq) under nitrogen atmosphere at 0 °C, [$Pd(PPh_3)_4$] (10 mg, 0.3 eq) and *N*-methylaniline (20 µL, 1.2 eq) were added. The reaction mixture was stirred 5 min at 0 °C and 2 h at room temperature. The mixture was diluted with DCM (20 mL) and washed with $KHSO_4$ 1 M (4×50 mL). The organic phase was dried over Na_2SO_4 and volatiles were removed under reduced pressure. The residue was purified by a Grace Reveleris system (column: Reveleris HP Silica 40 g; liquid load; flow rate: 33 mLmin-1; gradient: DCM/MeOH from 98/2 (v/v) to 8/2 (v/v) in 1 h) affording the desired product as a pale yellow foam.

4.19.6 Synthesis of Cbz-Arg(Mtr)-DKP3-f3-Asn(Trt)-Gly-OBn and benzyl group cleavage.

To a solution of H-Arg(Mtr)-DKP3-f3-OH (1 eq) in DMF (5 mL) under nitrogen atmosphere at 0 °C, HATU (1.2 eq), HOAt (1.2 eq) and DIPEA (3 eq) were added: the reaction mixture was stirred at 0 °C for 30 min, dipeptide (1.2 eq) was dissolved in DMF (5 mL) and added to the previous solution:

the reaction mixture was stirred at 0 °C for 1 h, then at room temperature overnight. The mixture was diluted with DCM (50 mL) and washed with $KHSO_4$ 1 M (4×80 mL), saturated aqueous $NaHCO_3$ (4×80 mL) and brine (1×100 mL). The organic phase was dried over Na_2SO_4 and volatiles were removed under reduced pressure.

To a solution of Cbz-Arg-DKP3-f3-Asn(Trt)-Gly-OBn (1 eq) in 10 ml THF/H_2O 1:1 (v/v), Pd/C 10% (10 mg, 0.03 mmol, 0.1 eq) was added. The mixture was purged under stirring with three cycles of vacuum/H_2 atmosphere and the reaction was stirred overnight under H_2 atmosphere. The reaction mixture was filtered on a celite pad and washed with MeOH. The filtered liquid was collected and concentrated affording the desired product as a white solid. Due to a very low quantity of compound, the sysnthesis was concluded without the actual purification, trying to characterize and detect the products using ESI-MS and NMR.

4.19.7 Cyclization

H-Arg(Mtr)-DKP3-f3-Asn(Trt)-Gly-OH was treated with TFA in the presence of ion scavengers thioanisole, ethanedithiol and phenol. The mixture was then cooled to 0 °C and flushed with N_2. Trimethylsilylbromide was added and the flask was opened, mixture was allowed to reach rt and stirred for 3 h. All volatiles were removed under reduced pressure and the acqueous phase was washed several times with ether and then concentrated to give the crude compound. Using exactly the same synthetic route also the non-functionalized version of the scaffold was obtained.

5. References

(1) Bray, F.; Ferlay, J.; Soerjomataram, I.; Siegel, R. L.; Torre, L. A.; Jemal, A. Global Cancer Statistics 2018: GLOBOCAN Estimates of Incidence and Mortality Worldwide for 36 Cancers in 185 Countries. *CA. Cancer J. Clin.* 2018, *68* (6), 394–424.

(2) Ma, X.; Yu, H. Global Burden of Cancer. *Yale J. Biol. Med.* 2006, *79* (3–4), 85–94.

(3) Mathers, C.; Organization, W. H. *The Global Burden of Disease: 2004 Update*; World Health Organization, 2008.

(4) Nagai, H.; Kim, Y. H. Cancer Prevention from the Perspective of Global Cancer Burden Patterns. *J. Thorac. Dis.* 2017, *9* (3), 448–451.

(5) Hanahan, D.; Weinberg, R. A. The Hallmarks of Cancer. *Cell* 2000, *100* (1), 57–70.

(6) WHO | The global burden of disease: 2004 update https://www.who.int/healthinfo/global_burden_disease/2004_report_update/en/ (accessed Apr 4, 2020).

(7) Saiki, I.; Fujii, H.; Yoneda, J.; Abe, F.; Nakajima, M.; Tsuruo, T.; Azuma, I. Role of Aminopeptidase N (CD13) in Tumor-Cell Invasion and Extracellular Matrix Degradation. *Int. J. Cancer* 1993, *54* (1), 137–143.

(8) Hynes, R. O. Integrins: Bidirectional, Allosteric Signaling Machines. *Cell* 2002, *110* (6), 673–687.

(9) Tarin, D. Cell and Tissue Interactions in Carcinogenesis and Metastasis and Their Clinical Significance. *Semin. Cancer Biol.* 2011, *21* (2), 72–82.

(10) Lazebnik, Y. What Are the Hallmarks of Cancer? *Nat. Rev. Cancer* 2010, *10* (4), 232–233.

(11) Hanahan, D.; Folkman, J. Patterns and Emerging Mechanisms of the Angiogenic Switch during Tumorigenesis. *Cell* 1996, *86* (3), 353–364.

(12) Chambers, A. F.; Groom, A. C.; MacDonald, I. C. Dissemination and Growth of Cancer Cells in Metastatic Sites. *Nat. Rev. Cancer* 2002, *2* (8), 563–572.

(13) Welch, D. R.; Cooper, C. R.; Hurst, D. R.; Lynch, C. C.; Martin, M. D.; Vaidya, K. S.; VanSaun, M. N.; Mastro, A. M. Metastasis Research Society–American Association for Cancer Research Joint Conference on Metastasis. *Cancer Res.* 2008, *68* (23), 9578–9582.

(14) Bacac, M.; Stamenkovic, I. Metastatic Cancer Cell. *Annu. Rev. Pathol. Mech. Dis.* 2008, *3* (1), 221–247.

(15) Martin, T. A.; Ye, L.; Sanders, A. J.; Lane, J.; Jiang, W. G. *Cancer Invasion and Metastasis: Molecular and Cellular Perspective*; Landes Bioscience, 2013.

(16) Seyfried, T. N.; Huysentruyt, L. C. On the Origin of Cancer Metastasis. *Crit. Rev. Oncog.* 2013, *18* (1–2), 43–73.

(17) Cancer invasion and metastasis: changing views - Duffy - 2008 - The Journal of Pathology - Wiley Online Library

(18) Steeg, P. S. Tumor Metastasis: Mechanistic Insights and Clinical Challenges. *Nat. Med.* 2006, *12* (8), 895–904.

(19) Yaeger, K. A.; Nair, M. N. Surgery for Brain Metastases. *Surg. Neurol. Int.* 2013, *4* (Suppl 4), S203–S208.

(20) Lorusso, G.; Rüegg, C. The Tumor Microenvironment and Its Contribution to Tumor Evolution toward Metastasis. *Histochem. Cell Biol.* 2008, *130* (6), 1091–1103.

(21) What is cancer? https://www.allaboutcancer.fi/facts-about-cancer/what-is-cancer/ (accessed May 10, 2020).

(22) Wyld, L.; Audisio, R. A.; Poston, G. J. The Evolution of Cancer Surgery and Future Perspectives. *Nat. Rev. Clin. Oncol.* 2015, *12* (2), 115–124.

(23) Papac, R. J. Origins of Cancer Therapy. *Yale J. Biol. Med.* 2001, *74* (6), 391–398.

(24) DeVita, V. T.; Chu, E. A History of Cancer Chemotherapy. *Cancer Res.* 2008, *68* (21), 8643–8653.

(25) Baskar, R.; Lee, K. A.; Yeo, R.; Yeoh, K.-W. Cancer and Radiation Therapy: Current Advances and Future Directions. *Int. J. Med. Sci.* 2012, *9* (3), 193–199.

(26) Baumann, M.; Krause, M.; Overgaard, J.; Debus, J.; Bentzen, S. M.; Daartz, J.; Richter, C.; Zips, D.; Bortfeld, T. Radiation Oncology in the Era of Precision Medicine. *Nat. Rev. Cancer* 2016, *16* (4), 234–249.

(27) Abdulkareem, I. H.; Zurmi, I. B. Review of Hormonal Treatment of Breast Cancer. *Niger. J. Clin. Pract.* 2012, *15* (1), 9.

(28) Puhalla, S.; Bhattacharya, S.; Davidson, N. E. Hormonal Therapy in Breast Cancer: A Model Disease for the Personalization of Cancer Care. *Mol. Oncol.* 2012, *6* (2), 222–236.

(29) Colleoni, M.; Giobbie-Hurder, A. Benefits and Adverse Effects of Endocrine Therapy. *Ann. Oncol.* 2010, *21* (Suppl 7), vii107–vii111.

(30) Lu, Z.-R.; Qiao, P. Drug Delivery in Cancer Therapy, Quo Vadis? *Mol. Pharm.* 2018, *15* (9), 3603–3616.

(31) Padma, V. V. An Overview of Targeted Cancer Therapy. *BioMedicine* 2015, *5* (4), 19.

(32) Corti, A.; Pastorino, F.; Curnis, F.; Arap, W.; Ponzoni, M.; Pasqualini, R. Targeted Drug Delivery and Penetration Into Solid Tumors. *Med. Res. Rev.* 2012, *32* (5), 1078–1091.

(33) Arruebo, M.; Vilaboa, N.; Sáez-Gutierrez, B.; Lambea, J.; Tres, A.; Valladares, M.; González-Fernández, A. Assessment of the Evolution of Cancer Treatment Therapies. *Cancers* 2011, *3* (3), 3279–3330.

(34) Urruticoechea, A.; Alemany, R.; Balart, J.; Villanueva, A.; Viñals, F.; Capellá, G. Recent Advances in Cancer Therapy: An Overview. *Curr. Pharm. Des.* 2010, *16* (1), 3–10.

(35) Patra, J. K.; Das; Fraceto, L.; Campos, E.; Rodríguez-Torres, M. D. P.; Acosta-Torres, L.; Diaz-Torres, L.; Grillo, R.; Swamy, M.; Sharma, S.; Habtemariam, S.; Shin, H. Nano Based Drug Delivery Systems: Recent Developments and Future Prospects. *J. Nanobiotechnology* 2018, *16*.

(36) Cheung, A.; Bax, H. J.; Josephs, D. H.; Ilieva, K. M.; Pellizzari, G.; Opzoomer, J.; Bloomfield, J.; Fittall, M.; Grigoriadis, A.; Figini, M.; Canevari, S.; Spicer, J. F.; Tutt, A. N.; Karagiannis, S. N. Targeting Folate Receptor Alpha for Cancer Treatment. *Oncotarget* 2016, *7* (32), 52553–52574.

(37) Vasir, J. K.; Labhasetwar, V. Targeted Drug Delivery in Cancer Therapy. *Technol. Cancer Res. Treat.* 2005, *4* (4), 363–374.

(38) Liang, X.-J.; Chen, C.; Zhao, Y.; Wang, P. C. Circumventing Tumor Resistance to Chemotherapy by Nanotechnology. *Methods Mol. Biol. Clifton NJ* 2010, *596*, 467–488.

(39) Thundimadathil, J. Cancer Treatment Using Peptides: Current Therapies and Future Prospects. *J. Amino Acids* 2012, *2012*, 967347.

(40) van Vlerken, L. E.; Duan, Z.; Little, S. R.; Seiden, M. V.; Amiji, M. M. Biodistribution and Pharmacokinetic Analysis of Paclitaxel and Ceramide Administered in Multifunctional Polymer-Blend Nanoparticles in Drug Resistant Breast Cancer Model. *Mol. Pharm.* 2008, *5* (4), 516–526.

(41) Krishna, R.; Mayer, L. D. Liposomal Doxorubicin Circumvents PSC 833-Free Drug Interactions, Resulting in Effective Therapy of Multidrug-Resistant Solid Tumors. *Cancer Res.* 1997, *57* (23), 5246–5253.

(42) Fracasso, P. M.; Westervelt, P.; Fears, C. L.; Rosen, D. M.; Zuhowski, E. G.; Cazenave, L. A.; Litchman, M.; Egorin, M. J.; Westerveldt, P.; Fears, C. A. Phase I Study of Paclitaxel in

Combination with a Multidrug Resistance Modulator, PSC 833 (Valspodar), in Refractory Malignancies. *J. Clin. Oncol. Off. J. Am. Soc. Clin. Oncol.* 2000, *18* (5), 1124–1134.

(43) Hasinoff, B. B.; Chee, G. L.; Thampatty, P.; Allan, W. P.; Yalowich, J. C. The Cardioprotective and DNA Topoisomerase II Inhibitory Agent Dexrazoxane (ICRF-187) Antagonizes Camptothecin-Mediated Growth Inhibition of Chinese Hamster Ovary Cells by Inhibition of DNA Synthesis. *Anticancer. Drugs* 1999, *10* (1), 47–54.

(44) Enbäck, J.; Laakkonen, P. Tumour-Homing Peptides: Tools for Targeting, Imaging and Destruction. *Biochem. Soc. Trans.* 2007, *35* (Pt 4), 780–783.

(45) Dorsam, R. T.; Gutkind, J. S. G-Protein-Coupled Receptors and Cancer. *Nat. Rev. Cancer* 2007, *7* (2), 79–94.

(46) Meng, L.; Yang, L.; Zhao, X.; Zhang, L.; Zhu, H.; Liu, C.; Tan, W. Targeted Delivery of Chemotherapy Agents Using a Liver Cancer-Specific Aptamer. *PLOS ONE* 2012, *7* (4), e33434.

(47) Aina, O. H.; Sroka, T. C.; Chen, M.-L.; Lam, K. S. Therapeutic Cancer Targeting Peptides. *Biopolymers* 2002, *66* (3), 184–199.

(48) Zhang, X.-X.; Eden, H. S.; Chen, X. Peptides in Cancer Nanomedicine: Drug Carriers, Targeting Ligands and Protease Substrates. *J. Control. Release Off. J. Control. Release Soc.* 2012, *159* (1), 2–13.

(49) Ehrlich, P. P. Ehrlich, Anwendung Und Wirkung von Salvarsan. Deutsche Medizinische Wochenschrift: 2437-2438. 1910.

(50) Valent, P.; Groner, B.; Schumacher, U.; Superti-Furga, G.; Busslinger, M.; Kralovics, R.; Zielinski, C.; Penninger, J. M.; Kerjaschki, D.; Stingl, G.; Smolen, J. S.; Valenta, R.; Lassmann, H.; Kovar, H.; Jäger, U.; Kornek, G.; Müller, M.; Sörgel, F. Paul Ehrlich (1854-1915) and His Contributions to the Foundation and Birth of Translational Medicine. *J. Innate Immun.* 2016, *8* (2), 111–120.

(51) Witkop, B. Paul Ehrlich and His Magic Bullets, Revisited. *Proc. Am. Philos. Soc.* 1999, *143* (4), 540–557.

(52) Lode, H. N.; Xiang, R.; Becker, J. C.; Gillies, S. D.; Reisfeld, R. A. Immunocytokines: A Promising Approach to Cancer Immunotherapy. *Pharmacol. Ther.* 1998, *80* (3), 277–292.

(53) Wang, R. E.; Niu, Y.; Wu, H.; Amin, M. N.; Cai, J. Development of NGR Peptide-Based Agents for Tumor Imaging. *Am. J. Nucl. Med. Mol. Imaging* 2011, *1* (1), 36–46.

(54) Kerbel, R.; Folkman, J. Clinical Translation of Angiogenesis Inhibitors. *Nat. Rev. Cancer* 2002, *2* (10), 727–739.

(55) Risau, W.; Flamme, I. Vasculogenesis. *Annu. Rev. Cell Dev. Biol.* 1995, *11* (1), 73–91.

(56) Hurwitz, H.; Fehrenbacher, L.; Novotny, W.; Cartwright, T.; Hainsworth, J.; Heim, W.; Berlin, J.; Baron, A.; Griffing, S.; Holmgren, E.; Ferrara, N.; Fyfe, G.; Rogers, B.; Ross, R.; Kabbinavar, F. Bevacizumab plus Irinotecan, Fluorouracil, and Leucovorin for Metastatic Colorectal Cancer. *N. Engl. J. Med.* 2004, *350* (23), 2335–2342.

(57) Corti, A.; Curnis, F.; Arap, W.; Pasqualini, R. The Neovasculature Homing Motif NGR: More than Meets the Eye. *Blood* 2008, *112* (7), 2628–2635.

(58) Arap, W.; Pasqualini, R.; Ruoslahti, E. Cancer Treatment by Targeted Drug Delivery to Tumor Vasculature in a Mouse Model. *Science* 1998, *279* (5349), 377–380.

(59) Folkman, J. Angiogenesis in Cancer, Vascular, Rheumatoid and Other Disease. *Nat. Med.* 1995, *1* (1), 27–31.

(60) Finn, O. J. Immuno-Oncology: Understanding the Function and Dysfunction of the Immune System in Cancer. *Ann. Oncol. Off. J. Eur. Soc. Med. Oncol.* 2012, *23 Suppl 8*, viii6-9.

(61) Hoos, A. Development of Immuno-Oncology Drugs - from CTLA4 to PD1 to the next Generations. *Nat. Rev. Drug Discov.* 2016, *15* (4), 235–247.

(62) Barros-Oliveira, M. da C.; Costa-Silva, D. R.; Andrade, D. B. de; Borges, U. S.; Tavares, C. B.; Borges, R. S.; Silva, J. de M.; Silva, B. B. da. Use of Anastrozole in the Chemoprevention and Treatment of Breast Cancer: A Literature Review. *Rev. Assoc. Medica Bras. 1992* 2017, *63* (4), 371–378.

(63) Fradet, Y. Bicalutamide (Casodex®) in the Treatment of Prostate Cancer. *Expert Rev. Anticancer Ther.* 2004, *4* (1), 37–48.

(64) Hackshaw, A.; Baum, M.; Fornander, T.; Nordenskjold, B.; Nicolucci, A.; Monson, K.; Forsyth, S.; Reczko, K.; Johansson, U.; Fohlin, H.; Valentini, M.; Sainsbury, R. Long-Term Effectiveness of Adjuvant Goserelin in Premenopausal Women With Early Breast Cancer. *JNCI J. Natl. Cancer Inst.* 2009, *101* (5), 341–349.

(65) Vogel, C. L.; Johnston, M. A.; Capers, C.; Braccia, D. Toremifene for Breast Cancer: A Review of 20 Years of Data. *Clin. Breast Cancer* 2014, *14* (1), 1–9.

(66) Schuster, S.; Biri-Kovács, B.; Szeder, B.; Farkas, V.; Buday, L.; Szabó, Z.; Halmos, G.; Mező, G. Synthesis and in Vitro Biochemical Evaluation of Oxime Bond-Linked Daunorubicin-GnRH-III Conjugates Developed for Targeted Drug Delivery. *Beilstein J. Org. Chem.* 2018, *14*, 756–771.

(67) Tripodi, A. A. P.; Tóth, S.; Enyedi, K. N.; Schlosser, G.; Szakács, G.; Mező, G. Development of Novel Cyclic NGR Peptide-Daunomycin Conjugates with Dual Targeting Property. *Beilstein J. Org. Chem.* 2018, *14*, 911–918.

(68) Cazzamalli, S.; Corso, A. D.; Neri, D. Targeted Delivery of Cytotoxic Drugs: Challenges, Opportunities and New Developments. *Chimia* 2017, *71* (10), 712–715.

(69) Srinivasarao, M.; Low, P. S. Ligand-Targeted Drug Delivery. *Chem. Rev.* 2017, *117* (19), 12133–12164.

(70) Srinivasarao, M.; Galliford, C. V.; Low, P. S. Principles in the Design of Ligand-Targeted Cancer Therapeutics and Imaging Agents. *Nat. Rev. Drug Discov.* 2015, *14* (3), 203–219.

(71) Vrettos, E. I.; Mező, G.; Tzakos, A. G. On the Design Principles of Peptide–Drug Conjugates for Targeted Drug Delivery to the Malignant Tumor Site. *Beilstein J. Org. Chem.* 2018, *14* (1), 930–954.

(72) Kapuvári, B.; Hegedüs, R.; Schulcz, Á.; Manea, M.; Tóvári, J.; Gacs, A.; Vincze, B.; Mező, G. Improved in Vivo Antitumor Effect of a Daunorubicin - GnRH-III Bioconjugate Modified by Apoptosis Inducing Agent Butyric Acid on Colorectal Carcinoma Bearing Mice. *Invest. New Drugs* 2016, *34* (4), 416–423.

(73) Schlage, P.; Mezo, G.; Orbán, E.; Bosze, S.; Manea, M. Anthracycline-GnRH Derivative Bioconjugates with Different Linkages: Synthesis, in Vitro Drug Release and Cytostatic Effect. *J. Control. Release Off. J. Control. Release Soc.* 2011, *156* (2), 170–178.

(74) Mezõ, G.; Biri-Kovács, B.; Pethõ, L.; Sabine, S.; Kiss, K.; Oláhné Szabó, R.; Ranđelović, I.; Tóvári, J. [Optimization of peptide-drug conjugates for targeted tumor therapy]. *Magy. Onkol.* 2019, *63* (4), 290–300.

(75) Rawla, P.; Sunkara, T.; Raj, J. P. Role of Biologics and Biosimilars in Inflammatory Bowel Disease: Current Trends and Future Perspectives. *J. Inflamm. Res.* 2018, *11*, 215–226.

(76) Baumgart, D. C.; Misery, L.; Naeyaert, S.; Taylor, P. C. Biological Therapies in Immune-Mediated Inflammatory Diseases: Can Biosimilars Reduce Access Inequities? *Front. Pharmacol.* 2019, *10*.

(77) Hirten, R. P.; Iacucci, M.; Shah, S.; Ghosh, S.; Colombel, J.-F. Combining Biologics in Inflammatory Bowel Disease and Other Immune Mediated Inflammatory Disorders. *Clin. Gastroenterol. Hepatol.* 2018, *16* (9), 1374–1384.

(78) Kaniewska, M.; Eder, P.; Gąsiorowska, A.; Gonciarz, M.; Kierkuś, J.; Małecka-Panas, E.; Rydzewska, G. Biosimilar Biological Drugs in the Treatment of Inflammatory Bowel Diseases. *Przegląd Gastroenterol.* 2019, *14* (4), 223–227.

(79) Her, M.; Kavanaugh, A. Alterations in Immune Function with Biologic Therapies for Autoimmune Disease. *J. Allergy Clin. Immunol.* 2016, *137* (1), 19–27.

(80) Marcucci, F.; Caserta, C. A.; Romeo, E.; Rumio, C. Antibody-Drug Conjugates (ADC) Against Cancer Stem-Like Cells (CSC)—Is There Still Room for Optimism? *Front. Oncol.* 2019, *9*.

(81) Lucas, A. T.; Robinson, R.; Schorzman, A. N.; Piscitelli, J. A.; Razo, J. F.; Zamboni, W. C. Pharmacologic Considerations in the Disposition of Antibodies and Antibody-Drug Conjugates in Preclinical Models and in Patients. *Antibodies* 2019, *8* (1), 3.

(82) Dan, N.; Setua, S.; Kashyap, V. K.; Khan, S.; Jaggi, M.; Yallapu, M. M.; Chauhan, S. C. Antibody-Drug Conjugates for Cancer Therapy: Chemistry to Clinical Implications. *Pharmaceuticals* 2018, *11* (2).

(83) Nejadmoghaddam, M.-R.; Minai-Tehrani, A.; Ghahremanzadeh, R.; Mahmoudi, M.; Dinarvand, R.; Zarnani, A.-H. Antibody-Drug Conjugates: Possibilities and Challenges. *Avicenna J. Med. Biotechnol.* 2019, *11* (1), 3–23.

(84) Ecker, D. M.; Jones, S. D.; Levine, H. L. The Therapeutic Monoclonal Antibody Market. *mAbs* 2015, *7* (1), 9–14.

(85) Casi, G.; Neri, D. Antibody–Drug Conjugates and Small Molecule–Drug Conjugates: Opportunities and Challenges for the Development of Selective Anticancer Cytotoxic Agents. *J. Med. Chem.* 2015, *58* (22), 8751–8761.

(86) AlDeghaither, D.; Smaglo, B. G.; Weiner, L. M. Beyond Peptides and MAbs - Current Status and Future Perspectives for Biotherapeutics with Novel Constructs. *J. Clin. Pharmacol.* 2015, *55* (0 3), S4–S20.

(87) Polakis, P. Antibody Drug Conjugates for Cancer Therapy. *Pharmacol. Rev.* 2016, *68* (1), 3–19.

(88) Perez, H. L.; Cardarelli, P. M.; Deshpande, S.; Gangwar, S.; Schroeder, G. M.; Vite, G. D.; Borzilleri, R. M. Antibody-Drug Conjugates: Current Status and Future Directions. *Drug Discov. Today* 2014, *19* (7), 869–881.

(89) Polatuzumab vedotin (Drug Description) » ADC Review https://www.adcreview.com/polatuzumab-vedotin-drug-description/ (accessed Apr 9, 2020).

(90) Joubert, N.; Denevault-Sabourin, C.; Bryden, F.; Viaud-Massuard, M.-C. Towards Antibody-Drug Conjugates and Prodrug Strategies with Extracellular Stimuli-Responsive Drug Delivery in the Tumor Microenvironment for Cancer Therapy. *Eur. J. Med. Chem.* 2017, *142*, 393–415.

(91) Uy, N.; Nadeau, M.; Stahl, M.; Zeidan, A. M. Inotuzumab Ozogamicin in the Treatment of Relapsed/Refractory Acute B Cell Lymphoblastic Leukemia. *J. Blood Med.* 2018, *9*, 67–74.

(92) Bertamini, L.; Nanni, J.; Marconi, G.; Abbenante, M.; Robustelli, V.; Bacci, F.; Matti, A.; Paolini, S.; Sartor, C.; Monaco, S. L.; Fontana, M. C.; De Polo, S.; Cavo, M.; Curti, A.; Martinelli, G.; Papayannidis, C. Inotuzumab Ozogamicin Is Effective in Relapsed/Refractory Extramedullary B Acute Lymphoblastic Leukemia. *BMC Cancer* 2018, *18*.

(93) Appelbaum, F. R.; Bernstein, I. D. Gemtuzumab Ozogamicin for Acute Myeloid Leukemia. *Blood* 2017, *130* (22), 2373–2376.

(94) Baron, J.; Wang, E. S. Gemtuzumab Ozogamicin for Treatment of Acute Myeloid Leukemia. *Expert Rev. Clin. Pharmacol.* 2018, *11* (6), 549–559.

(95) Satomaa, T.; Pynnönen, H.; Vilkman, A.; Kotiranta, T.; Pitkänen, V.; Heiskanen, A.; Herpers, B.; Price, L. S.; Helin, J.; Saarinen, J. Hydrophilic Auristatin Glycoside Payload Enables Improved Antibody-Drug Conjugate Efficacy and Biocompatibility. *Antibodies* 2018, *7* (2).

(96) Zhao, N.; Qin, Y.; Liu, H.; Cheng, Z. Tumor-Targeting Peptides: Ligands for Molecular Imaging and Therapy. *Anticancer Agents Med. Chem.* 2018, *18* (1), 74–86.

(97) Zhuang, C.; Guan, X.; Ma, H.; Cong, H.; Zhang, W.; Miao, Z. Small Molecule-Drug Conjugates: A Novel Strategy for Cancer-Targeted Treatment. *Eur. J. Med. Chem.* 2019, *163*, 883–895.

(98) Kapoor, P.; Singh, H.; Gautam, A.; Chaudhary, K.; Kumar, R.; Raghava, G. P. S. TumorHoPe: A Database of Tumor Homing Peptides. *PloS One* 2012, *7* (4), e35187.

(99) Li, Z. J.; Cho, C. H. Peptides as Targeting Probes against Tumor Vasculature for Diagnosis and Drug Delivery. *J. Transl. Med.* 2012, *10 Suppl 1*, S1.

(100) Accardo, A.; Aloj, L.; Aurilio, M.; Morelli, G.; Tesauro, D. Receptor Binding Peptides for Target-Selective Delivery of Nanoparticles Encapsulated Drugs. *Int. J. Nanomedicine* 2014, *9*, 1537–1557.

(101) Zhong, Y.; Meng, F.; Deng, C.; Zhong, Z. Ligand-Directed Active Tumor-Targeting Polymeric Nanoparticles for Cancer Chemotherapy. *Biomacromolecules* 2014, *15* (6), 1955–1969.

(102) Petrenko, V. A.; Jayanna, P. K. Phage Protein-Targeted Cancer Nanomedicines. *FEBS Lett.* 2014, *588* (2), 341–349.

(103) Shapira, S.; Fokra, A.; Arber, N.; Kraus, S. Peptides for Diagnosis and Treatment of Colorectal Cancer. *Curr. Med. Chem.* 2014, *21* (21), 2410–2416.

(104) Dai, T.; Li, N.; Zhang, L.; Zhang, Y.; Liu, Q. A New Target Ligand Ser-Glu for PEPT1-Overexpressing Cancer Imaging. *Int. J. Nanomedicine* 2016, *11*, 203–212.

(105) Su, H.; Koo, J. M.; Cui, H. One-Component Nanomedicine. *J. Control. Release Off. J. Control. Release Soc.* 2015, *219*, 383–395.

(106) Räder, A. F. B.; Weinmüller, M.; Reichart, F.; Schumacher-Klinger, A.; Merzbach, S.; Gilon, C.; Hoffman, A.; Kessler, H. Orally Active Peptides: Is There a Magic Bullet? *Angew. Chem. Int. Ed Engl.* 2018, *57* (44), 14414–14438.

(107) Vergote, I.; Leamon, C. P. Vintafolide: A Novel Targeted Therapy for the Treatment of Folate Receptor Expressing Tumors. *Ther. Adv. Med. Oncol.* 2015, *7* (4), 206–218.

(108) Cazzamalli, S.; Corso, A. D.; Neri, D. Linker Stability Influences the Anti-Tumor Activity of Acetazolamide-Drug Conjugates for the Therapy of Renal Cell Carcinoma. *J. Control. Release Off. J. Control. Release Soc.* 2017, *246*, 39–45.

(109) Ahmad Fuaad, A. A. H.; Azmi, F.; Skwarczynski, M.; Toth, I. Peptide Conjugation via CuAAC 'Click' Chemistry. *Molecules* 2013, *18* (11), 13148–13174.

(110) Merrifield, R. B. Solid-Phase Peptide Synthesis. III. An Improved Synthesis of Bradykinin*. *Biochemistry* 1964, *3* (9), 1385–1390.

(111) Chan, W.; White, P. *Fmoc Solid Phase Peptide Synthesis: A Practical Approach*; Oxford University Press, 1999.

(112) Amblard, M.; Fehrentz, J.-A.; Martinez, J.; Subra, G. Methods and Protocols of Modern Solid Phase Peptide Synthesis. *Mol. Biotechnol.* 2006, *33* (3), 239–254.

(113) Atherton, E.; Fox, H.; Harkiss, D.; Logan, C. J.; Sheppard, R. C.; Williams, B. J. A Mild Procedure for Solid Phase Peptide Synthesis: Use of Fluorenylmethoxycarbonylamino-Acids. *J. Chem. Soc. Chem. Commun.* 1978, No. 13, 537–539.

(114) Khalil, I. A.; Kogure, K.; Akita, H.; Harashima, H. Uptake Pathways and Subsequent Intracellular Trafficking in Nonviral Gene Delivery. *Pharmacol. Rev.* 2006, *58* (1), 32–45.

(115) Giancotti, F. G.; Ruoslahti, E. Integrin Signaling. *Science* 1999, *285* (5430), 1028–1032.

(116) Desgrosellier, J. S.; Cheresh, D. A. Integrins in Cancer: Biological Implications and Therapeutic Opportunities. *Nat. Rev. Cancer* 2010, *10* (1), 9–22.

(117) Alberts, B.; Johnson, A.; Lewis, J.; Raff, M.; Roberts, K.; Walter, P. Integrins. *Mol. Biol. Cell 4th Ed.* 2002.

(118) Lowell, C. A.; Mayadas, T. N. Overview-Studying Integrins in Vivo. *Methods Mol. Biol. Clifton NJ* 2012, *757*, 369–397.

(119) Seguin, L.; Desgrosellier, J. S.; Weis, S. M.; Cheresh, D. A. Integrins and Cancer: Regulators of Cancer Stemness, Metastasis, and Drug Resistance. *Trends Cell Biol.* 2015, *25* (4), 234–240.

(120) Rathinam, R.; Alahari, S. K. Important Role of Integrins in the Cancer Biology. *Cancer Metastasis Rev.* 2010, *29* (1), 223–237.

(121) Juliano, R. L.; Varner, J. A. Adhesion Molecules in Cancer: The Role of Integrins. *Curr. Opin. Cell Biol.* 1993, *5* (5), 812–818.

(122) Danen, E. H. J. *Integrins: An Overview of Structural and Functional Aspects*; Landes Bioscience, 2013.

(123) Stergios J. Moschos, M. D. Integrins and Cancer https://www.cancernetwork.com/bookfilm-review/integrins-and-cancer (accessed Mar 28, 2020).

(124) Takada, Y.; Ye, X.; Simon, S. The Integrins. *Genome Biol.* 2007, *8* (5), 215.

(125) Schneider, D.; Engelman, D. Involvement of Transmembrane Domain Interactions in Signal Transduction by / Integrins. *J. Biol. Chem.* 2004, *279*, 9840–9846.

(126) Arnaout, M. A.; Goodman, S. L.; Xiong, J.-P. Structure and Mechanics of Integrin-Based Cell Adhesion. *Curr. Opin. Cell Biol.* 2007, *19* (5), 495–507.

(127) Bianconi, D.; Unseld, M.; Prager, G. W. Integrins in the Spotlight of Cancer. *Int. J. Mol. Sci.* 2016, *17* (12).

(128) Nieberler, M.; Reuning, U.; Reichart, F.; Notni, J.; Wester, H.-J.; Schwaiger, M.; Weinmüller, M.; Räder, A.; Steiger, K.; Kessler, H. Exploring the Role of RGD-Recognizing Integrins in Cancer. *Cancers* 2017, *9* (9).

(129) Ruoslahti, E.; Pierschbacher, M. D. New Perspectives in Cell Adhesion: RGD and Integrins. *Science* 1987, *238* (4826), 491–497.

(130) Aumailley, M.; Gurrath, M.; Müller, G.; Calvete, J.; Timpl, R.; Kessler, H. Arg-Gly-Asp Constrained within Cyclic Pentapoptides Strong and Selective Inhibitors of Cell Adhesion to Vitronectin and Laminin Fragment P1. *FEBS Lett.* 1991, *291* (1), 50–54.

(131) Stupp, R.; Hegi, M. E.; Gorlia, T.; Erridge, S. C.; Perry, J.; Hong, Y.-K.; Aldape, K. D.; Lhermitte, B.; Pietsch, T.; Grujicic, D.; Steinbach, J. P.; Wick, W.; Tarnawski, R.; Nam, D.-H.; Hau, P.; Weyerbrock, A.; Taphoorn, M. J. B.; Shen, C.-C.; Rao, N.; Thurzo, L.; Herrlinger, U.; Gupta, T.; Kortmann, R.-D.; Adamska, K.; McBain, C.; Brandes, A. A.; Tonn, J. C.; Schnell, O.; Wiegel, T.; Kim, C.-Y.; Nabors, L. B.; Reardon, D. A.; van den Bent, M. J.; Hicking, C.; Markivskyy, A.; Picard, M.; Weller, M.; European Organisation for Research and Treatment of Cancer (EORTC); Canadian Brain Tumor Consortium; CENTRIC study team. Cilengitide

Combined with Standard Treatment for Patients with Newly Diagnosed Glioblastoma with Methylated MGMT Promoter (CENTRIC EORTC 26071-22072 Study): A Multicentre, Randomised, Open-Label, Phase 3 Trial. *Lancet Oncol.* 2014, *15* (10), 1100–1108.

(132) Nabors, L. B.; Fink, K. L.; Mikkelsen, T.; Grujicic, D.; Tarnawski, R.; Nam, D. H.; Mazurkiewicz, M.; Salacz, M.; Ashby, L.; Zagonel, V.; Depenni, R.; Perry, J. R.; Hicking, C.; Picard, M.; Hegi, M. E.; Lhermitte, B.; Reardon, D. A. Two Cilengitide Regimens in Combination with Standard Treatment for Patients with Newly Diagnosed Glioblastoma and Unmethylated MGMT Gene Promoter: Results of the Open-Label, Controlled, Randomized Phase II CORE Study. *Neuro-Oncol.* 2015, *17* (5), 708–717.

(133) Tucci, M.; Stucci, S.; Felici, C.; Cafforio, P.; Resta, L.; Rossi, R.; Silvestris, F. Cilengitide Restrains the Osteoclast-like Bone Resorbing Activity of Myeloma Plasma Cells. *Br. J. Haematol.* 2016, *173* (1), 59–69.

(134) Alva, A.; Slovin, S.; Daignault, S.; Carducci, M.; DiPaola, R.; Pienta, K.; Agus, D.; Cooney, K.; Chen, A.; Smith, D. C.; Hussain, M. Phase II Study of Cilengitide (EMD 121974, NSC 707544) in Patients with Non-Metastatic Castration Resistant Prostate Cancer, NCI-6735. A Study by the DOD/PCF Prostate Cancer Clinical Trials Consortium. *Invest. New Drugs* 2012, *30* (2), 749–757.

(135) Xiong, J.-P.; Stehle, T.; Zhang, R.; Joachimiak, A.; Frech, M.; Goodman, S. L.; Arnaout, M. A. Crystal Structure of the Extracellular Segment of Integrin Alpha Vbeta3 in Complex with an Arg-Gly-Asp Ligand. *Science* 2002, *296* (5565), 151–155.

(136) Liu, Z.; Wang, F.; Chen, X. Integrin Avβ3-Targeted Cancer Therapy. *Drug Dev. Res.* 2008, *69* (6), 329–339.

(137) Mingozzi, M.; Dal Corso, A.; Marchini, M.; Guzzetti, I.; Civera, M.; Piarulli, U.; Arosio, D.; Belvisi, L.; Potenza, D.; Pignataro, L.; Gennari, C. Cyclic IsoDGR Peptidomimetics as Low-Nanomolar Avβ3 Integrin Ligands. *Chem. Weinh. Bergstr. Ger.* 2013, *19* (11), 3563–3567.

(138) Marchini, M.; Mingozzi, M.; Colombo, R.; Guzzetti, I.; Belvisi, L.; Vasile, F.; Potenza, D.; Piarulli, U.; Arosio, D.; Gennari, C. Cyclic RGD Peptidomimetics Containing Bifunctional Diketopiperazine Scaffolds as New Potent Integrin Ligands. *Chem. - Eur. J.* 2012, *18* (20), 6195–6207.

(139) Panzeri, S.; Zanella, S.; Arosio, D.; Vahdati, L.; Dal Corso, A.; Pignataro, L.; Paolillo, M.; Schinelli, S.; Belvisi, L.; Gennari, C.; Piarulli, U. Cyclic IsoDGR and RGD Peptidomimetics Containing Bifunctional Diketopiperazine Scaffolds Are Integrin Antagonists. *Chem. – Eur. J.* 2015, *21* (16), 6265–6271.

(140) Ressurreição, A. S. M.; Bordessa, A.; Civera, M.; Belvisi, L.; Gennari, C.; Piarulli, U. Synthesis and Conformational Studies of Peptidomimetics Containing a New Bifunctional

Diketopiperazine Scaffold Acting as a Beta-Hairpin Inducer. *J. Org. Chem.* 2008, *73* (2), 652–660.

(141) da Ressurreição, A. S. M.; Vidu, A.; Civera, M.; Belvisi, L.; Potenza, D.; Manzoni, L.; Ongeri, S.; Gennari, C.; Piarulli, U. Cyclic RGD-Peptidomimetics Containing Bifunctional Diketopiperazine Scaffolds as New Potent Integrin Ligands. *Chem. Weinh. Bergstr. Ger.* 2009, *15* (45), 12184–12188.

(142) Zanella, S.; Angerani, S.; Pina, A.; López Rivas, P.; Giannini, C.; Panzeri, S.; Arosio, D.; Caruso, M.; Gasparri, F.; Fraietta, I.; Albanese, C.; Marsiglio, A.; Pignataro, L.; Belvisi, L.; Piarulli, U.; Gennari, C. Tumor Targeting with an IsoDGR–Drug Conjugate. *Chem. – Eur. J.* 2017, *23* (33), 7910–7914.

(143) Razak, K.; Newland, A. C. The Significance of Aminopeptidases and Haematopoietic Cell Differentiation. *Blood Rev.* 1992, *6* (4), 243–250.

(144) Luan, Y.; Xu, W. The Structure and Main Functions of Aminopeptidase N. *Curr. Med. Chem.* 2007, *14* (6), 639–647.

(145) Riemann, D.; Kehlen, A.; Langner, J. CD13--Not Just a Marker in Leukemia Typing. *Immunol. Today* 1999, *20* (2), 83–88.

(146) Santiago, C.; Mudgal, G.; Reguera, J.; Recacha, R.; Albrecht, S.; Enjuanes, L.; Casasnovas, J. M. Allosteric Inhibition of Aminopeptidase N Functions Related to Tumor Growth and Virus Infection. *Sci. Rep.* 2017, *7* (1), 1–14.

(147) Langner, J.; Langner, J.; Ansorge, S. *Ectopeptidases: Cd13/Aminopeptidase N and Cd26/Dipeptidylpeptidase IV in Medicine and Biology*; Springer Science & Business Media, 2002.

(148) Lu, C.; Amin, M. A.; Fox, D. A. CD13/Aminopeptidase N Is a Potential Therapeutic Target for Inflammatory Disorders. *J. Immunol.* 2020, *204* (1), 3–11.

(149) Taylor, A. Aminopeptidases: Structure and Function. *FASEB J. Off. Publ. Fed. Am. Soc. Exp. Biol.* 1993, *7* (2), 290–298.

(150) Taylor, A. Aminopeptidases: Towards a Mechanism of Action. *Trends Biochem. Sci.* 1993, *18* (5), 167–171.

(151) Sanz, Y. Aminopeptidases. In *Industrial Enzymes: Structure, Function and Applications*; Polaina, J., MacCabe, A. P., Eds.; Springer Netherlands: Dordrecht, 2007; pp 243–260.

(152) Wong, A. H. M.; Zhou, D.; Rini, J. M. The X-Ray Crystal Structure of Human Aminopeptidase N Reveals a Novel Dimer and the Basis for Peptide Processing. *J. Biol. Chem.* 2012, *287* (44), 36804–36813.

(153) Schreiber, C. L.; Smith, B. D. Molecular Imaging of Aminopeptidase N in Cancer and Angiogenesis. *Contrast Media Mol. Imaging* 2018, *2018*.

(154) Look, A. T.; Ashmun, R. A.; Shapiro, L. H.; Peiper, S. C. Human Myeloid Plasma Membrane Glycoprotein CD13 (Gp150) Is Identical to Aminopeptidase N. *J. Clin. Invest.* 1989, *83* (4), 1299–1307.

(155) Wickström, M.; Larsson, R.; Nygren, P.; Gullbo, J. Aminopeptidase N (CD13) as a Target for Cancer Chemotherapy. *Cancer Sci.* 2011, *102* (3), 501–508.

(156) Fukasawa, K.; Fujii, H.; Saitoh, Y.; Koizumi, K.; Aozuka, Y.; Sekine, K.; Yamada, M.; Saiki, I.; Nishikawa, K. Aminopeptidase N (APN/CD13) Is Selectively Expressed in Vascular Endothelial Cells and Plays Multiple Roles in Angiogenesis. *Cancer Lett.* 2006, *243* (1), 135–143.

(157) Hashida, H.; Takabayashi, A.; Kanai, M.; Adachi, M.; Kondo, K.; Kohno, N.; Yamaoka, Y.; Miyake, M. Aminopeptidase N Is Involved in Cell Motility and Angiogenesis: Its Clinical Significance in Human Colon Cancer. *Gastroenterology* 2002, *122* (2), 376–386.

(158) Zhang, X.; Xu, W. Aminopeptidase N (APN/CD13) as a Target for Anti-Cancer Agent Design. *Curr. Med. Chem.* 2008, *15* (27), 2850–2865.

(159) Mina-Osorio, P. The Moonlighting Enzyme CD13: Old and New Functions to Target. *Trends Mol. Med.* 2008, *14* (8), 361–371.

(160) Mina-Osorio, P.; Ortega, E. Aminopeptidase N (CD13) Functionally Interacts with FcγRs in Human Monocytes. *J. Leukoc. Biol.* 2005, *77* (6), 1008–1017.

(161) Aminopeptidase N (APN)/CD13-dependent CXCR4 downregulation is associated with diminished cell migration, proliferation and invasion. - PubMed - NCBI

(162) Yang, E.; Shim, J. S.; Woo, H.-J.; Kim, K.-W.; Kwon, H. J. Aminopeptidase N/CD13 Induces Angiogenesis through Interaction with a pro-Angiogenic Protein, Galectin-3. *Biochem. Biophys. Res. Commun.* 2007, *363* (2), 336–341.

(163) Petrović, N. Ž.; Schacke, W.; Shapiro, L. H. CD13/Aminopeptidase N in Tumor Growth and Angiogenesis; 2004.

(164) Bhagwat, S. V.; Petrovic, N.; Okamoto, Y.; Shapiro, L. H. The Angiogenic Regulator CD13/APN Is a Transcriptional Target of Ras Signaling Pathways in Endothelial Morphogenesis. *Blood* 2003, *101* (5), 1818–1826.

(165) Chiaretti, S.; Zini, G.; Bassan, R. Diagnosis and Subclassification of Acute Lymphoblastic Leukemia. *Mediterr. J. Hematol. Infect. Dis.* 2014, *6* (1).

(166) Ahmadzadeh, A.; Saedi, S.; Jaseb, K.; Asnafi, A. A.; Alghasi, A.; Saki, N. T-Cell Acute Lymphoblastic Leukemia with Del (7) (Q11.2q22) and Aberrant Expression of Myeloid Markers. *Int. J. Hematol.-Oncol. Stem Cell Res.* 2013, *7* (4), 40–44.

(167) Curnis, F.; Arrigoni, G.; Sacchi, A.; Fischetti, L.; Arap, W.; Pasqualini, R.; Corti, A. Differential Binding of Drugs Containing the NGR Motif to CD13 Isoforms in Tumor Vessels, Epithelia, and Myeloid Cells. *Cancer Res.* 2002, *62* (3), 867–874.

(168) Dixon, J.; Kaklamanis, L.; Turley, H.; Hickson, I. D.; Leek, R. D.; Harris, A. L.; Gatter, K. C. Expression of Aminopeptidase-n (CD 13) in Normal Tissues and Malignant Neoplasms of Epithelial and Lymphoid Origin. *J. Clin. Pathol.* 1994, *47* (1), 43–47.

(169) *Aminopeptidases in Biology and Disease*; Hooper, N. M., Lendeckel, U., Eds.; Proteases in Biology and Disease; Springer US, 2004.

(170) Chávez-Gutiérrez, L.; Matta-Camacho, E.; Osuna, J.; Horjales, E.; Joseph-Bravo, P.; Maigret, B.; Charli, J.-L. Homology Modeling and Site-Directed Mutagenesis of Pyroglutamyl Peptidase II INSIGHTS INTO OMEGA-VERSUS AMINOPEPTIDASE SPECIFICITY IN THE M1 FAMILY. *J. Biol. Chem.* 2006, *281* (27), 18581–18590.

(171) Ito, K.; Nakajima, Y.; Onohara, Y.; Takeo, M.; Nakashima, K.; Matsubara, F.; Ito, T.; Yoshimoto, T. Crystal Structure of Aminopeptidase N (Proteobacteria Alanyl Aminopeptidase) from Escherichia Coli and Conformational Change of Methionine 260 Involved in Substrate Recognition. *J. Biol. Chem.* 2006, *281* (44), 33664–33676.

(172) Addlagatta, A.; Matthews, B. W. Structure of the Angiogenesis Inhibitor Ovalicin Bound to Its Noncognate Target, Human Type 1 Methionine Aminopeptidase. *Protein Sci.* 2006, *15* (8), 1842–1848.

(173) Chen, L.; Lin, Y.-L.; Peng, G.; Li, F. Structural Basis for Multifunctional Roles of Mammalian Aminopeptidase N. *Proc. Natl. Acad. Sci. U. S. A.* 2012, *109* (44), 17966–17971.

(174) Máté, G.; Kertész, I.; Enyedi, K. N.; Mező, G.; Angyal, J.; Vasas, N.; Kis, A.; Szabó, É.; Emri, M.; Bíró, T.; Galuska, L.; Trencsényi, G. In Vivo Imaging of Aminopeptidase N (CD13) Receptors in Experimental Renal Tumors Using the Novel Radiotracer (68)Ga-NOTA-c(NGR). *Eur. J. Pharm. Sci. Off. J. Eur. Fed. Pharm. Sci.* 2015, *69*, 61–71.

(175) Enyedi, K. N.; Tóth, S.; Szakács, G.; Mező, G. NGR-Peptide-Drug Conjugates with Dual Targeting Properties. *PloS One* 2017, *12* (6), e0178632.

(176) Corti, A.; Curnis, F.; Rossoni, G.; Marcucci, F.; Gregorc, V. Peptide-Mediated Targeting of Cytokines to Tumor Vasculature: The NGR-HTNF Example. *BioDrugs Clin. Immunother. Biopharm. Gene Ther.* 2013, *27* (6), 591–603.

(177) Colombo, G.; Curnis, F.; De Mori, G. M. S.; Gasparri, A.; Longoni, C.; Sacchi, A.; Longhi, R.; Corti, A. Structure-Activity Relationships of Linear and Cyclic Peptides Containing the NGR Tumor-Homing Motif. *J. Biol. Chem.* 2002, *277* (49), 47891–47897.

(178) Zhang, J.; Lu, X.; Wan, N.; Hua, Z.-C.; Wang, Z.; Huang, H.; Yang, M.; Wang, F. 68Ga-DOTA-NGR as a Novel Molecular Probe for APN-Positive Tumor Imaging Using MicroPET. *Nucl. Med. Biol.* 2014.

(179) Curnis, F.; Sacchi, A.; Borgna, L.; Magni, F.; Gasparri, A.; Corti, A. Enhancement of Tumor Necrosis Factor Alpha Antitumor Immunotherapeutic Properties by Targeted Delivery to Aminopeptidase N (CD13). *Nat. Biotechnol.* 2000, *18* (11), 1185–1190.

(180) Corti, A.; Ponzoni, M. Tumor Vascular Targeting with Tumor Necrosis Factor Alpha and Chemotherapeutic Drugs. *Ann. N. Y. Acad. Sci.* 2004, *1028*, 104–112.

(181) Ellerby, H. M.; Arap, W.; Ellerby, L. M.; Kain, R.; Andrusiak, R.; Rio, G. D.; Krajewski, S.; Lombardo, C. R.; Rao, R.; Ruoslahti, E.; Bredesen, D. E.; Pasqualini, R. Anti-Cancer Activity of Targeted pro-Apoptotic Peptides. *Nat. Med.* 1999, *5* (9), 1032–1038.

(182) Gregorc, V.; Gaafar, R. M.; Favaretto, A.; Grossi, F.; Jassem, J.; Polychronis, A.; Bidoli, P.; Tiseo, M.; Shah, R.; Taylor, P.; Novello, S.; Muzio, A.; Bearz, A.; Greillier, L.; Fontana, F.; Salini, G.; Lambiase, A.; O'Brien, M. NGR-HTNF in Combination with Best Investigator Choice in Previously Treated Malignant Pleural Mesothelioma (NGR015): A Randomised, Double-Blind, Placebo-Controlled Phase 3 Trial. *Lancet Oncol.* 2018, *19* (6), 799–811.

(183) D'Onofrio, N.; Caraglia, M.; Grimaldi, A.; Marfella, R.; Servillo, L.; Paolisso, G.; Balestrieri, M. L. Vascular-Homing Peptides for Targeted Drug Delivery and Molecular Imaging: Meeting the Clinical Challenges. *Biochim. Biophys. Acta* 2014, *1846* (1), 1–12.

(184) Corti, A.; Gasparri, A.; Ghitti, M.; Sacchi, A.; Sudati, F.; Fiocchi, M.; Buttiglione, V.; Perani, L.; Gori, A.; Valtorta, S.; Moresco, R.; Pastorino, F.; Ponzoni, M.; Musco, G.; Curnis, F. Glycine N -Methylation in NGR-Tagged Nanocarriers Prevents Isoaspartate Formation and Integrin Binding without Impairing CD13 Recognition and Tumor Homing. *Adv. Funct. Mater.* 2017, *27*, 1701245.

(185) Negussie, A. H.; Miller, J. L.; Reddy, G.; Drake, S. K.; Wood, B. J.; Dreher, M. R. Synthesis and in Vitro Evaluation of Cyclic NGR Peptide Targeted Thermally Sensitive Liposome. *J. Control. Release Off. J. Control. Release Soc.* 2010, *143* (2), 265–273.

(186) Satpati, D.; Sharma, R.; Sarma, H. D.; Dash, A. Comparative Evaluation of 68 Ga-Labeled NODAGA, DOTAGA, and HBED-CC-Conjugated CNGR Peptide Chelates as Tumor-Targeted Molecular Imaging Probes. *Chem. Biol. Drug Des.* 2018, *91* (3), 781–788.

(187) Arap, W.; Pasqualini, R.; Ruoslahti, E. Chemotherapy Targeted to Tumor Vasculature. *Curr. Opin. Oncol.* 1998, *10* (6), 560–565.

(188) Mukhopadhyay, S.; Barnés, C. M.; Haskel, A.; Short, S. M.; Barnes, K. R.; Lippard, S. J. Conjugated Platinum(IV)-Peptide Complexes for Targeting Angiogenic Tumor Vasculature. *Bioconjug. Chem.* 2008, *19* (1), 39–49.

(189) Ndinguri, M. W.; Solipuram, R.; Gambrell, R. P.; Aggarwal, S.; Hammer, R. P. Peptide Targeting of Platinum Anti-Cancer Drugs. *Bioconjug. Chem.* 2009, *20* (10), 1869–1878.

(190) Zhang, Z.; Hatta, H.; Ito, T.; Nishimoto, S. Synthesis and Photochemical Properties of Photoactivated Antitumor Prodrugs Releasing 5-Fluorouracil. *Org. Biomol. Chem.* 2005, *3* (4), 592–596.

(191) Vats, K.; Satpati, D.; Sharma, R.; Kumar, C.; Sarma, H. D.; Dash, A. 99m Tc-Labeled NGR-Chlorambucil Conjugate, 99m Tc-HYNIC-CLB-c(NGR) for Targeted Chemotherapy and Molecular Imaging. *J. Label. Compd. Radiopharm.* 2017, *60* (9), 431–438.

(192) Vats, K.; Satpati, D.; Sharma, R.; Kumar, C.; Sarma, H. D.; Banerjee, S. Preparation and Comparative Evaluation of 99mTc-HYNIC-CNGR and 99mTc-HYNIC-PEG2-CNGR as Tumor-Targeting Molecular Imaging Probes. *J. Label. Compd. Radiopharm.* 2018, *61* (2), 68–76.

(193) Kirikoshi, R.; Manabe, N.; Takahashi, O. Succinimide Formation from an NGR-Containing Cyclic Peptide: Computational Evidence for Catalytic Roles of Phosphate Buffer and the Arginine Side Chain. *Int. J. Mol. Sci.* 2017, *18* (2).

(194) Violand, B. N.; Schlittler, M. R.; Toren, P. C.; Siegel, N. R. Formation of Isoaspartate 99 in Bovine and Porcine Somatotropins. *J. Protein Chem.* 1990, *9* (1), 109–117.

(195) Meinwald, Y. C.; Stimson, E. R.; Scheraga, H. A. Deamidation of the Asparaginyl-Glycyl Sequence. *Int. J. Pept. Protein Res.* 1986, *28* (1), 79–84.

(196) Geiger, T.; Clarke, S. Deamidation, Isomerization, and Racemization at Asparaginyl and Aspartyl Residues in Peptides. Succinimide-Linked Reactions That Contribute to Protein Degradation. *J. Biol. Chem.* 1987, *262* (2), 785–794.

(197) Corti, A.; Curnis, F. Isoaspartate-Dependent Molecular Switches for Integrin–Ligand Recognition. *J. Cell Sci.* 2011, *124* (4), 515–522.

(198) Kempkes, L. J. M.; Martens, J.; Grzetic, J.; Berden, G.; Oomens, J. Deamidation Reactions of Asparagine- and Glutamine-Containing Dipeptides Investigated by Ion Spectroscopy. *J. Am. Soc. Mass Spectrom.* 2016, *27* (11), 1855–1869.

(199) Robinson, A. B. Molecular Clocks, Molecular Profiles, and Optimum Diets: Three Approaches to the Problem of Aging. *Mech. Ageing Dev.* 1979, *9* (3–4), 225–236.

(200) Robinson, N. E. Protein Deamidation. *Proc. Natl. Acad. Sci. U. S. A.* 2002, *99* (8), 5283–5288.

(201) Robinson, N. E.; Robinson, A. B. Prediction of Protein Deamidation Rates from Primary and Three-Dimensional Structure. *Proc. Natl. Acad. Sci. U. S. A.* 2001, *98* (8), 4367–4372.

(202) Effects of acidic N + 1 residues on asparagine deamidation rates in solution and in the solid state - Journal of Pharmaceutical Sciences

(203) Tyler-Cross, R.; Schirch, V. Effects of Amino Acid Sequence, Buffers, and Ionic Strength on the Rate and Mechanism of Deamidation of Asparagine Residues in Small Peptides. *J. Biol. Chem.* 1991, *266* (33), 22549–22556.

(204) Curnis, F.; Cattaneo, A.; Longhi, R.; Sacchi, A.; Gasparri, A. M.; Pastorino, F.; Di Matteo, P.; Traversari, C.; Bachi, A.; Ponzoni, M.; Rizzardi, G.-P.; Corti, A. Critical Role of Flanking Residues in NGR-to-IsoDGR Transition and CD13/Integrin Receptor Switching. *J. Biol. Chem.* 2010, *285* (12), 9114–9123.

(205) Spitaleri, A.; Ghitti, M.; Mari, S.; Alberici, L.; Traversari, C.; Rizzardi, G.-P.; Musco, G. Use of Metadynamics in the Design of IsoDGR-Based Avβ3 Antagonists to Fine-Tune the Conformational Ensemble. *Angew. Chem. Int. Ed Engl.* 2011, *50* (8), 1832–1836.

(206) Frank, A. O.; Otto, E.; Mas-Moruno, C.; Schiller, H. B.; Marinelli, L.; Cosconati, S.; Bochen, A.; Vossmeyer, D.; Zahn, G.; Stragies, R.; Novellino, E.; Kessler, H. Conformational Control of Integrin-Subtype Selectivity in IsoDGR Peptide Motifs: A Biological Switch. *Angew. Chem. Int. Ed Engl.* 2010, *49* (48), 9278–9281.

(207) Seidi, K.; Jahanban-Esfahlan, R.; Monhemi, H.; Zare, P.; Minofar, B.; Daei Farshchi Adli, A.; Farajzadeh, D.; Behzadi, R.; Mesgari Abbasi, M.; Neubauer, H. A.; Moriggl, R.; Zarghami, N.; Javaheri, T. NGR (Asn-Gly-Arg)-Targeted Delivery of Coagulase to Tumor Vasculature Arrests Cancer Cell Growth. *Oncogene* 2018, *37* (29), 3967–3980.

(208) Enyedi, K. N.; Czajlik, A.; Knapp, K.; Láng, A.; Majer, Z.; Lajkó, E.; Kőhidai, L.; Perczel, A.; Mező, G. Development of Cyclic NGR Peptides with Thioether Linkage: Structure and Dynamics Determining Deamidation and Bioactivity. *J. Med. Chem.* 2015, *58* (4), 1806–1817.

(209) Hoppenz, P.; Els-Heindl, S.; Beck-Sickinger, A. G. Peptide-Drug Conjugates and Their Targets in Advanced Cancer Therapies. *Front. Chem.* 2020, *8*.

(210) Böhme, D.; Beck-Sickinger, A. Drug Delivery and Release Systems for Targeted Tumor Therapy†‡. *J. Pept. Sci. Off. Publ. Eur. Pept. Soc.* 2015, *21*.

(211) Szlachcic, A.; Zakrzewska, M.; Lobocki, M.; Jakimowicz, P.; Otlewski, J. Design and Characteristics of Cytotoxic Fibroblast Growth Factor 1 Conjugate for Fibroblast Growth Factor Receptor-Targeted Cancer Therapy. *Drug Des. Devel. Ther.* 2016, *10*, 2547–2560.

(212) Tan, G.-J.; Peng, Z.-K.; Lu, J.-P.; Tang, F.-Q. Cathepsins Mediate Tumor Metastasis. *World J. Biol. Chem.* 2013, *4* (4), 91–101.

(213) Withana, N. P.; Saito, T.; Ma, X.; Garland, M.; Liu, C.; Kosuge, H.; Amsallem, M.; Verdoes, M.; Ofori, L. O.; Fischbein, M.; Arakawa, M.; Cheng, Z.; McConnell, M. V.; Bogyo, M. Dual Modality Activity Based Probes as Molecular Imaging Agents for Vascular Inflammation. *J. Nucl. Med.* 2016, jnumed.115.171553.

(214) Barve, A.; Jin, W.; Cheng, K. Prostate Cancer Relevant Antigens and Enzymes for Targeted Drug Delivery. *J. Control. Release Off. J. Control. Release Soc.* 2014, *187*, 118–132.

(215) Chitkara, D.; Mittal, A.; Behrman, S. W.; Kumar, N.; Mahato, R. I. Self-Assembling, Amphiphilic Polymer-Gemcitabine Conjugate Shows Enhanced Antitumor Efficacy against Human Pancreatic Adenocarcinoma. *Bioconjug. Chem.* 2013, *24* (7), 1161–1173.

(216) García-Manteiga, J.; Molina-Arcas, M.; Casado, F. J.; Mazo, A.; Pastor-Anglada, M. Nucleoside Transporter Profiles in Human Pancreatic Cancer Cells: Role of HCNT1 in 2',2'-Difluorodeoxycytidine- Induced Cytotoxicity. *Clin. Cancer Res. Off. J. Am. Assoc. Cancer Res.* 2003, *9* (13), 5000–5008.

(217) Santini, D.; Schiavon, G.; Vincenzi, B.; Cass, C. E.; Vasile, E.; Manazza, A. D.; Catalano, V.; Baldi, G. G.; Lai, R.; Rizzo, S.; Giacobino, A.; Chiusa, L.; Caraglia, M.; Russo, A.; Mackey, J.; Falcone, A.; Tonini, G. Human Equilibrative Nucleoside Transporter 1 (HENT1) Levels Predict Response to Gemcitabine in Patients with Biliary Tract Cancer (BTC). *Curr. Cancer Drug Targets* 2011, *11* (1), 123–129.

(218) Huang, P.; Chubb, S.; Hertel, L. W.; Grindey, G. B.; Plunkett, W. Action of 2',2'-Difluorodeoxycytidine on DNA Synthesis. *Cancer Res.* 1991, *51* (22), 6110–6117.

(219) Wall, M. E.; Wani, M. C.; Cook, C. E.; Palmer, K. H.; McPhail, A. T.; Sim, G. A. Plant Antitumor Agents. I. The Isolation and Structure of Camptothecin, a Novel Alkaloidal Leukemia and Tumor Inhibitor from Camptotheca Acuminata1,2. *J. Am. Chem. Soc.* 1966.

(220) Wall, M. E.; Wani, M. C. Camptothecin and Taxol: From Discovery to Clinic. *J. Ethnopharmacol.* 1996, *51* (1), 239–254.

(221) Znojek, P.; Willmore, E.; Curtin, N. J. Preferential Potentiation of Topoisomerase I Poison Cytotoxicity by PARP Inhibition in S Phase. *Br. J. Cancer* 2014, *111* (7), 1319–1326.

(222) Lee, M. H.; Kim, J. Y.; Han, J. H.; Bhuniya, S.; Sessler, J. L.; Kang, C.; Kim, J. S. Direct Fluorescence Monitoring of the Delivery and Cellular Uptake of a Cancer-Targeted RGD Peptide-Appended Naphthalimide Theragnostic Prodrug. *J. Am. Chem. Soc.* 2012, *134* (30), 12668–12674.

(223) Sun, L.; Fuselier, J. A.; Coy, D. H. Effects of Camptothecin Conjugated to a Somatostatin Analog Vector on Growth of Tumor Cell Lines in Culture and Related Tumors in Rodents. *Drug Deliv.* 2004, *11* (4), 231–238.

(224) Cassinelli, G. The Roots of Modern Oncology: From Discovery of New Antitumor Anthracyclines to Their Clinical Use: *Tumori J.* 2016.

(225) McGowan, J. V.; Chung, R.; Maulik, A.; Piotrowska, I.; Walker, J. M.; Yellon, D. M. Anthracycline Chemotherapy and Cardiotoxicity. *Cardiovasc. Drugs Ther.* 2017, *31* (1), 63–75.

(226) Volkova, M.; Russell, R. Anthracycline Cardiotoxicity: Prevalence, Pathogenesis and Treatment. *Curr. Cardiol. Rev.* 2011, *7* (4), 214–220.

(227) Murphy, T.; Yee, K. W. L. Cytarabine and Daunorubicin for the Treatment of Acute Myeloid Leukemia. *Expert Opin. Pharmacother.* 2017, *18* (16), 1765–1780.

(228) Hannon, M. J. Supramolecular DNA Recognition. *Chem. Soc. Rev.* 2007, *36* (2), 280–295.

(229) Mezo, G.; Manea, M.; Szabó, I.; Vincze, B.; Kovács, M. New Derivatives of GnRH as Potential Anticancer Therapeutic Agents. *Curr. Med. Chem.* 2008, *15* (23), 2366–2379.

(230) Yang, F.; Teves, S. S.; Kemp, C. J.; Henikoff, S. Doxorubicin, DNA Torsion, and Chromatin Dynamics. *Biochim. Biophys. Acta* 2014, *1845* (1), 84–89.

(231) Thomssen, C.; Schmitt, M.; Goretzki, L.; Oppelt, P.; Pache, L.; Dettmar, P.; Jänicke, F.; Graeff, H. Prognostic Value of the Cysteine Proteases Cathepsins B and Cathepsin L in Human Breast Cancer. *Clin. Cancer Res. Off. J. Am. Assoc. Cancer Res.* 1995, *1* (7), 741–746.

(232) Mai, J.; Waisman, D. M.; Sloane, B. F. Cell Surface Complex of Cathepsin B/Annexin II Tetramer in Malignant Progression. *Biochim. Biophys. Acta* 2000, *1477* (1–2), 215–230.

(233) Orbán, E.; Mezo, G.; Schlage, P.; Csík, G.; Kulić, Z.; Ansorge, P.; Fellinger, E.; Möller, H. M.; Manea, M. In Vitro Degradation and Antitumor Activity of Oxime Bond-Linked

Daunorubicin-GnRH-III Bioconjugates and DNA-Binding Properties of Daunorubicin-Amino Acid Metabolites. *Amino Acids* 2011, *41* (2), 469–483.

(234) Garrigues, H. J.; Rubinchikova, Y. E.; Dipersio, C. M.; Rose, T. M. Integrin AlphaVbeta3 Binds to the RGD Motif of Glycoprotein B of Kaposi's Sarcoma-Associated Herpesvirus and Functions as an RGD-Dependent Entry Receptor. *J. Virol.* 2008, *82* (3), 1570–1580.

(235) Goodman, S. L.; Grote, H. J.; Wilm, C. Matched Rabbit Monoclonal Antibodies against Av-Series Integrins Reveal a Novel Avβ3-LIBS Epitope, and Permit Routine Staining of Archival Paraffin Samples of Human Tumors. *Biol. Open* 2012, *1* (4), 329–340.

(236) Wayner, E. A.; Carter, W. G. Identification of Multiple Cell Adhesion Receptors for Collagen and Fibronectin in Human Fibrosarcoma Cells Possessing Unique Alpha and Common Beta Subunits. *J. Cell Biol.* 1987, *105* (4), 1873–1884.

(237) Kemperman, H.; Wijnands, Y. M.; Roos, E. AV Integrins on HT-29 Colon Carcinoma Cells: Adhesion to Fibronectin Is Mediated Solely by Small Amounts of AVβ6, and AVβ5 Is Codistributed with Actin Fibers. *Exp. Cell Res.* 1997, *234* (1), 156–164.

(238) Ma, W.; Kang, F.; Wang, Z.; Yang, W.; Li, G.; Ma, X.; Li, G.; Chen, K.; Zhang, Y.; Wang, J. (99m)Tc-Labeled Monomeric and Dimeric NGR Peptides for SPECT Imaging of CD13 Receptor in Tumor-Bearing Mice. *Amino Acids* 2013, *44* (5), 1337–1345.

(239) Chen, N.-T.; Wu, C.-Y.; Chung, C.-Y.; Hwu, Y.; Cheng, S.-H.; Mou, C.-Y.; Lo, L.-W. Probing the Dynamics of Doxorubicin-DNA Intercalation during the Initial Activation of Apoptosis by Fluorescence Lifetime Imaging Microscopy (FLIM). *PloS One* 2012, *7* (9), e44947.

(240) Mohan, P.; Rapoport, N. Doxorubicin as a Molecular Nanotheranostic Agent: Effect of Doxorubicin Encapsulation in Micelles or Nanoemulsions on the Ultrasound-Mediated Intracellular Delivery and Nuclear Trafficking. *Mol. Pharm.* 2010, *7* (6), 1959–1973.

(241) Shaikh, A. Y.; Shih, J. A. Chemotherapy-Induced Cardiotoxicity. *Curr. Heart Fail. Rep.* 2012, *9* (2), 117–127.

(242) Chatterjee, K.; Zhang, J.; Honbo, N.; Karliner, J. S. Doxorubicin Cardiomyopathy. *Cardiology* 2010, *115* (2), 155–162.

(243) Karukstis, K. K.; Thompson, E. H.; Whiles, J. A.; Rosenfeld, R. J. Deciphering the Fluorescence Signature of Daunomycin and Doxorubicin. *Biophys. Chem.* 1998, *73* (3), 249–263.

(244) Motlagh, N. S. H.; Parvin, P.; Ghasemi, F.; Atyabi, F. Fluorescence Properties of Several Chemotherapy Drugs: Doxorubicin, Paclitaxel and Bleomycin. *Biomed. Opt. Express* 2016, *7* (6), 2400–2406.

(245) Simonart, T.; Hermans, P.; Schandene, L.; Van Vooren, J. P. Phenotypic Characteristics of Kaposi's Sarcoma Tumour Cells Derived from Patch-, Plaque- and Nodular-Stage Lesions: Analysis of Cell Cultures Isolated from AIDS and Non-AIDS Patients and Review of the Literature. *Br. J. Dermatol.* 2000, *143* (3), 557–563.

(246) Ensoli, B.; Sgadari, C.; Barillari, G.; Sirianni, M. C.; Stürzl, M.; Monini, P. Biology of Kaposi's Sarcoma. *Eur. J. Cancer Oxf. Engl. 1990* 2001, *37* (10), 1251–1269.

(247) Cancian, L.; Hansen, A.; Boshoff, C. Cellular Origin of Kaposi's Sarcoma and Kaposi's Sarcoma-Associated Herpesvirus-Induced Cell Reprogramming. *Trends Cell Biol.* 2013, *23* (9), 421–432.

(248) Schreiner, C.; Bauer, J.; Margolis, M.; Juliano, R. L. Expression and Role of Integrins in Adhesion of Human Colonic Carcinoma Cells to Extracellular Matrix Components. *Clin. Exp. Metastasis* 1991, *9* (2), 163–178.

(249) Fontijn, D.; Duyndam, M. C. A.; van Berkel, M. P. A.; Yuana, Y.; Shapiro, L. H.; Pinedo, H. M.; Broxterman, H. J.; Boven, E. CD13/Aminopeptidase N Overexpression by Basic Fibroblast Growth Factor Mediates Enhanced Invasiveness of 1F6 Human Melanoma Cells. *Br. J. Cancer* 2006, *94* (11), 1627–1636.

(250) Garrigues, H. J.; Rubinchikova, Y. E.; Dipersio, C. M.; Rose, T. M. Integrin AlphaVbeta3 Binds to the RGD Motif of Glycoprotein B of Kaposi's Sarcoma-Associated Herpesvirus and Functions as an RGD-Dependent Entry Receptor. *J. Virol.* 2008, *82* (3), 1570–1580.

(251) Ensoli, B.; Stürzl, M. Kaposi's Sarcoma: A Result of the Interplay among Inflammatory Cytokines, Angiogenic Factors and Viral Agents. *Cytokine Growth Factor Rev.* 1998, *9* (1), 63–83.

(252) Chandran, B. Early Events in Kaposi's Sarcoma-Associated Herpesvirus Infection of Target Cells. *J. Virol.* 2010, *84* (5), 2188–2199.

(253) Browning, P. J.; Sechler, J. M.; Kaplan, M.; Washington, R. H.; Gendelman, R.; Yarchoan, R.; Ensoli, B.; Gallo, R. C. Identification and Culture of Kaposi's Sarcoma-like Spindle Cells from the Peripheral Blood of Human Immunodeficiency Virus-1-Infected Individuals and Normal Controls. *Blood* 1994, *84* (8), 2711–2720.

(254) Bhagwat, S. V.; Lahdenranta, J.; Giordano, R.; Arap, W.; Pasqualini, R.; Shapiro, L. H. CD13/APN Is Activated by Angiogenic Signals and Is Essential for Capillary Tube Formation. *Blood* 2001, *97* (3), 652–659.

(255) Schreiner, C.; Bauer, J.; Margolis, M.; Juliano, R. L. Expression and Role of Integrins in Adhesion of Human Colonic Carcinoma Cells to Extracellular Matrix Components. *Clin. Exp. Metastasis* 1991, *9* (2), 163–178.

(256) Burvenich, I.; Schoonooghe, S.; Vervoort, L.; Dumolyn, C.; Coene, E.; Vanwalleghem, L.; Van Huysse, J.; Praet, M.; Cuvelier, C.; Mertens, N.; De Vos, F.; Slegers, G. Monoclonal Antibody 14C5 Targets Integrin Alphavbeta5. *Mol. Cancer Ther.* 2008, *7* (12), 3771–3779.

(257) Thundimadathil, J. Cancer Treatment Using Peptides: Current Therapies and Future Prospects. *J. Amino Acids* 2012, *2012*, 967347.

(258) Frank, A. O.; Otto, E.; Mas-Moruno, C.; Schiller, H. B.; Marinelli, L.; Cosconati, S.; Bochen, A.; Vossmeyer, D.; Zahn, G.; Stragies, R.; Novellino, E.; Kessler, H. Conformational Control of Integrin-Subtype Selectivity in IsoDGR Peptide Motifs: A Biological Switch. *Angew. Chem. Int. Ed Engl.* 2010, *49* (48), 9278–9281.

(259) Spitaleri, A.; Ghitti, M.; Mari, S.; Alberici, L.; Traversari, C.; Rizzardi, G.-P.; Musco, G. Use of Metadynamics in the Design of IsoDGR-Based Avβ3 Antagonists to Fine-Tune the Conformational Ensemble. *Angew. Chem. Int. Ed Engl.* 2011, *50* (8), 1832–1836.

(260) Mingozzi, M.; Dal Corso, A.; Marchini, M.; Guzzetti, I.; Civera, M.; Piarulli, U.; Arosio, D.; Belvisi, L.; Potenza, D.; Pignataro, L.; Gennari, C. Cyclic IsoDGR Peptidomimetics as Low-Nanomolar Avβ3 Integrin Ligands. *Chem. Weinh. Bergstr. Ger.* 2013, *19* (11), 3563–3567.

(261) Orbán, E.; Mezo, G.; Schlage, P.; Csík, G.; Kulić, Z.; Ansorge, P.; Fellinger, E.; Möller, H. M.; Manea, M. In Vitro Degradation and Antitumor Activity of Oxime Bond-Linked Daunorubicin-GnRH-III Bioconjugates and DNA-Binding Properties of Daunorubicin-Amino Acid Metabolites. *Amino Acids* 2011, *41* (2), 469–483.

(262) Tripodi, A. A. P.; Tóth, S.; Enyedi, K. N.; Schlosser, G.; Szakács, G.; Mező, G. Development of Novel Cyclic NGR Peptide-Daunomycin Conjugates with Dual Targeting Property. *Beilstein J. Org. Chem.* 2018, *14*, 911–918.

(263) Enyedi, K. N.; Tóth, S.; Szakács, G.; Mező, G. NGR-Peptide-Drug Conjugates with Dual Targeting Properties. *PloS One* 2017, *12* (6), e0178632.

(264) Scholzen, T.; Gerdes, J. The Ki-67 Protein: From the Known and the Unknown. *J. Cell. Physiol.* 2000, *182* (3), 311–322.

(265) Folkman, J. Tumor Angiogenesis. *Adv. Cancer Res.* 1985, *43*, 175–203.

(266) Kuntzman, R.; Mark, L. C.; Brand, L. C.; Jacobson, B. M.; Levin, W.; Conney, A. H. Metabolism of Drugs and Carcinogens by Human Liver Enzymes. *J. Pharmacol. Exp. Ther.* 1966, *152* (1), 151–156.

(267) Mittal, V. K.; Bhullar, J. S.; Jayant, K. Animal Models of Human Colorectal Cancer: Current Status, Uses and Limitations. *World J. Gastroenterol.* 2015, *21* (41), 11854–11861.

(268) Kapuvári, B.; Hegedüs, R.; Schulcz, Á.; Manea, M.; Tóvári, J.; Gacs, A.; Vincze, B.; Mező, G. Improved in Vivo Antitumor Effect of a Daunorubicin - GnRH-III Bioconjugate Modified by Apoptosis Inducing Agent Butyric Acid on Colorectal Carcinoma Bearing Mice. *Invest. New Drugs* 2016, *34* (4), 416–423.

(269) Liao, H.-W.; Hung, M.-C. Intracaecal Orthotopic Colorectal Cancer Xenograft Mouse Model. *Bio-Protoc.* 2017, *7* (11).

(270) Parasuraman, S. Toxicological Screening. *J. Pharmacol. Pharmacother.* 2011, *2* (2), 74–79.

6. Appendix

6.1 ESI-MS spectra of bioconjugates

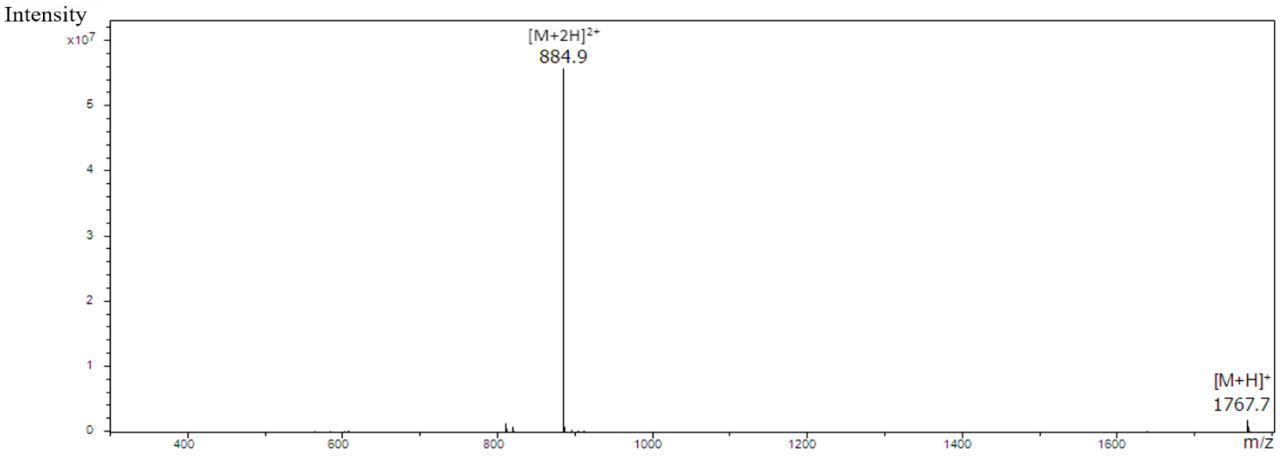

Figure 29: ESI-MS spectrum of conjugate **2** (Nle) containing bioconjugate.

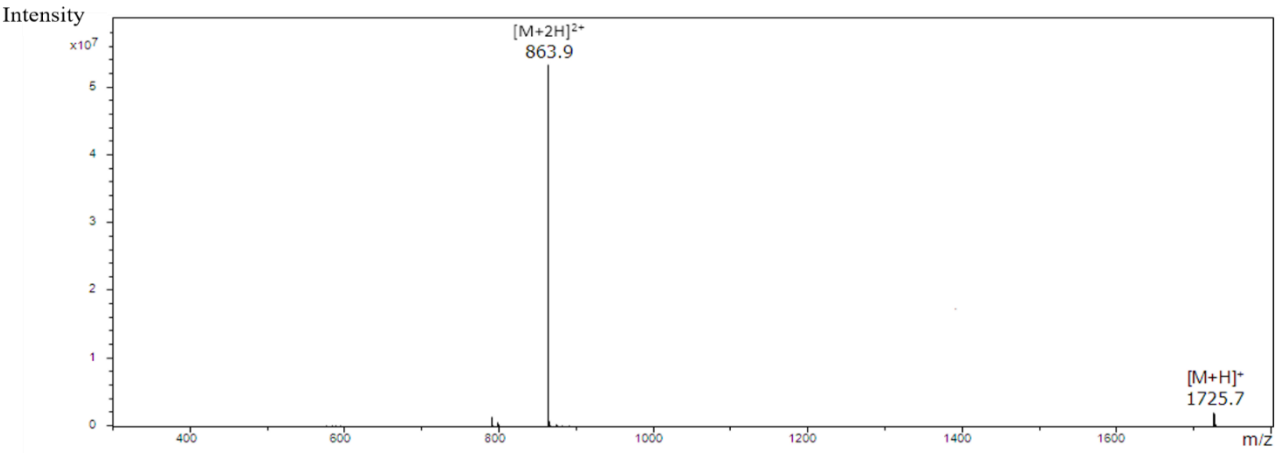

Figure 30: ESI-MS spectrum of conjugate **3** (Ala) containing bioconjugate.

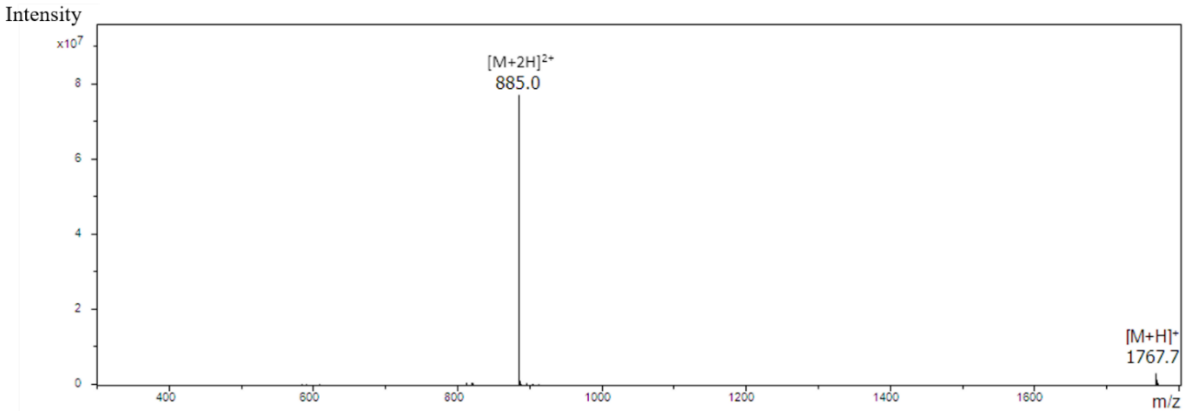

Figure 31: ESI-MS spectrum of conjugate **4** (Leu) containing bioconjugate.

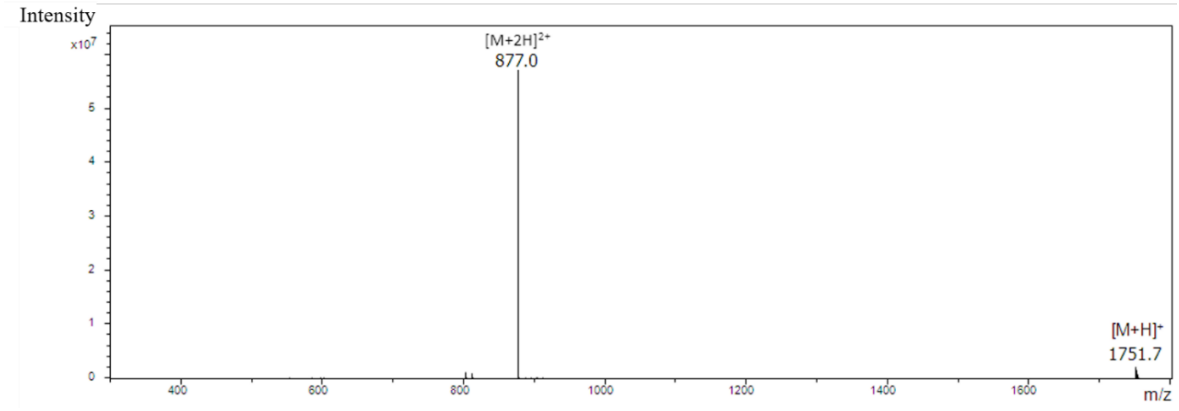

Figure 32*:* ESI-MS spectrum of conjugate **5** (Pro) containing biocojugate.

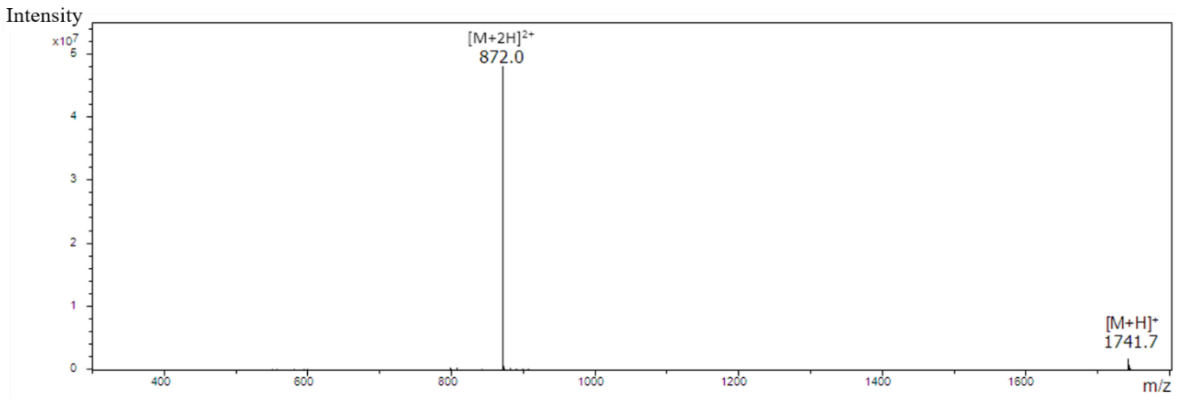

Figure 33: ESI-MS spectrum of conjugate **6** (Ser) containing bioconjugate.

6.2 Chemostability measurements

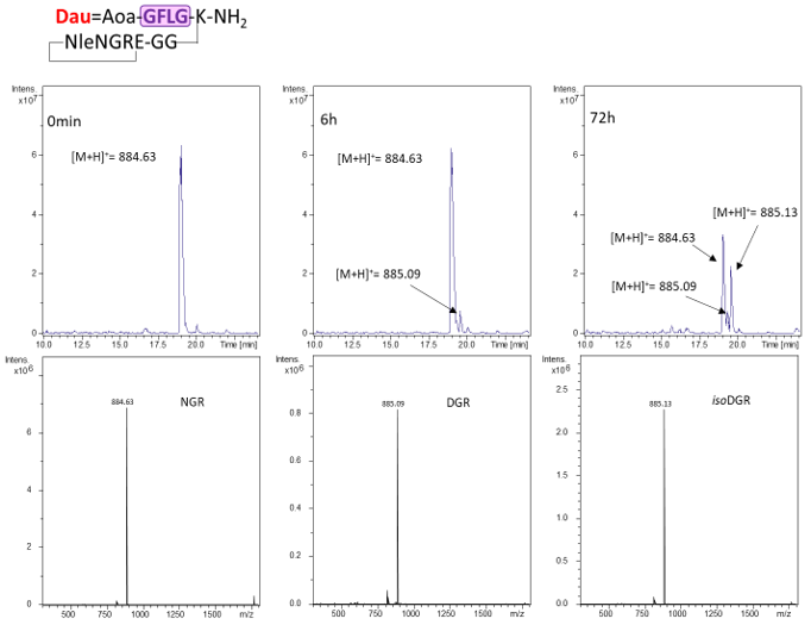

Figure 34: Chemostability of conjugate **2**: Dau=Aoa-GFLGK(c[NleNGRE]-GG)-NH_2

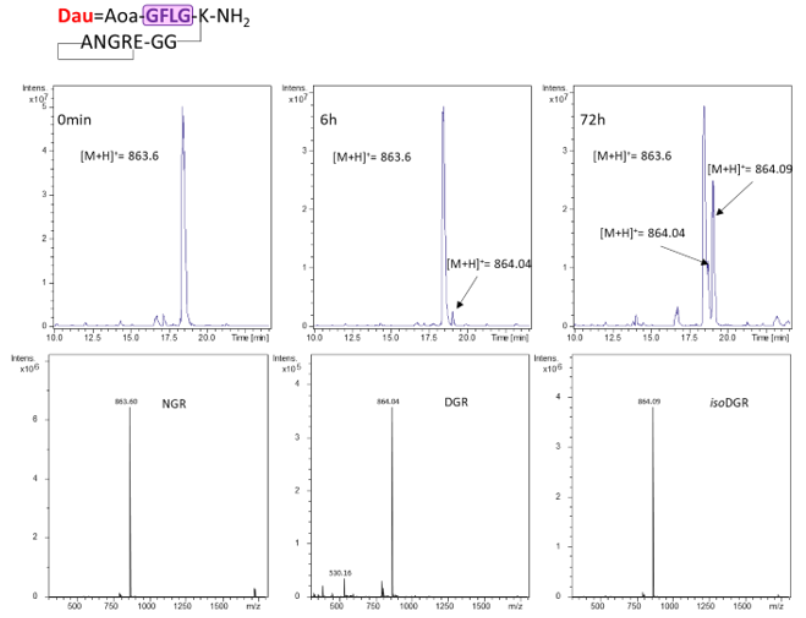

Figure 35: Chemostability of conjugate **3**: Dau=Aoa-GFLGK(c[ANGRE]-GG)-NH_2

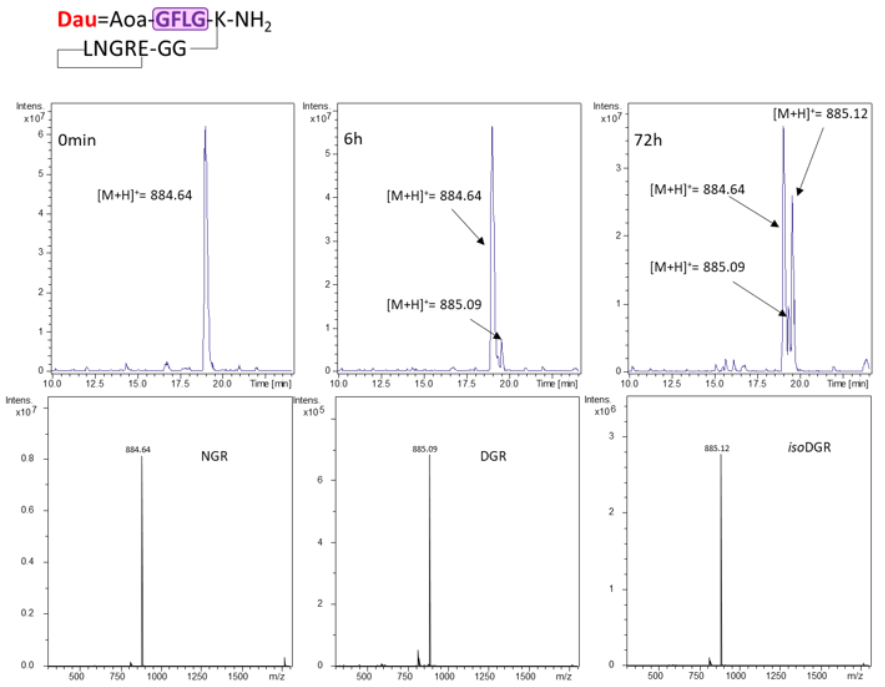

Figure 36: Chemostability of conjugate **4**: Dau=Aoa-GFLGK(c[LNGRE]-GG)-NH_2

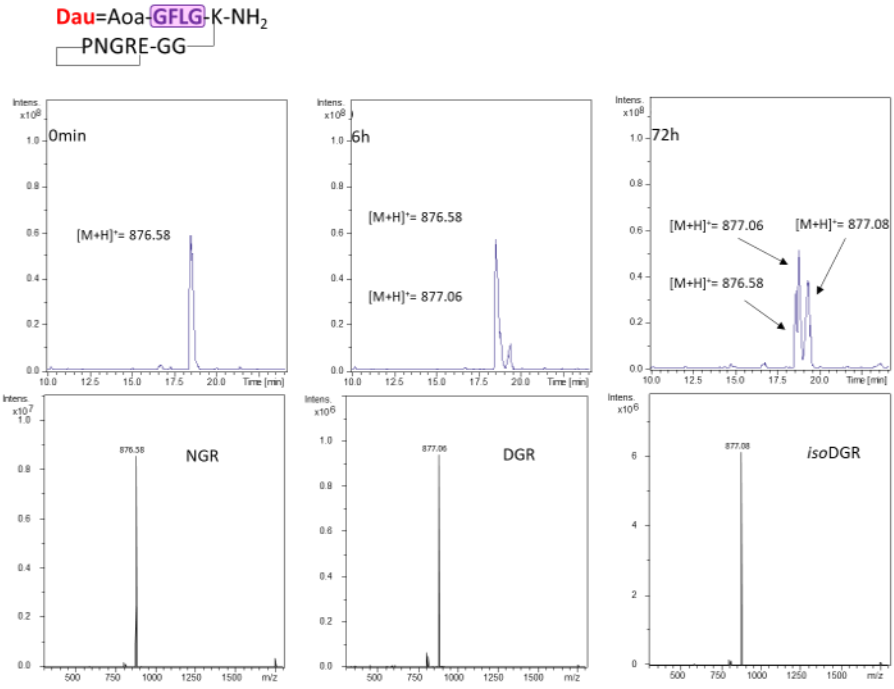

Figure 37: Chemostability of conjugate **5**: Dau=Aoa-GFLGK(c[PNGRE]-GG)-NH_2

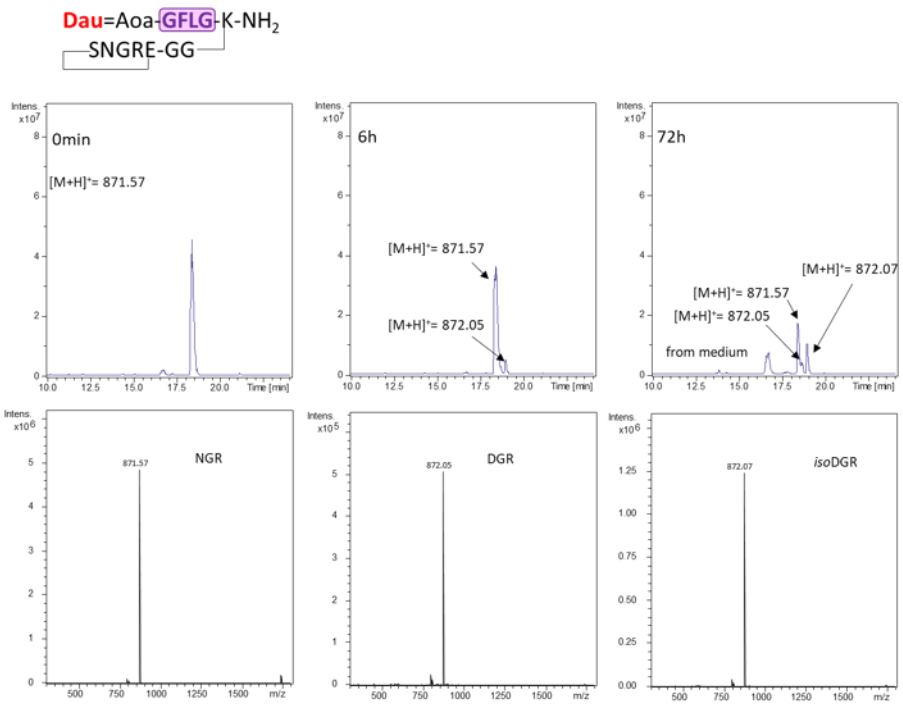

Figure 38: Chemostability of conjugate **6**: Dau=Aoa-GFLGK(c[SNGRE]-GG)-NH_2

6.3 Lysosomal degradation studies

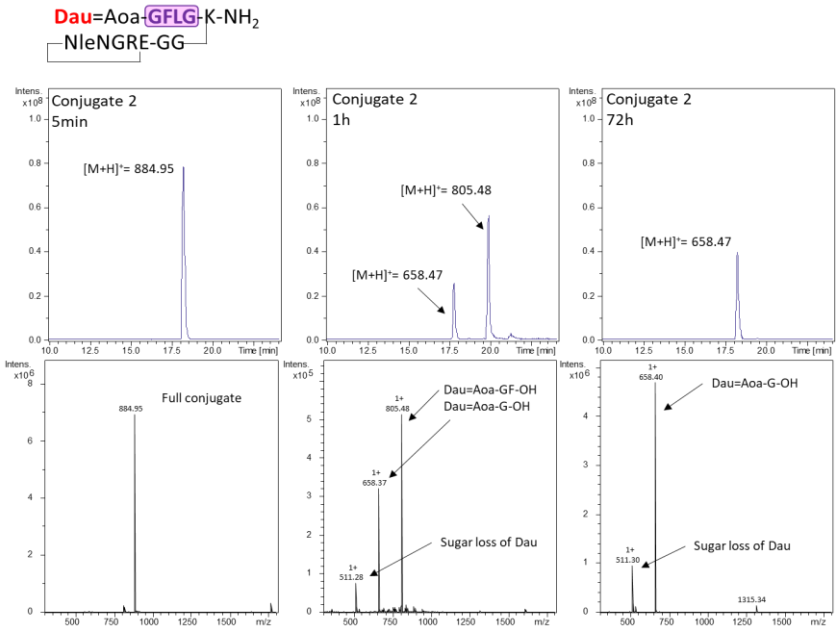

Figure 39: Lysosomal degradation of Conjugate **2**: Dau=Aoa-GFLGK(c[NleNGRE]-GG)-NH_2

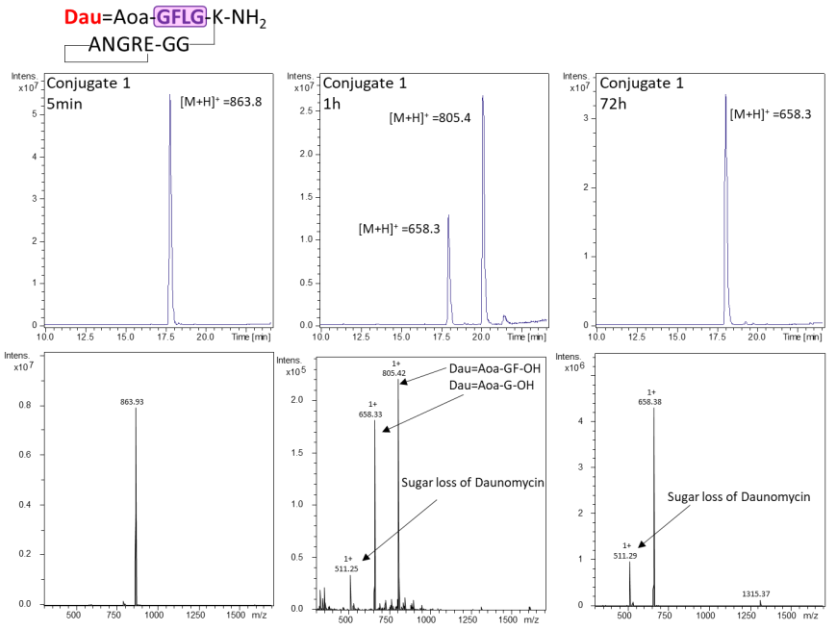

Figure 40: Lysosomal degradation of Conjugate **3**: Dau=Aoa-GFLGK(c[ANGRE]-GG)-NH_2

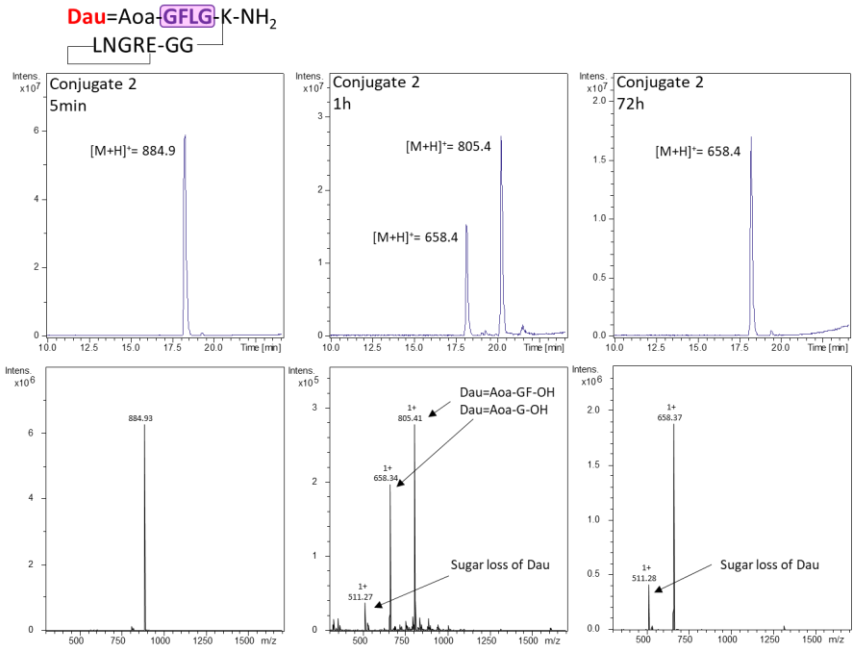

Figure 41: Lysosomal degradation of Conjugate **4**: Dau=Aoa-GFLGK(c[LNGRE]-GG)-NH_2

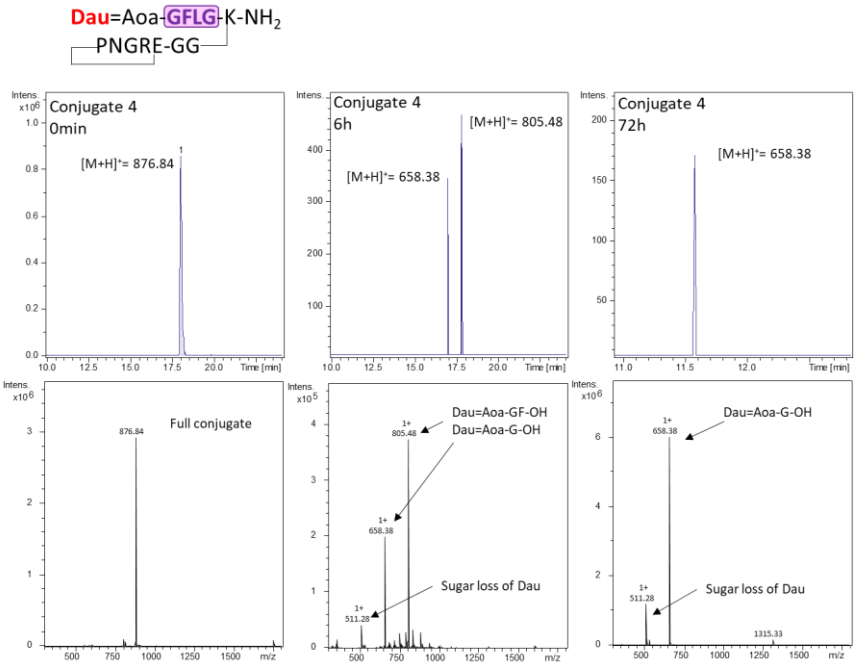

Figure 42: Lysosomal degradation of Conjugate **5**: Dau=Aoa-GFLGK(c[PNGRE]-GG)-NH_2

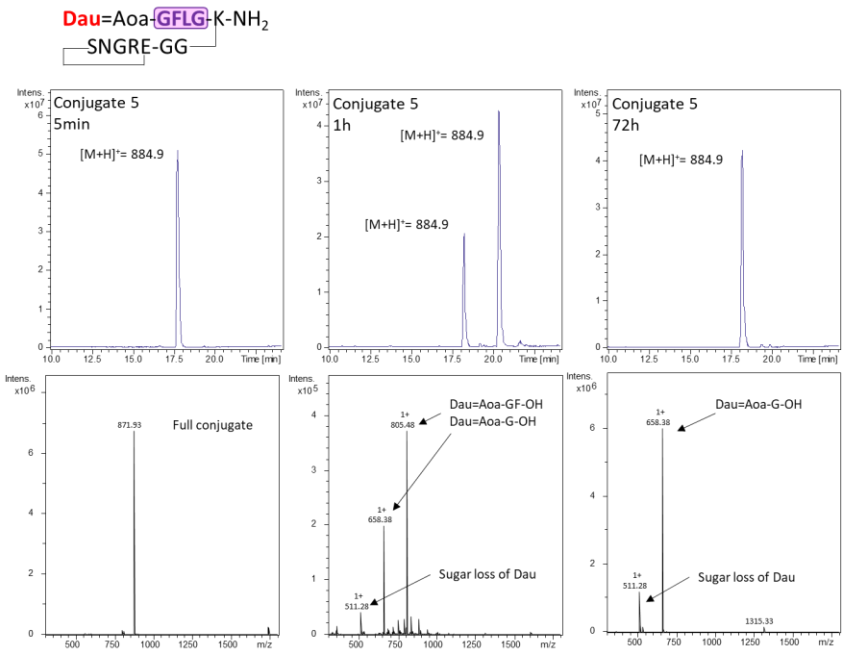

Figure 43*:* Lysosomal degradation of Conjugate **6**: Dau=Aoa-GFLGK(c[SNGRE]-GG)-NH_2

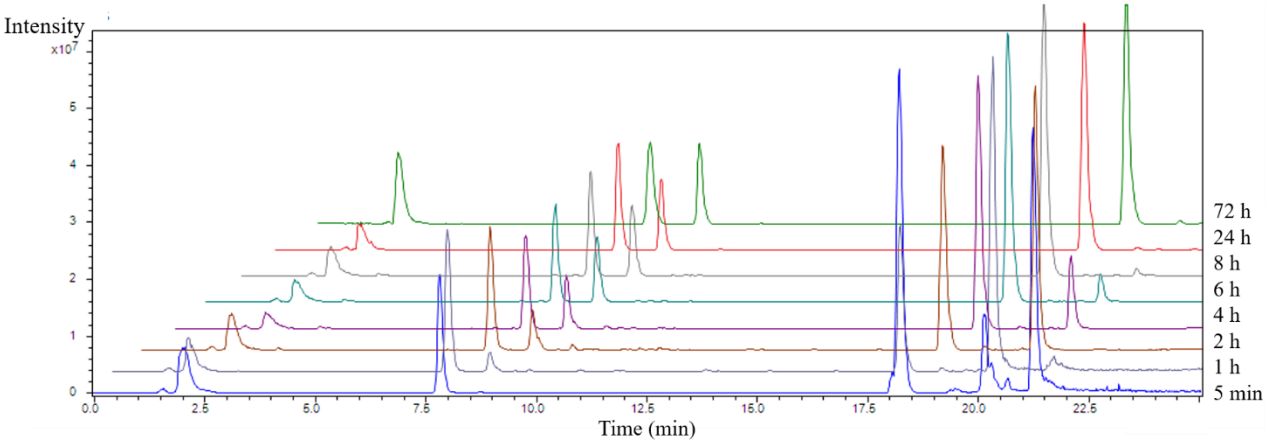

Figure 44: Degradation of cyclic NleNGRE-Dau bioconjugate by rat liver lysosomal homogenate. Detectable cleavage sites of lysosomal enzymes, RP-HPLC chromatogram of the bioconjugate on 5 min, 1, 2, 4, 6, 8, 24 and 72 h incubation with lysosomal homogenate at 37 °C (*peak of Dau=Aoa-G-OH).

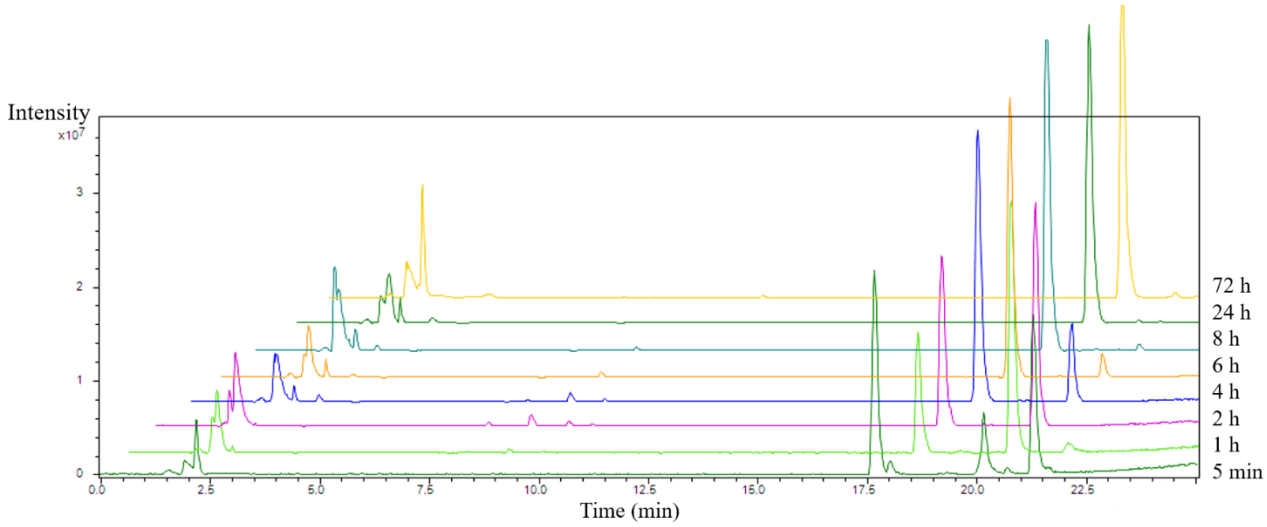

Figure 45: Degradation of cyclic ANGRE-Dau bioconjugate by rat liver lysosomal homogenate. Detectable cleavage sites of lysosomal enzymes, RP-HPLC chromatogram of the bioconjugate on 5 min, 1, 2, 4, 6, 8, 24 and 72 h incubation with lysosomal homogenate at 37 °C (*peak of Dau=Aoa-G-OH).

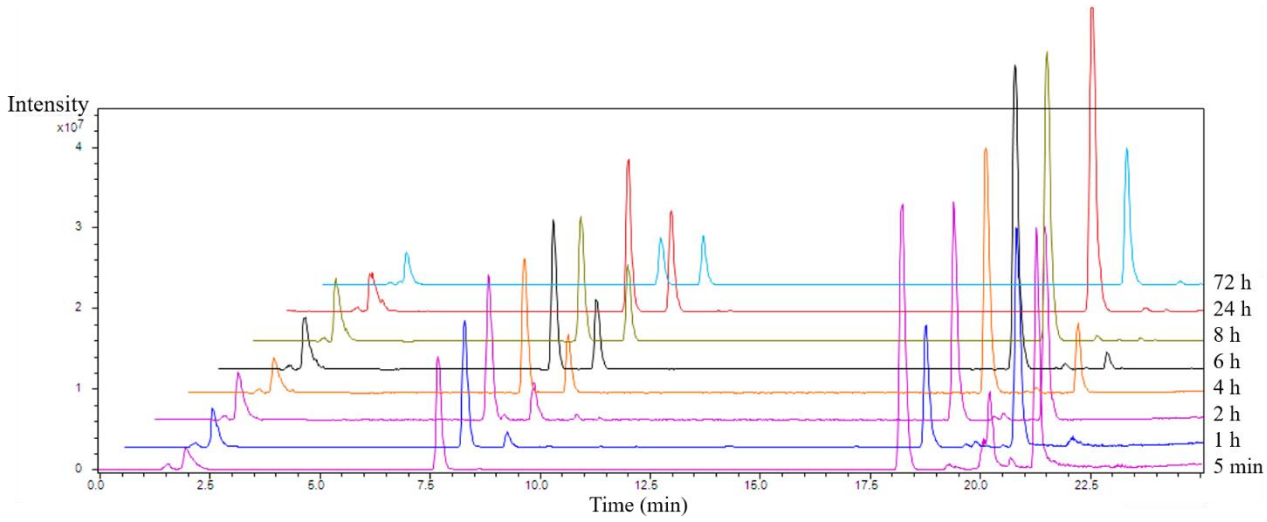

Figure 46: Degradation of cyclic LNGRE-Dau bioconjugate by rat liver lysosomal homogenate. Detectable cleavage sites of lysosomal enzymes, RP-HPLC chromatogram of the bioconjugate on 5 min, 1, 2, 4, 6, 8, 24 and 72 h incubation with lysosomal homogenate at 37 °C (*peak of Dau=Aoa-G-OH).

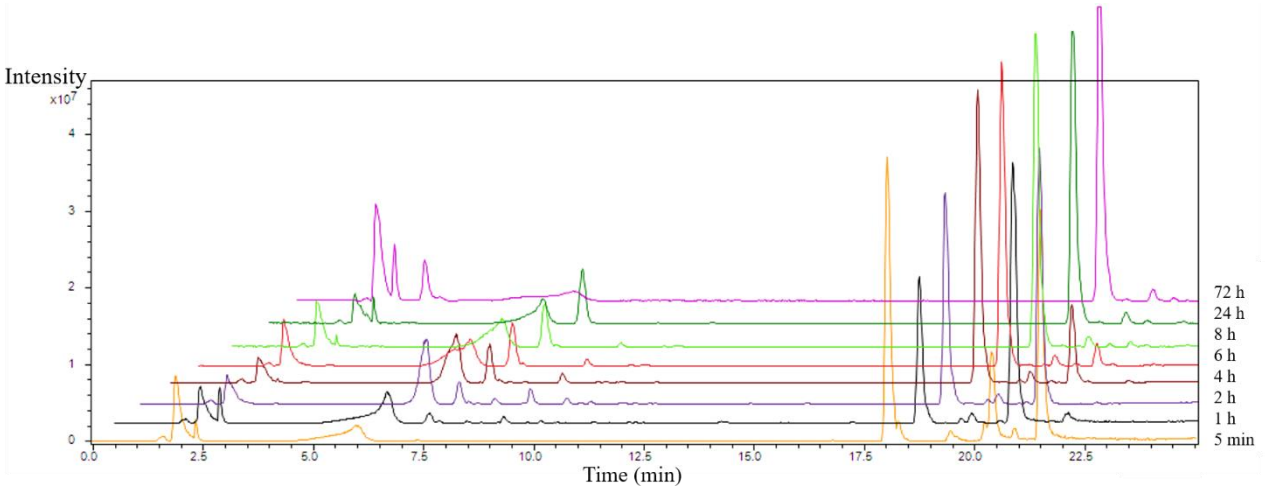

Figure 47*:* Degradation of cyclic PNGRE-Dau bioconjugate by rat liver lysosomal homogenate. Detectable cleavage sites of lysosomal enzymes, RP-HPLC chromatogram of the bioconjugate on 5 min, 1, 2, 4, 6, 8, 24 and 72 h incubation with lysosomal homogenate at 37 °C (*peak of Dau=Aoa-G-OH).

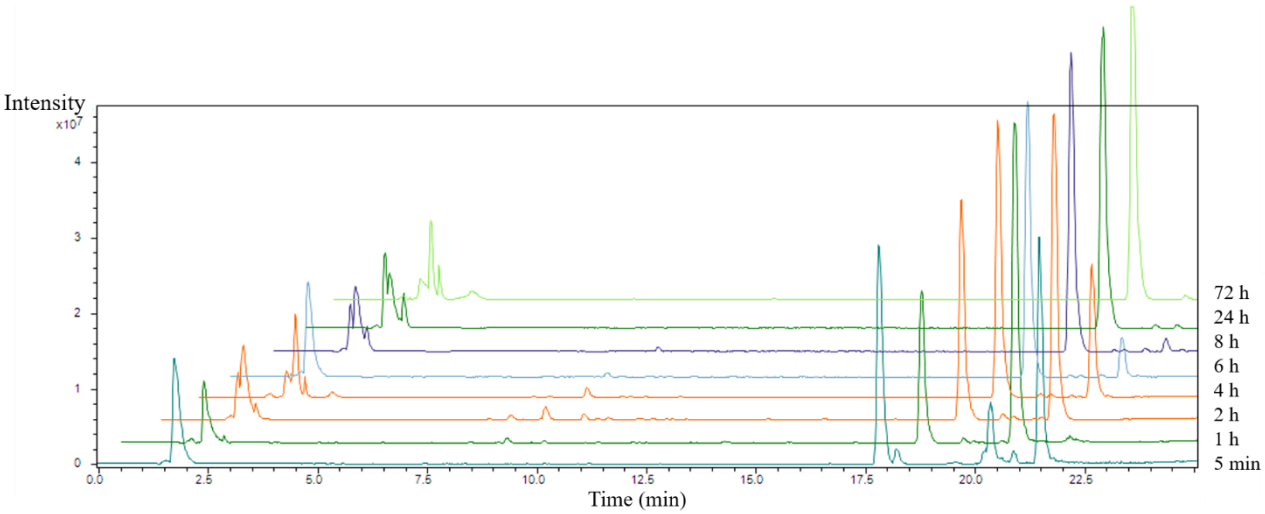

Figure 48*:* Degradation of cyclic SNGRE-Dau bioconjugate by rat liver lysosomal homogenate. Detectable cleavage sites of lysosomal enzymes, RP-HPLC chromatogram of the bioconjugate on 5 min, 1, 2, 4, 6, 8, 24 and 72 h incubation with lysosomal homogenate at 37 °C (*peak of Dau=Aoa-G-OH).

6.4 Stability studies in sodium acetate solution

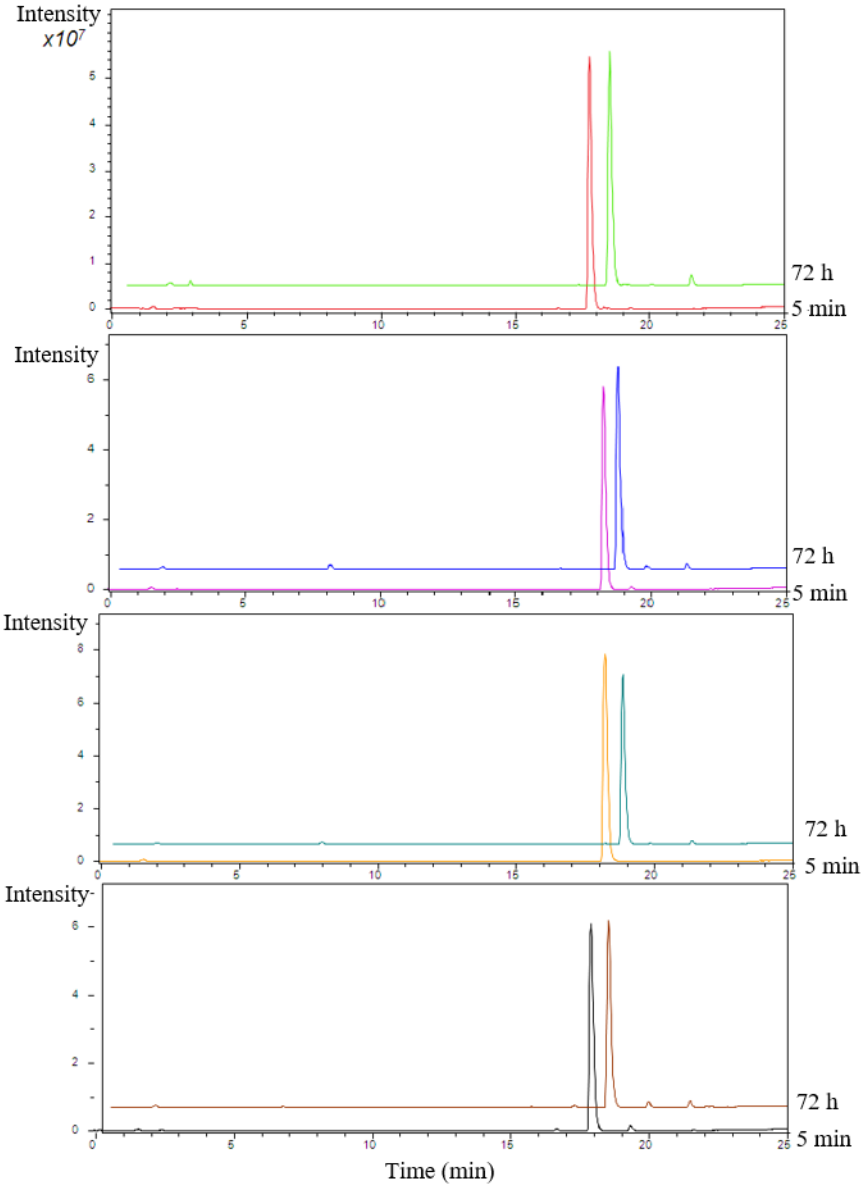

Figure 49*:* The LC-MS basepeak after 5 min and after 72 h incubation (37 °C, pH 4.8, 0.2 M sodium acetate solution) of conjugates **3**, **2**, **5** and **6**, respectively.

6.5 DKP scaffold NMR and MS spectra

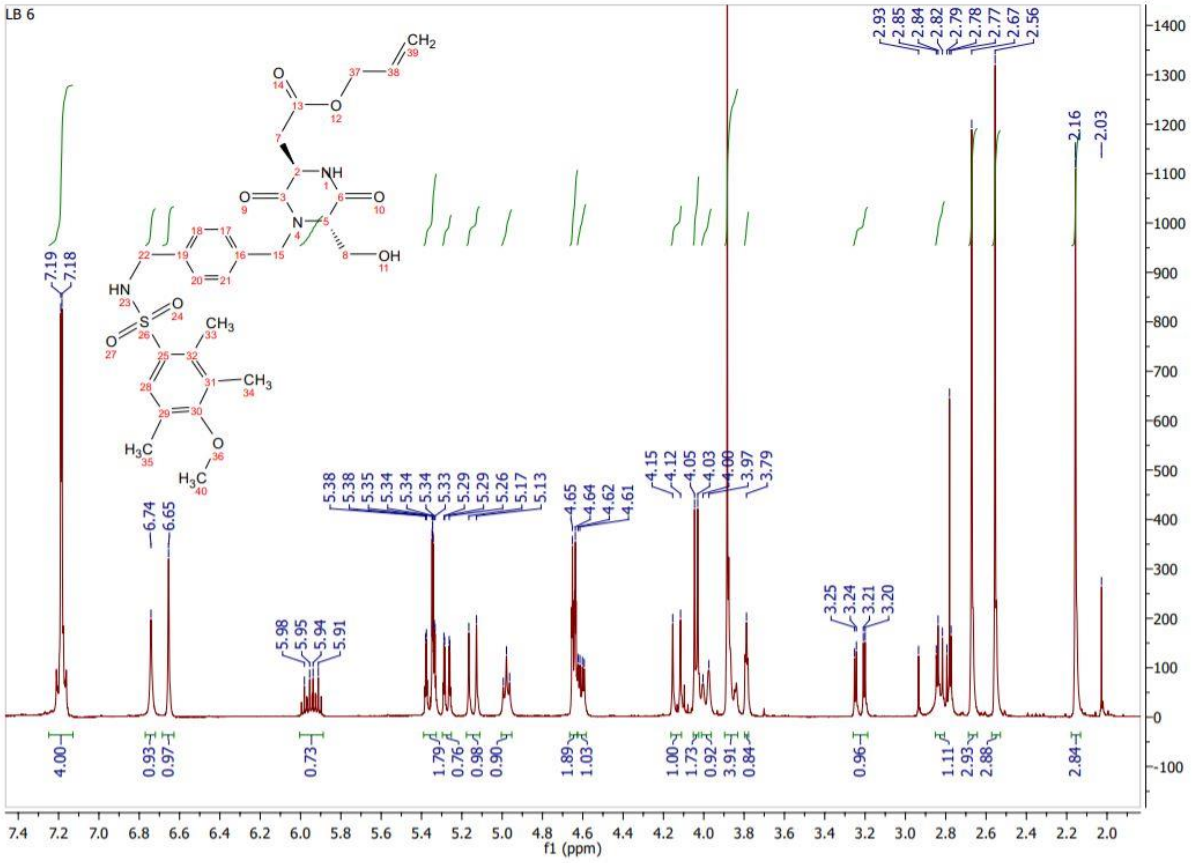

Figure 50: DKP3-f3-OH

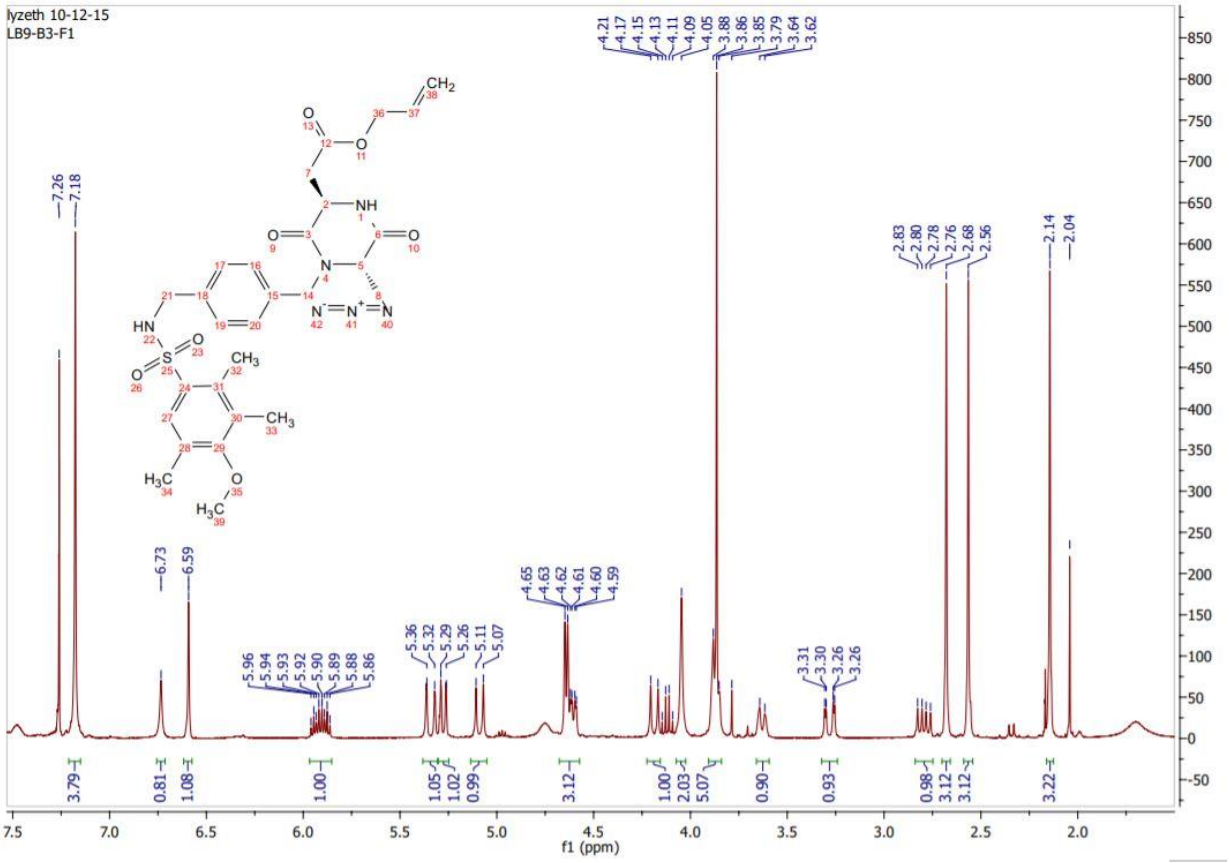

Figure 51: N3-DKP3-f3-OAll

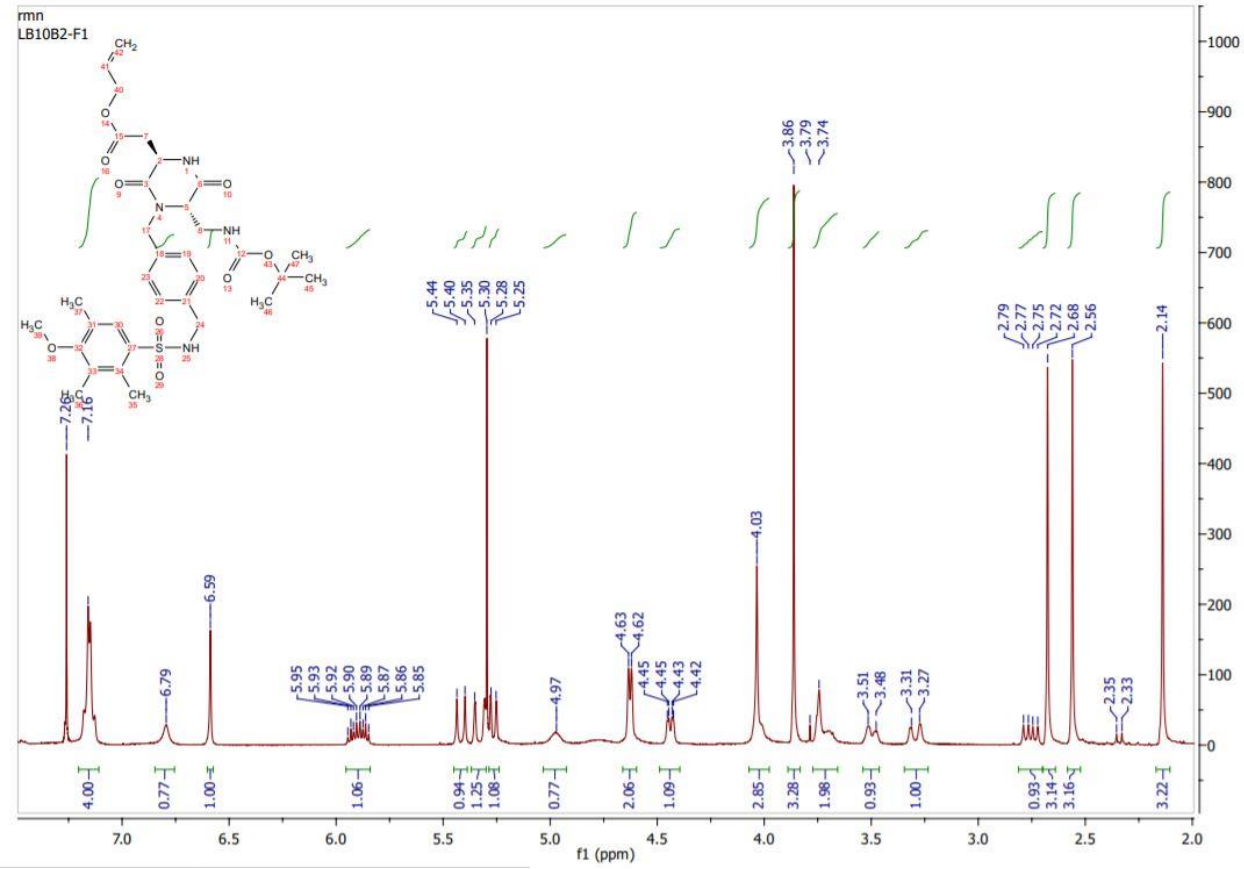

Figure 52: Boc-DKP3-f3-OAll

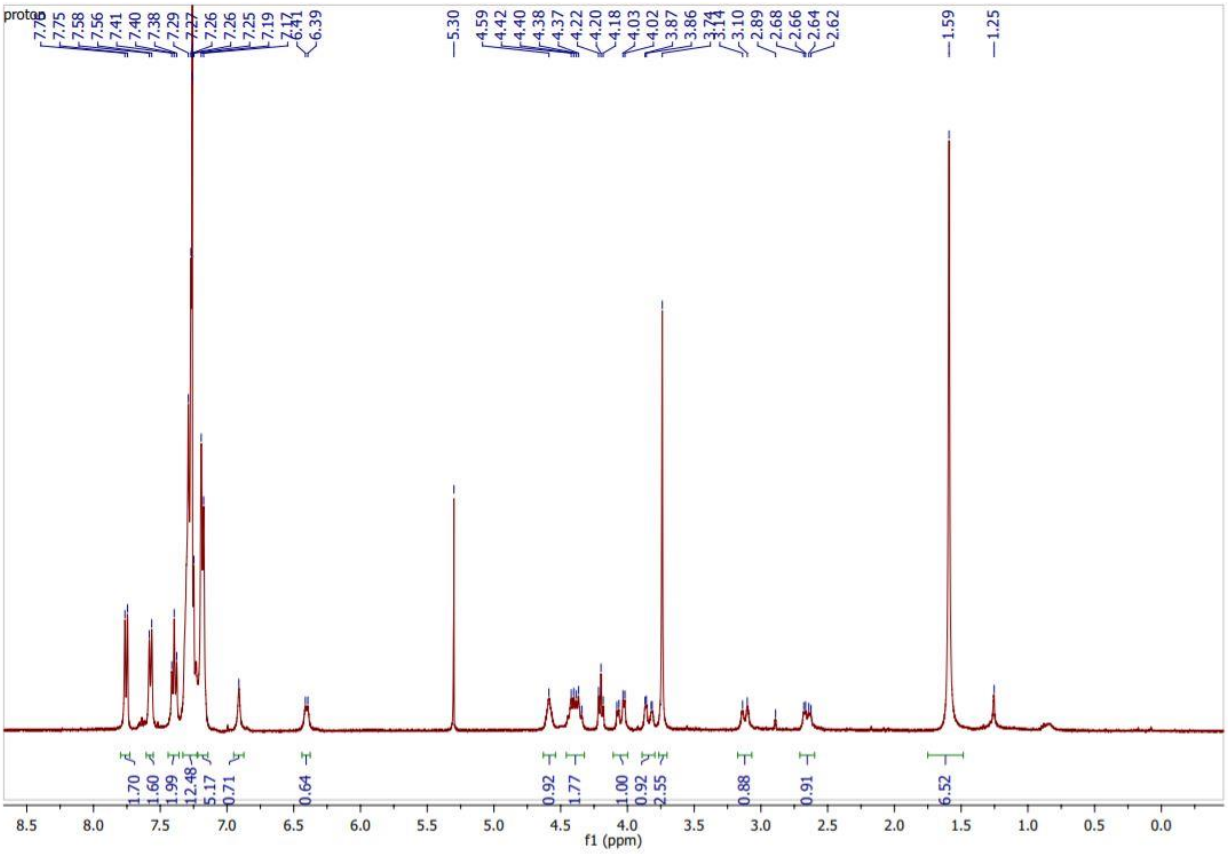

Figure 53: Dipeptide Fmoc-Asn(Trt)-Gly-OBn

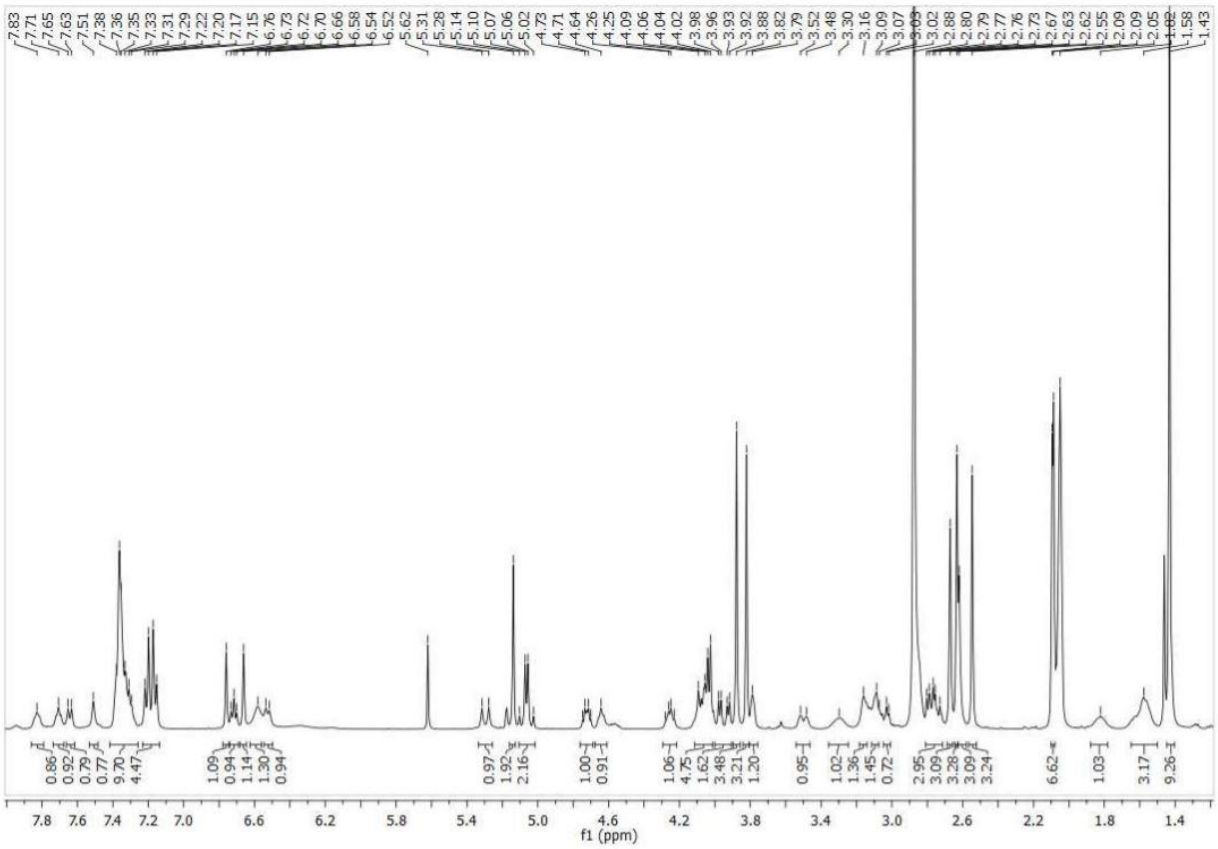

Figure 54: Cbz-Arg(Mtr)-DKP3-f3-Asn(Trt)-Gly-OBn

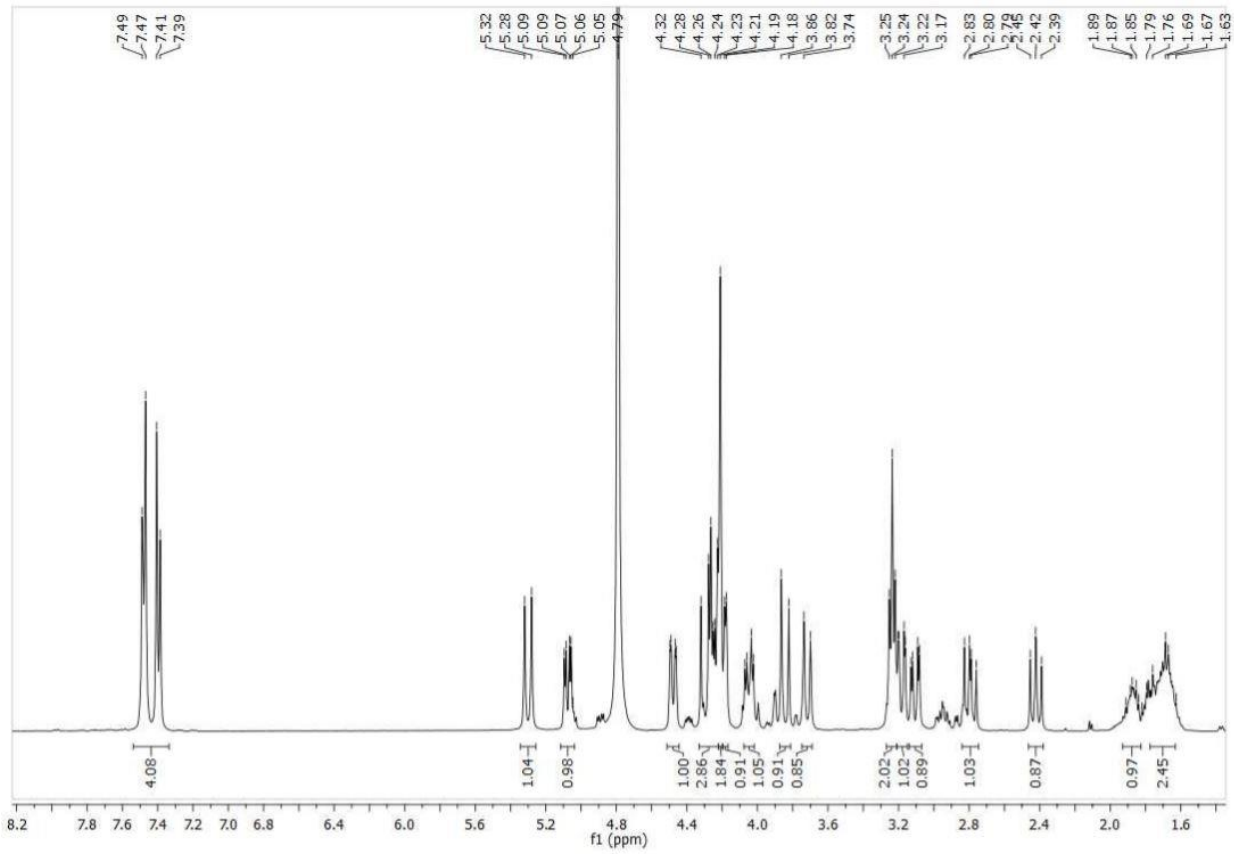

Figure 55: Cyclo[DKP3-f3-NGR]

EÖTVÖS LORÁND UNIVERSITY
DECLARATION FORM
for disclosure of a doctoral dissertation

I. The data of the doctoral dissertation:

Name of the author: Andrea Angelo Pierluigi Tripodi
MTMT-identifier: 10064573
Title and subtitle of the doctoral dissertation: Development of a novel class of cyclic NGR peptides for targeted drug delivery
DOI-identifier[72]: 10.15476/ELTE.2020.127
Name of the doctoral school: School of Chemistry
Name of the doctoral programme: Synthetic Chemistry, Materials Science and Biomolecular Chemistry
Name and scientific degree of the supervisor: Prof. Dr. Mező Gábor, Head of the Research Group of Peptide Chemistry
Workplace of the supervisor: Department of Organic Chemistry, Research Group of Peptide Chemistry, Eötvös Loránd University

II. Declarations

1. As the author of the doctoral dissertation,[73]
a) I agree to public disclosure of my doctoral dissertation after obtaining a doctoral degree in the storage of ELTE Digital Institutional Repository. I authorize the administrator of the Department of Doctoral, Habilitational and International Affairs of the Dean's Office of the facultry of Science to upload the dissertation and the abstract to ELTE Digital Institutional Repository, and I authorize the administrator to fill all the declarations that are required in this procedure.
b) I request to defer public disclosure to the University Library and the ELTE Digital Institutional Repository until the date of announcement of the patent or protection. For details, see the attached application form;[74]
c) I request in case the doctoral dissertation contains qualified data pertaining to national security, to disclose the doctoral dissertation publicly to the University Library and the ELTE Digital Institutional Repository ensuing the lapse of the period of the qualification process.;[75]
d) I request to defer public disclosure to the University Library and the ELTE Digital Institutional Repository, in case there is a publishing contract concluded during the doctoral procedure or up until the award of the degree. However, the bibliographical data of the work shall be accessible to the public. If the publication of the doctoral dissertation will not be carried out within a year from the award of the degree subject to the publishing contract, I agree to the public disclosure of the doctoral dissertation and abstract to the University Library and the ELTE Digital Institutional Repository.[76]
2. As the author of the doctoral dissertation, I declare that
a) the doctoral dissertation and abstract uploaded to the ELTE Digital Institutional Repository are entirely the result of my own intellectual work and as far as I know, I did not infringe anyone's intellectual property rights.;
b) the printed version of the doctoral dissertation and the abstract are identical with the doctoral dissertation files (texts and diagrams) submitted on electronic device.
3. As the author of the doctoral dissertation, I agree to the inspection of the dissertation and the abstract by uploading them to a plagiarism checker software.

Budapest, 01.09.2020

Andrea Angelo Pierluigi Tripodi

Signature of dissertation author

72 Filled by the administrator of the faculty offices.
73 The relevant part shall be underlined.
74 Submitting the doctoral dissertation to the Disciplinary Doctoral Council, the patent or protection application form and the request for deferment of public disclosure shall also be attached.
75 Submitting the doctoral dissertation, the notarial deed pertaining to the qualified data shall also be attached.
76 Submitting the doctoral dissertation, the publishing contract shall also be attached.